FRACTURE AND FLOW IN GLASS

BY

B. STAVRINIDIS, BSc

A thesis submitted to the University of Keele
for the Degree of Doctor of Philosophy

Department of Physics
University of Keele
Keele, Staffordshire

March 1980

To Christine and Nicholas

ABSTRACT

The indentation creep behaviour and the apparent healing of cracks are studied in several silicate glasses in different environments and at different temperatures.

The results obtained do not confirm previous findings that the indentation creep rates are environment dependent. The impact of these results on recent theories relating indentation creep rates and tensile fracture is discussed.

It is found possible to describe all the indentation creep results at different temperatures with a universal indentation creep equation.

The closure of cracks upon unloading and the load-bearing character of closed cracks are studied in some detail. It is found that the load-bearing capacity of closed cracks increases with aging time and with the temperature of heat-treatment at rates which are dependent upon the composition of the glass. The results are interpreted qualitatively in terms of the chemical action of water on glass.

ACKNOWLEDGEMENTS

I would like to thank my supervisor Dr.D.G.Holloway for many helpful and encouraging discussions and for his critical reading of my reports which finally resulted in this thesis. I would also like to thank

Professor W.Fuller	for the provision of laboratory facilities
Mr.F.Rowerth and Messrs.G.Dudley, E.J.T.Greasley, G.Marsh, M.P.Wallace and S.B.Cartledge	for the use of technical and workshop facilities
Messrs.M.T.Cheney and M.Daniels	for the preparation of the photographs
My parents in law and the University of Keele	for their financial support
and my wife, Christine	for the patience and care with which she prepared the graphs and typed this thesis.

CONTENTS

CONTENTS (continued)

CONTENTS (continued)

GENERAL INTRODUCTION

Glass is often regarded as a simple, ideally brittle and chemically inert material. There is however extensive experimental evidence that glass exhibits microplasticity and unusual chemical reactivity under common circumstances.

Evidence of microplasticity can be readily seen as the grooves and indentations formed when a hard object is slid or pressed on a glass surface. With the increasing sophistication of the techniques of fracture mechanics, the energy absorbed during fracture can be measured and is found to be up to 10 times the estimated value of the surface free energy.

It is also found that the ultimate strength of undamaged glass specimens is far below the theoretical strength of glass. Some investigators have taken the view that all these phenomena are related to the limited plastic deformation that glass can undergo at room temperature and have attempted to explore this possibility quantitatively. The characteristics needed for such an investigation are the tensile or compressive yield stress, Y, that is, the stress level at which plastic (irrecoverable) deformation occurs in uniaxial tension or compression and also the yield criterion which is the condition that must be satisfied by the principal stresses in three dimensional stress distributions. Previous experience has taught that in the case of metals with well defined plastic properties, the yield stress can be obtained conveniently by an indentation test in which the hardness (defined as the mean pressure under an indenter of specific geometry) is measured. In particular it is found that the tensile yield stress of some metals and alloys coincides with one third of the

value of hardness. Hardness testing was adopted as a means for obtaining the flow stress for glass, although a different conversion factor had to be introduced to suit the highly elastic nature of these materials.

Marsh (1964), who introduced the flow concept for glasses in a quantitative way, reported observations that the indentation hardness of soda glass decreases with the time of loading and interpreted this as a reduction of the flow stress with duration of load; this in turn could explain the reduction of the breaking strength of glass samples subjected to prolonged loading, (static fatigue).

Marsh's work was extended by Gunasekera (1970) who showed that the hardness of soda-lime-silica glass is dependent not only on the loading time, but also on the test environment. The variation of hardness with loading time and environment was found to be compatible with the fracture behaviour of glass in different environments. Further work by Weidmann and Holloway (1974a,b), showed that in soda-lime-silica glass the variation of the crack speed with applied stress and also static fatigue phenomena can be expressed quantitatively in terms of the variation of the hardness with time under similar test conditions.

The possibility of extending this work to cover glasses with different composition was appealing. It would be interesting to compare the variation of hardness for different glasses under different environments and temperatures with the fracture behaviour of these glasses under the same test conditions. Initially, the objective of the present study was to attempt such a correlation.

As a matter of tactics, indentation experiments were carried

out early in the present study on soda-lime-silica glass at room temperature. Similar experiments have already been carried out by Marsh (1964) and by Gunasekera (1970). Surprisingly, a widespread and fundamental disagreement was found between the results of the present study and those obtained by the previously mentioned authors*. In particular, the duration of loading was found not to affect the hardness of soda-lime-silica glass as remarkably as reported by Marsh (1964) and by Gunasekera (1970) and, in direct conflict with Gunasekera's results, the hardness of glass was found to be independent of the test environment. A lot of effort has been spent in the present study to reveal possible sources of the discrepancy observed but no conclusion has been reached.

Despite the conflict, the variation of the hardness of soda-lime-silica glass at high temperature and also the variation of hardness of different glass compositions with the loading time were carried out as originally intended.

Because the quantitative model of plastic flow proposed by Weidmann and Holloway was based in effect on the results of Gunasekera's indentation hardness study but also on the results on slow crack propagation, it also appeared useful to perform key-experiments on the variation of the crack speed with applied stress under different test conditions. These experiments produced results in excellent agreement with those reported by Weidmann and Holloway (and others). In the course of the slow crack propagation experiments curious phenomena involving what appeared to be crack healing, i.e. crack closure resulting in a load

---

* Other independent investigators have reported results from similar experiments which are in direct conflict with both those obtained by Gunasekera and those of the present author.

bearing interface were observed. Some of these phenomena have been observed by previous members of this laboratory and other investigators but a detailed quantitative study has not previously been attempted. In fact, crack healing seems to be a natural consequence of Griffith's (1920) theory of brittle fracture for glass. Griffith postulated that fracture of glass is controlled by the First Law of Thermodynamics: In an elastic solid containing a crack under load thermodynamic equilibrium is attained when the total energy*, U, of the system remains constant in respect to the crack length, C, that is

$$\frac{dU}{dC} = 0$$

For small displacements from the equilibrium crack length the pre-existing crack in the body advances or retreats depending on the sign of $\frac{dU}{dC}$. Therefore, fracture in Griffith's theory is a reversible thermodynamic process. Energy from the body is absorbed and converted only into surface free energy as the crack advances (ideally brittle fracture). The same amount of energy must be expected to be released as the crack closes over the same length.

It was thought then that an investigation of the closure and the load bearing properties of closed cracks in glass may lead to a better understanding of the flow and fracture properties of glass. The experiments which have been carried out suggest however that surface chemical reactivity may play a significant role in the occurrence of the apparent healing and that the phenomenon is not a manifestation of the crack reversibility implied by Griffith's equation.

---

* The total energy U in this context comprises of the work done by the applied loads, the elastic strain energy stored in the body and the surface free energy of the pre-existing crack.

Under these circumstances the presentation of the thesis in two more or less separate sections appeared almost unavoidable.

The first section deals with the hardness and flow of glass; several ideas expressed in the past are reviewed and the consequences of the present results are discussed.

The second section deals with closure and load bearing phenomena of cracks in different glasses including an organic glass. Several factors affecting these phenomena are studied in some detail and possible mechanisms for interpretation of the results are discussed.

PART I

INDENTATION CREEP IN GLASS

CHAPTER 1

HARDNESS AND FLOW

1.1 General

The hardness of a solid is a readily appreciated quality generally understood as the resistance to surface deformation by scratching or indentation. This quality is technologically important and despite the fact that many metals and minerals have been in use for thousands of years the earliest known scale and method for quantitatively assessing the hardness of solids did not appear until 1820. This is Mohs' hardness scale and is based on the ability of certain minerals to scratch others. A scale was developed in which ten minerals were ranked so that any one would scratch all the others below it but not those above it. In practice the hardness of any solid could be classed among hardness values of the 10 selected minerals in Mohs' scale. Many other techniques for the evaluation of the hardness of solids have appeared since then based on the measurement of the extent of "damage" produced on the surface of solids under specific and sometimes standardized conditions. Among these methods are scratch, abrasion, and indentation (penetration) methods. The methods most widely used for determining the hardness of solids are indentation (static) methods. These

involve the penetration of an indenter of a specific geometry into a solid surface under constant load for a specified time known as loading time. The size of the permanent indentation produced on the test surface is subsequently measured and the hardness number is determined using one of the expressions:

$$\text{Hardness number} = \frac{\text{Indenter Load}}{\text{actual area of impression}} \qquad (1.1a)$$

or,

$$\text{Hardness number} = \frac{\text{Indenter Load}}{\text{projected area of impression}} \qquad (1.1b)$$

Some of the existing indentation techniques are:

a) The Brinell method in which a small steel ball is used as an indenter and the Brinell hardness number is given by equation (1.1a)

b) The Rockwell methods in which spherical or conical indenters are used and the Rockwell hardness number is determined by the depth of the penetration under a standard load. There are different Rockwell hardness scales depending on the geometry and size of the indenter used and on the applied load.

c) The Knoop method in which a rhombic-based diamond pyramid is used in which the angles between the two longer and the two shorter edges respectively, are $172^\circ\ 30'$ and 130°. The Knoop hardness number is given by equation (1.1b).

d) The Vickers method in which a square-based diamond pyramid with an included angle of 136° between opposite faces is used. The Vickers hardness number H_v is found from equation (1.1a).

Recenctly, a novel hardness method has been developed by the Shell Development Company* in which a conical indenter of known hardness is pressed on the surface of the material under test and the hardness of the latter is measured by the amount

---

* Offshore Research Focus (Department of Energy), December 1979, no 16, page 10.

of deformation of the indenter.

The Brinell method, once very popular in metallurgy, yields hardness numbers which are load and indenter-size dependent: a high load or/and a very small-diameter ball has to be used to produce permanent well-defined indents particularly on the surface of harder metals. In the latter case, significant deformation of the indenter complicates routine hardness tests.

Early experiments showed that the Brinell method could provide consistent hardness numbers when the load on the indenter was such that the diameter of the resulting indentation was around 0.375 times the diameter of the indenter. Under these conditions the angle subtended by the tangent planes to the surfaces of the ball is $\sim 136^{\circ}$, figure 1.1. These observations led Smith and Sandland (1925) "in full appreciation of the popularity of the Brinell test" to introduce a diamond pyramid indenter with an angle of 136° between opposite faces figure 1.2a. The resulting indentations are well-defined, figure 1.2b, and in fact the Vickers hardness numbers are independent of the size of the indenter and of the applied load. The difficulty of indenter deformation was also eliminated.

Nonetheless, some early investigators observed an apparent load dependence of the hardness of solids and several terms have evolved to distinguish the hardness obtained under small loads from that obtained under high loads (sometimes as high as 10^4 N). Among these terms are: microhardness, microindentation hardness, and micro-load hardness. However a load-limit below which these terms are appropriate has not been agreed.

In the present study the term hardness will be adopted, for the load range used (1 - 50 N).

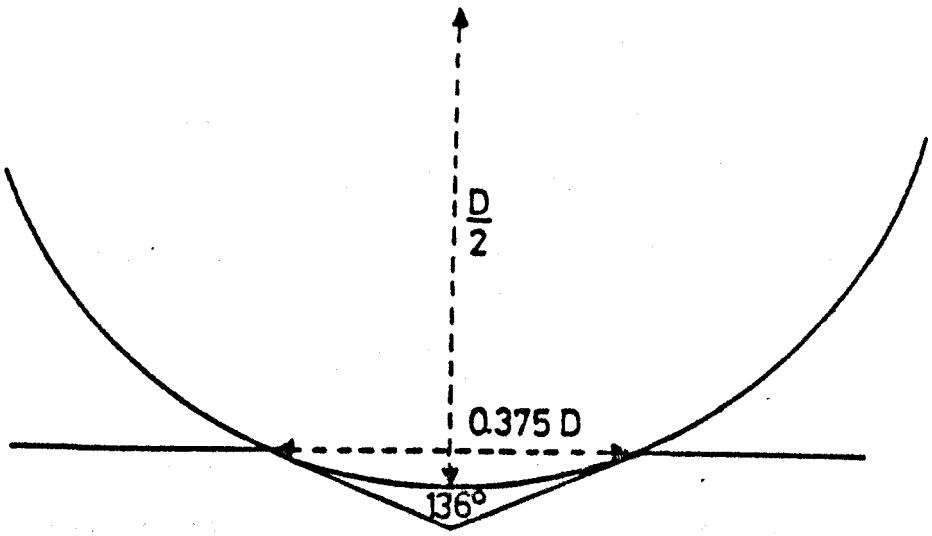

Figure 1.1 Conditions under which a ball indenter is equivalent to a pyramid indenter.

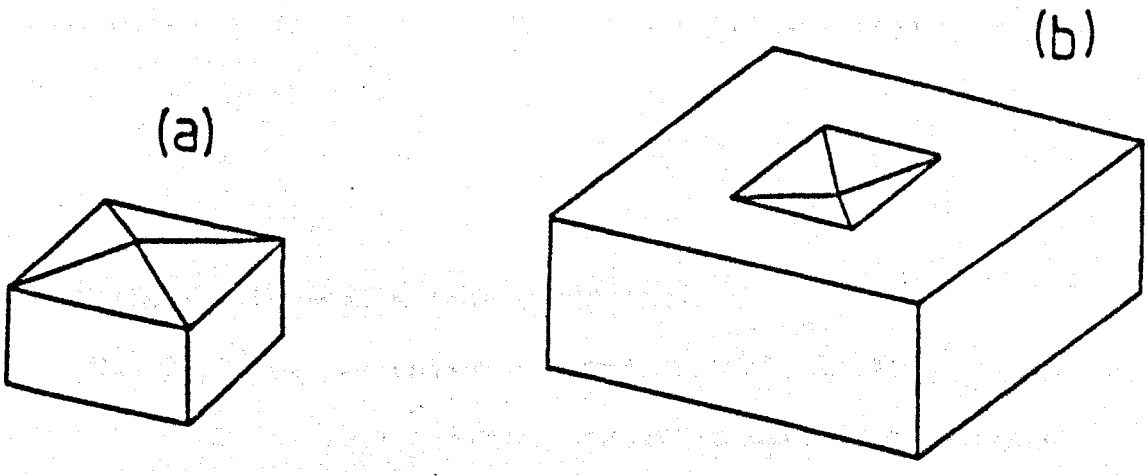

Figure 1.2 Diagram of (a) Vickers diamond indenter and (b) Vickers indentation produced by a Vickers indenter.

From the general definition of hardness, equation (1.1a), it is found that in the case of a pyramid-shaped impression with an included angle θ between the opposite faces, the actual area of the indentation is $d^2(2\sin\frac{\theta}{2})^{-1}$ where d is the length of the base diagonal. For the Vickers diamond indenter $\theta = 136^\circ$ and hence equation (1.1a) gives the Vickers hardness number, H_v, as

$$H_v = \frac{2P\sin 68^\circ}{d^2} \qquad (1.2)$$

where P is the load and d is the average base diagonal length of the indentation which is usually measured after removal of the load. Previous and also this work showed that the change in the length of the diagonals upon removal of the indenter (i.e. elastic recovery) is small and within the experimental error of measurements.

In the early and occasionally in the recent literature hardness numbers are quoted in Kg mm^{-2}. The relationship between these units and the SI units used in the present thesis is 1 Kg mm^{-2} = 9.8 MN m^{-2}.

1.2 Relation between hardness and flow.

The fact that indentation hardness tests involve plastic deformation of the test material indicates that a correlation may exist between the hardness number and the stress level at which plastic deformation takes place. Early investigators (reviewed by Nadai 1931 and Hill 1950) showed that the indentation process can be treated as a penetration of a flat die into a rigid-plastic material in which elastic strains are not taken into account (ideally plastic materials) and represent approximately

the real elastic-plastic materials in which elastic strains are small compared with plastic strains. On this basis a theory was developed, the rigid die theory, which predicts that the ratio of the average pressure on the die to the uniaxial yield stress is ~ 3. In this theory the criterion for plastic deformation is that of von Mises, which states that yielding occurs under a general state of combined stresses in which the principal (orthogonal) stresses are P_1, P_2, P_3, when the following parameter Y reaches a critical value

$$Y^2 = \frac{1}{2}\left[(P_1 - P_2)^2 + (P_2 - P_3)^2 + (P_3 - P_1)^2\right] \qquad (1.3)$$

Thus, the hydrostatic component plays no part in the plastic deformation of the material. This is equivalent to the statement that yield will occur when the elastic shear strain energy density reaches a critical value.

Indeed it was found (Tabor, 1951) that for metals and alloys which do not work-harden appreciably the ratio of the Brinell hardness number to the ultimate tensile strength is constant and approximately equal to 3. It was also found that for fully work-hardened metals the ratio of the Brinell or Vickers hardness number to the yield stress, Y, of the material is about 3, that is,

$$\frac{H_v}{Y} \simeq 3 \qquad (1.4)$$

The yield stress, Y, is the tensile stress at which permanent deformation first takes place and represents the upper limit of loading in service. Tabor (1951) showed further that for metals which work-harden and therefore do not have a

constant yield stress, equation (1.4) still holds provided that Y is taken as the flow stress at 8% strain corresponding to the mean surface strain imposed by a Vickers indenter. These empirical observations implied that a quick and non-destructive test such as the hardness test could produce useful information about the deformation of certain materials.

The validity of the equation (1.4) is confined however, to materials with low values of yield stress Y. As will be shown later in this chapter, for materials with high values of Y or more precisely, with low values of $\frac{E}{Y}$, the ratio $\frac{H_v}{Y}$ is less than three and varies with the ratio $\frac{E}{Y}$ for the material.

1.3 Hardness and flow of glass

It is customary to begin an introductory account of the hardness of glass with a clarifying definition. In glass technology, a glass is termed hard or soft depending on its softening temperature i.e. the temperature at which the viscosity is $10^{6.6}$ Nsm^{-2}. Thus a hard glass has a higher softening point than a soft glass. In the context of the present thesis this definition of hardness will be put aside; hardness will mean exclusively the quantity measured by an indentation test*.

When the Vickers indentation test was applied to silicate glasses (Taylor, 1950) permanent, well-defined indentations were produced even with the lightest loads, and this is in contrast to the result of a ball indentation test when fracture of the glass invariably occurs before any visible permanent

* When the term hardness is used in a comparative and qualitative sense, the distinction between the two definitions seems to be less important if one considers the observations of Bastic (1950) and Prod'homme (1968) that a linear relation exists between the Vickers hardness and the softening point of a variety of glasses.

indent is formed. However the ball indentation test has proved to be a useful tool for studying fracture phenomena in glass (e.g. Lawn and Wilshaw, 1975). It is characteristic of Vickers indentations on glass that radial and/or circular cracks often occur around the indentations, figure 1.3. When loads below 1 N are used, these cracks do not appear, although their existence can be verified by slight etching of the glass surface. The literature on the hardness of glass contains a large number of conflicting experimental results. Among these are results on the load dependence of the Vickers hardness of glass. Various authors reported that the Vickers hardness of glass increases as the applied load increases, (e.g. Prod'homme, 1968, in the load range 0.5 - 3 N); others reported that the Vickers hardness of glass decreases with increasing load (e.g. Bartenev, Razumovskaya and Sanditov, 1969, in the load range 0.05 - 1 N) and others reported load independence of the Vickers hardness (e.g. Ainsworth, 1954, in the load range 0.1 - 1 N). However, load dependence of the hardness of glass does not seem to be connected with the presence of cracks around the indentation.

The fact that plastic indentations and also plastic furrows can be produced on the glass surface seems to provide evidence that glass exhibits micro - plasticity despite its macroscopic brittle behaviour. As in the case of metals the hardness test has been used to estimate the flow stress of glasses. But is must be pointed out that in the case of glass no other way has been developed as yet to provide the flow stress.

Ainsworth (1954) seems to be the first author to estimate the flow stress for a glass from its Vickers hardness number.

He resolved the effective stress acting on the glass surface

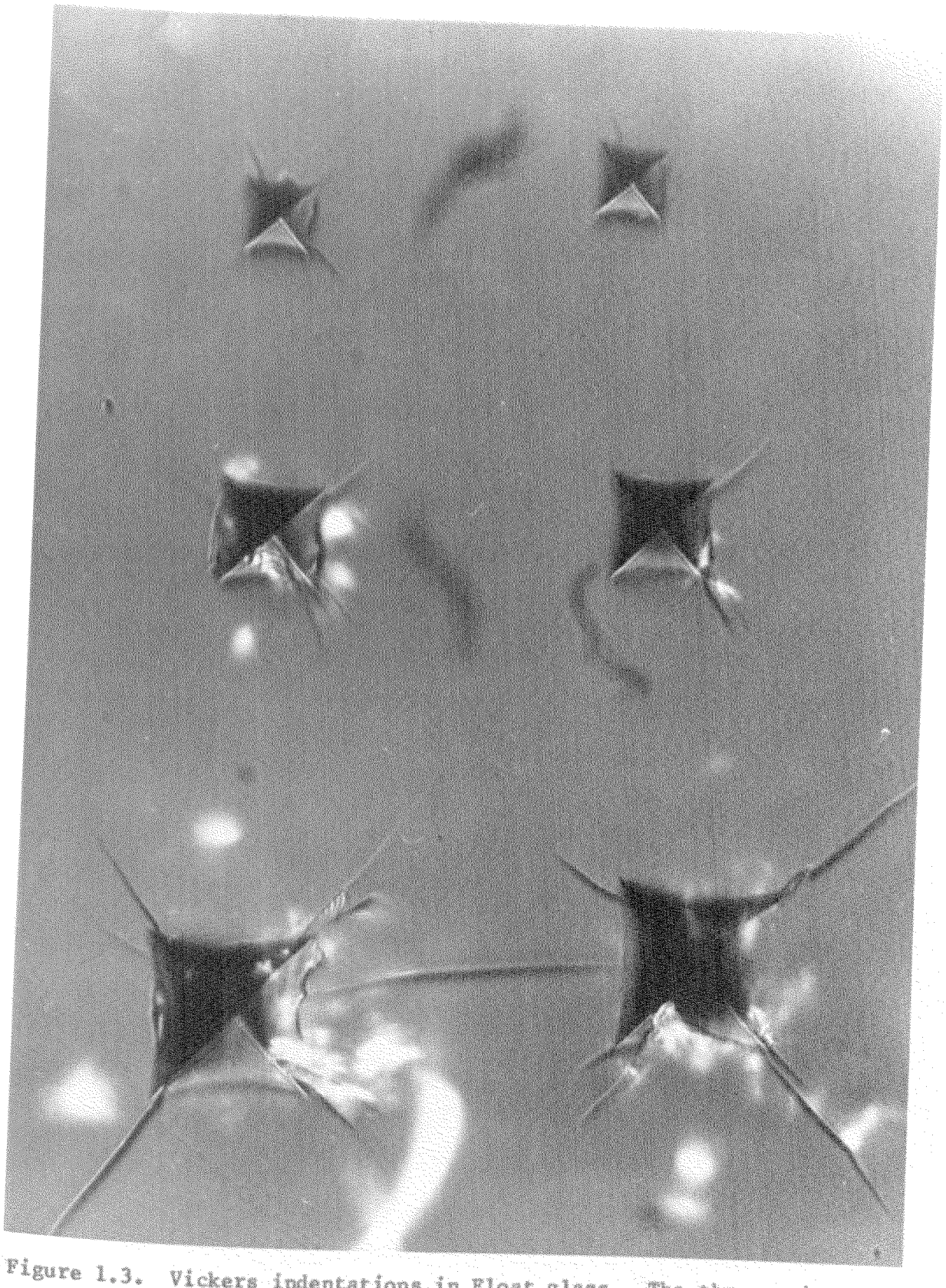

Figure 1.3. Vickers indentations in Float glass. The three pairs of indentations from top to bottom were produced by loads of 2, 3, and 5 N respectively (mag. x 1000).

in contact with the indenter into components parallel and perpendicular to the area of contact and argued that the important, effective stress is that which is parallel to the contact area and which is "tensile" in nature; and that as the indenter sinks into the material, the area of contact increases until the magnitude of this stress is reduced to the value of flow stress. Then $Y = H_v \cos 68^\circ$ or,

$$\frac{H_v}{Y} = 2.7 \qquad (1.5)$$

Thus, Ainsworth's simple approach provided virtually the same relation between flow stress and hardness number as that found for metals (equation 1.4).

Marsh (1964) argued that plastic deformation is not only responsible for the formation of indentations, but also for various phenomena observed in the fracture of glass. Thus, the fact that the fracture energy of glass is higher than the surface free energy was attributed to the energy dissipation at the tip of the crack where a small plastic zone is formed. If glass were an ideally brittle material its fracture energy would be equal to the surface free energy. It is also established that the maximum strength of undamaged glass specimens is $\sim \frac{E}{20}$ where E is Young's modulus, while the theoretical estimates of the strength of glass are between $\frac{E}{10}$ and $\frac{E}{3}$. According to Marsh the lower observed strengths are due to plastic deformation which takes place just prior to fracture. In this connection Marsh argued that since the maximum observed strength of glass ($\sim \frac{E}{20}$) is well above the flow stress predicted by the simple relation $\frac{H_v}{3} \sim 3$ but even pristine glass does not exhibit

macroscopic flow before fracture, the relation between H_v and Y needed re-examination. Similar problems are encountered with other highly elastic materials (e.g.glassy polymers) which can accommodate large elastic strains before failure.

In Marsh's view the mode of deformation in highly elastic materials is different from that in simple elastic-plastic materials (most metals and alloys) in which yielding occurs at very low elastic strains. In the latter case, the material under the indenter flows upwards forming a lip around the indentation "piling-up" mode. The alternative deformation mode proposed by Marsh for the highly-elastic materials is that of "radial flow". Previous work by Samuels and Mulhearn (1957) and Mulhearn (1959) showed that equal strain contours beneath Vickers and Brinell indentations form a series of concentric hemispheres. Marsh regarded this radial distribution of strain as analogous to the stress distribution around an expanding spherical cavity under a uniformly distributed internal pressure. The problem of the expansion of spherical and cylindrical cavities under internal pressure had been thoroughly studied because of its connection with the autofrettage of pressure vessels and gun-barrels (Hill, 1950). The solution to this problem predicts that the value of the internal pressure P, required inside a cavity of radius a to produce plastic flow to a radius c ($c > a$) is proportional to the yield stress of the materials and to $\ln(\frac{c}{a})$. The ratio $\frac{c}{a}$ (which is related to the strains around the cavity) could be expressed in terms of the ratio $\frac{E}{Y}$ for the material and therefore the solution predicts that $\frac{P}{Y}$ varies with $\frac{E}{Y}$ of the material containing the cavity.

Marsh regarded the internal pressure, P, in the cavity as

analogous to the Vickers hardness, H_v, and after "certain simplifications" of the exact solution given by Hill (1950) to the spherical cavity problem for the ratio $\frac{P}{Y}$ he deduced that

$$\frac{H_v}{Y} = C + KB\ln Z \qquad (1.6)$$

where $B = \frac{3}{3-\lambda}$, $Z = \frac{3}{\lambda + 3\mu - \lambda\mu}$ and $\lambda = 6(1-2\nu)\frac{Y}{E}$

and $\mu = (1+\nu)\frac{Y}{E}$. C and K are constants, both equal to 2/3 in the spherical cavity theory, although in Marsh's view for the indentation process the values differ from 2/3 "as the constraints will be less around a hemispherical cavity".

Although Marsh's analogy of the indentation process with the expansion of a spherical shell and the simplified treatment of this solution may seem somewhat arbitrary, it was shown that the form of equation (1.6) was verified by experiment.

Using the compressive yield stress and the Vickers hardness numbers measured for a variety of materials covering a wide range of $\frac{E}{Y}$ the results were plotted in the form of $\frac{H_v}{Y}$ against the quantity BlnZ which in effect is a function of $\frac{E}{Y}$, figure 1.4. The results show a remarkable agreement with the theory: $\frac{P}{Y}$ was found to vary linearly with BlnZ (the values of the constants C and K determined from figure 1.4 were found to be 0.28 and 0.6 respectively). Thus, Marsh claimed to have demonstrated that for materials with low values of BlnZ or equivalent with low values of $\frac{E}{Y}$ (below ~ 150) the deformation mode is that of radial flow and the corresponding ratio $\frac{H_v}{Y}$ is less than three and varies with $\frac{E}{Y}$, in contrast to materials with $\frac{E}{Y} > 150$ for which $\frac{H_v}{Y} \sim 3$ and the deformation mode is that of "piling-up". For practical purposes, values of $\frac{H_v}{E}$ were plotted against $\frac{Y}{E}$ for materials with different

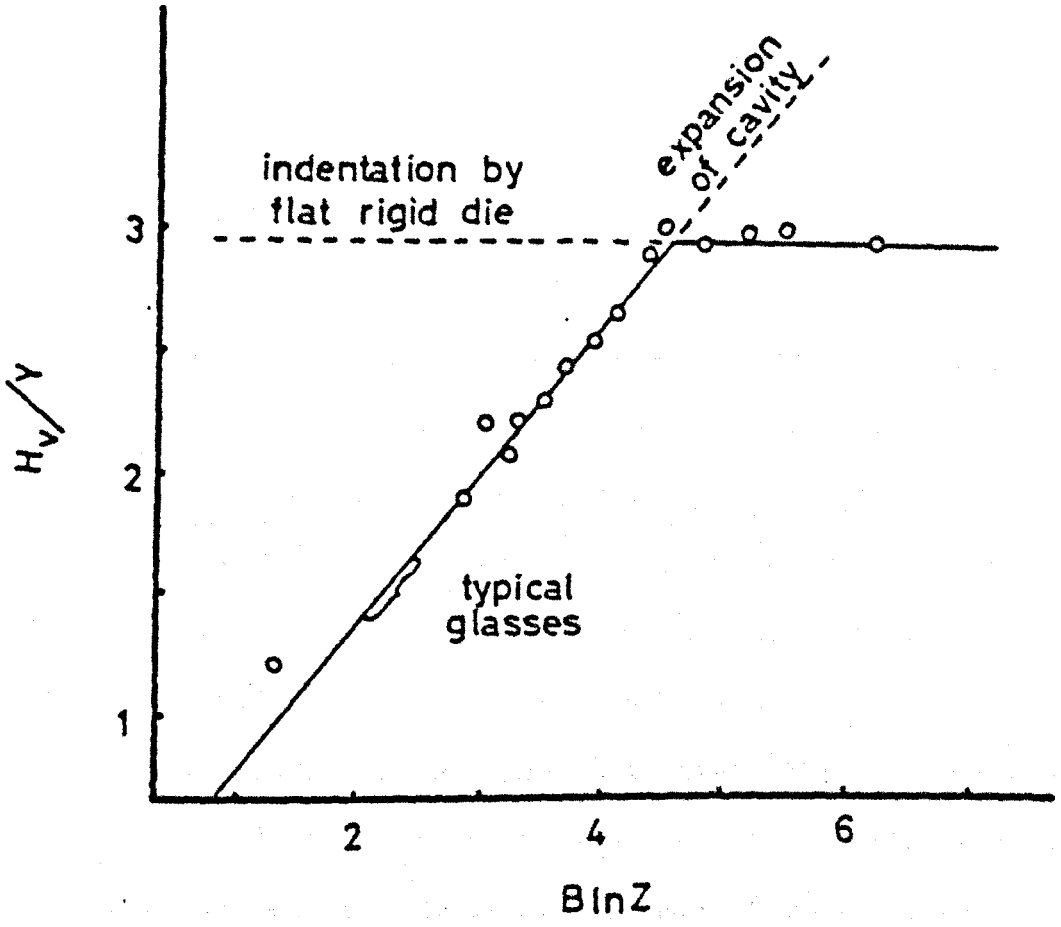

Figure 1.4 Variation of the ratio H_v/Y with BlnZ = f(E/Y), for different materials, after Marsh (1964).

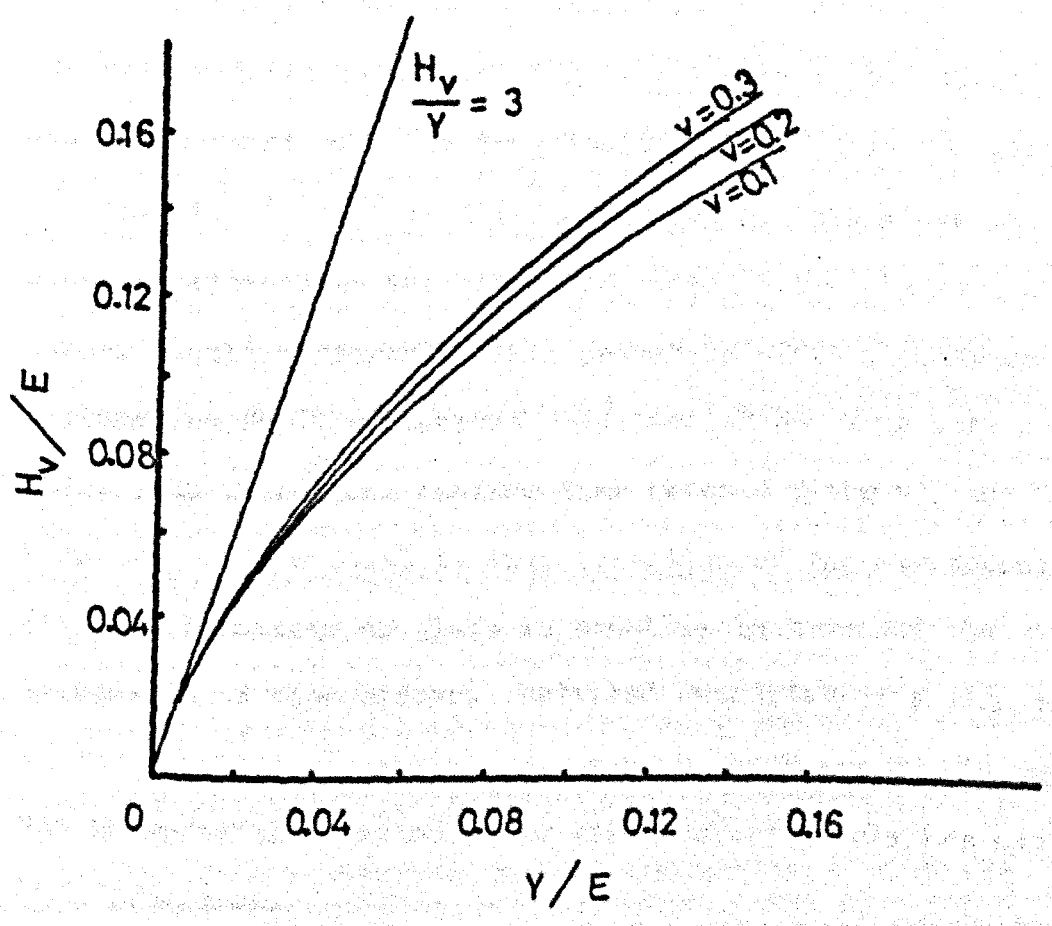

Figure 1.5 Variation of the ratio H_v/Y with Y/E for different materials after Marsh (1964).

Poisson ratios, figure 1.5. From known values of $\frac{H_v}{E}$ this graph showed that for silicate glasses $\frac{H_v}{Y} \simeq 1.6$.

It is interesting to note that Hirst and Howse (1968) and Johnson (1970) have investigated the relationship between $\frac{P}{Y}$ (where P is average pressure on the indenter) and $\frac{E}{Y}$ for different materials using wedges of various angles. Their results were compatible with a relationship between $\frac{P}{Y}$ and $\frac{E}{Y}$ predicted by a theory in which the indentation process was regarded analogous to the expansion of a cylindrical cavity under internal pressure.

On the basis of the spherical cavity theory, Marsh showed that the yield stresses (calculated from indentation hardness measurements) and the fracture stresses of undamaged glass specimens in air correlate well for several glasses, loading times and temperatures. He further showed that the flow stress of soda glass (determined of course from Vickers hardness numbers) reduces as the loading time increases but tends to reach a contant value at long loading times while for very short loading time ($\sim 10^{-5}$ s) the flow stress of this glass is extremely high and approaches the time-independent value observed at 77 K (under liquid nitrogen). This seemed to offer a phenomenological explanation for the observed reduction of breaking stress of glass with increasing loading time (static fatigue), and Marsh suggested that a complete interpretation of the macroscopic fracture behaviour of glass is possible in terms of the time-dependence of flow stress. Detailed quantitative explanation of the fracture properties of glass on the basis of his theory was referred to a future paper which unfortunately has never been published.

His work however was continued by Gunasekera (1970) who

also found that the Vickers hardness of soda-lime-silica glass decreases with increasing duration of loading but most importantly he also observed that the rate of decrease depends upon the test environment. A dry environment was found to reduce appreciably the rate of decrease of hardness. This apparently corresponded phenomenologically to the environment sensitivity of static fatigue. Further detailed work by Weidmann and Holloway (1974a) and others revealed that the rate of slow crack growth is stress and environment dependent.

In principle indentation creep, crack creep, and static fatigue in glass might be explicable on the basis of a common mechanism. A tentative explanation of these phenomena on the basis of plastic flow was attempted by Weidmann and Holloway (1974b). They claimed that static fatigue data from precracked soda-lime-silica glass specimens correlate well with the stress and environment sensitivity of the rate of crack growth in this glass: failure of precracked glass specimens occurs when one of the pre-existing cracks grows under the applied stress until it reaches a critical size at which catastrophic failure takes place. On the other hand fracture mechanics methods could predict a relation between the rate of crack growth, V, and the rate of change of the yield stress, $\frac{dY}{dt}$, at the boundary of a small plastic zone ahead of the crack tip. The observed relationship between the results from indentation creep (from which the variation of flow stress with time was obtained) and from slow crack propagation studied in different environments agreed with that predicted between V and $\frac{dY}{dt}$. It was also found possible to correlate quantitatively the rate of change of flow stress with static fatigue data for "pristine" glass samples.

These ideas are not universally accepted. Several other authors have expressed different views regarding the nature of deformation of glass during the indentation process and these will be discussed in a later chapter.

CHAPTER 2

EXPERIMENTAL: APPARATUS AND MEASUREMENTS

2.1 Introduction

The main series of experiments carried out in the present study consisted of indentation tests on four different glasses for different loading times in different environments and temperatures. For these experiments three indentation machines and a few other simple pieces of apparatus were used. In this chapter a brief description is given of the apparatus used followed by an account of the experimental techniques used to produce the specimens and to perform the indentation tests.

2.2 Machines

A hardness testing machine is in principle a device by which an indenter and a specimen with a smooth surface are brought into contact at very slow rate under a known constant load. The contact is maintained for the desired time (loading time) and then the indenter is withdrawn. This procedure can be made electromagnetically, hydraulically etc. In the present work three manually operated hardness testers were used with two different specimen-indenter configurations, figure 2.1. In the first

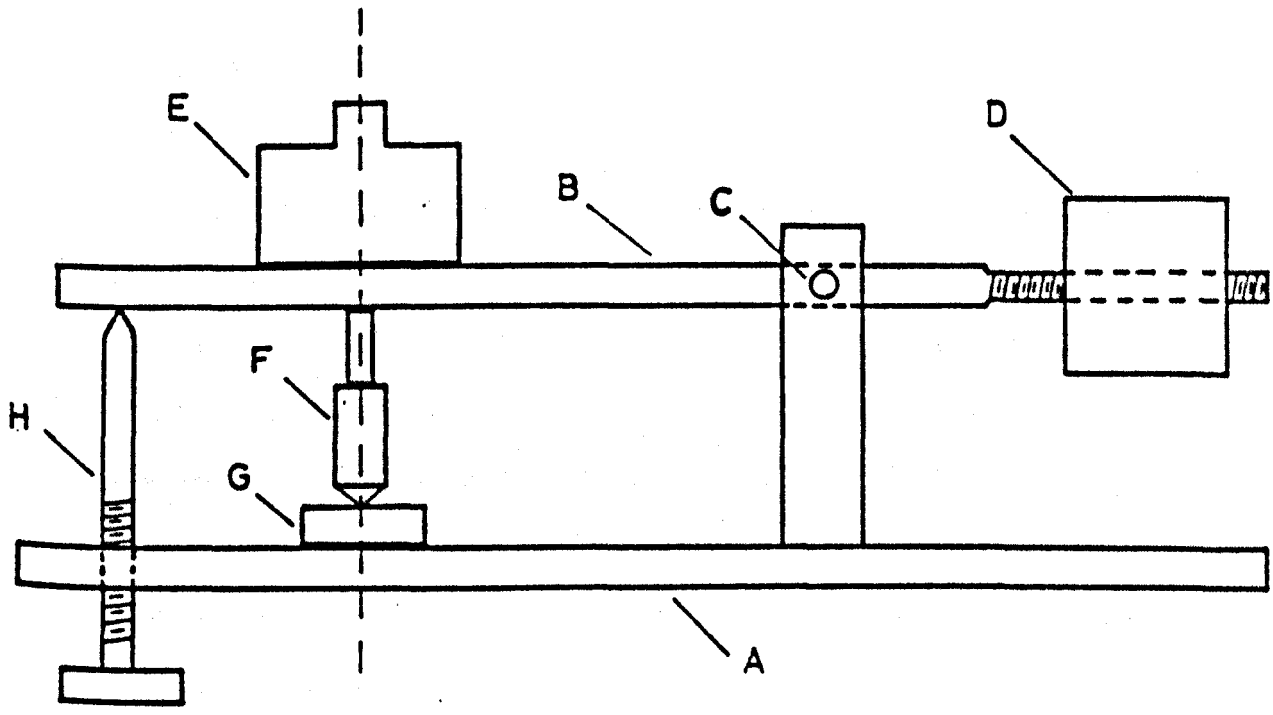

A	Base	E	Weight
B	Lever arm	F	Indenter
C	Pivot	G	Specimen
D	Counter weight	H	Loading-unloading screw

Figure 2.1 Schematic representation of the manually operated hardness tester. The position of the specimen and the indenter can be interchanged.

configuration the indenter is firmly fixed to a horizontal base so that its tip is pointing upwards. The specimen is held in one side and underneath a lever arm which can rotate about a horizontal axis passing through the pivoting points. The surface of the specimen to be tested lies opposite the indenter tip. The balancing of the lever arm is achieved by adjusting a counterweight on a screwed spindle at the end of the arm. The load is placed on the balanced arm, above the specimen so that its center of gravity is aligned with the vertical axis of the indenter.

This type of arrangement is used in a commercial hardness testing machine available as an accessory for the inverted Vickers projection microscope (Cooke, Troughton & Simms Ltd.) available in this laboratory, figure 2.2. (In inverted microscopes the specimen is positioned above the objective lens). In this case the lever arm and the supporting frame is fixed on the stage of the inverted microscope and the diamond indenter is permanently fixed on the top of an objective lens. The indentation is made by lowering the stage of the microscope towards the objective lens using the fine-focusing drum.

A series of indentation tests were carried out by the present author using this machine.

In the second type of specimen-indenter configuration the specimen is placed on a horizontal base and the indenter is fixed on the balanced pivoting arm and is pointing downwards. A hardness tester based on this arrangement was constructed and used by Gunasekera (1970) in this laboratory and its brief description here follows that given by Gunasekera (1970), figure2.3. The balancing arm carrying the indenter, the counter weight and

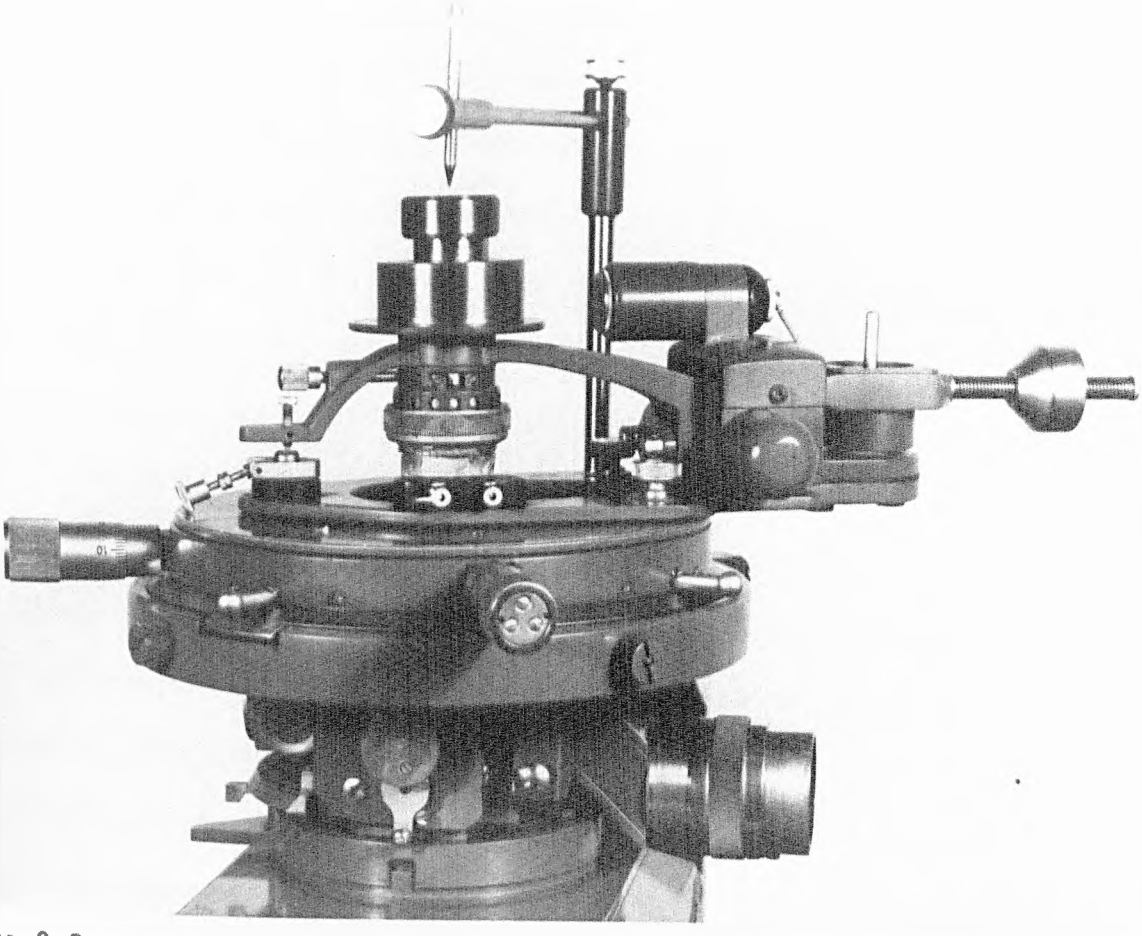

Figure 2.2. The Cooke, Troughton & Simms hardness tester.

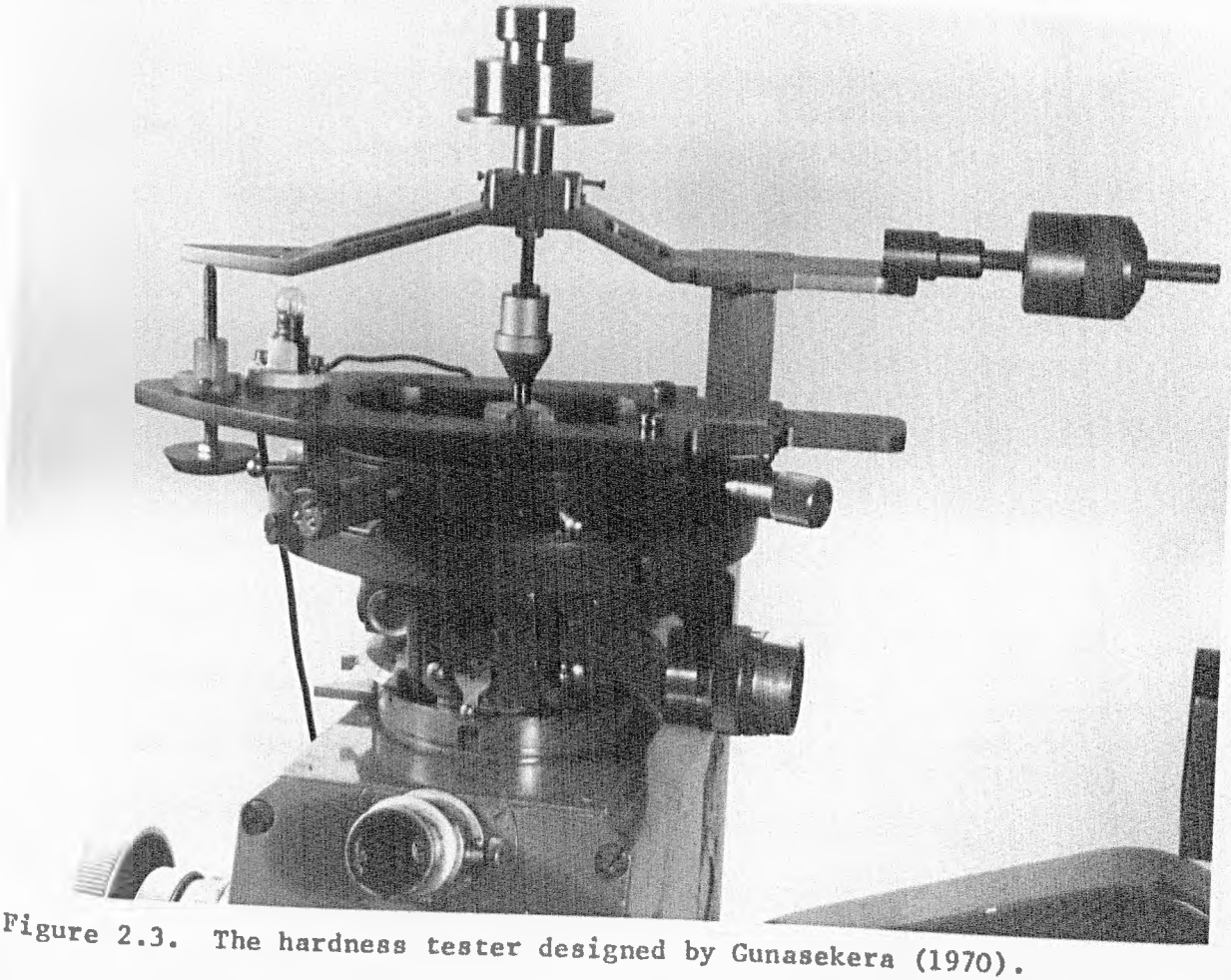

Figure 2.3. The hardness tester designed by Gunasekera (1970).

a knife edge was slotted to reduce the weight without reducing its rigidity. The base of the machine consists of a horizontal plate carrying a vertical stand, which is v-grooved to accomodate the knife edge of the lever arm, and a simple screw to facilitate loading and unloading. On turning this screw clockwise the loaded lever arm pivots until the indenter comes into contact with the specimen and the full load is supported by the specimen. When the contact between the screw and the lever arm is broken, a small electrical lamp connected in series with the contact, is extinguished. For unloading the screw is turned anticlockwise until it touches and lifts the lever arm.

The diamond holder is attached to the machine through a vertical screw, by means of which the position (height) of the indenter can be adjusted to suit the thickness of the specimen. Fine adjustment of the length of the indenter screw was always necessary for the production of square indentations, since these require that the axis of the indenter be normal to the specimen surface. This machine was originally intended to produce indentations, the size of which could be measured directly under the microscope while the indenter was still on the specimen under load. For this purpose a large hole was opened in the base plate of the machine so that when the machine was placed on the table of the inverted Vickers projection microscope the indentation could be observed and measured from below through the microscope.

Using this experimental arrangement, Gunasekera was able to perform indentation tests on glass in air and in two different liquid environments for loading times ranging from 20 to 10^5 seconds. A large number of indentation tests were carried out

at room temperature in the present study using this particular machine.

A new hardness testing machine was constructed in order to measure hardness at high temperatures. The new machine was like that described above, with only a few modifications and minor improvements, figures 2.4a,b. The distance between the vertical axis of the indenter and the pivoting axis of the lever arm was increased by 25% to reduce the error in applied loads, P, resulting from small displacements of the centre of gravity of the weight from the vertical axis of the indenter. Further reproducible positioning of the weight along the axis of the indenter was ensured by constructing a circular weight, weighing 2.94 N. This weight could be placed on a circular plate which had a peripheral edge slightly higher than the level of its surface so that lateral movement of the weight was restricted. The axis of this circular plate was aligned with that of the indenter and of the weight. Also, in order to increase the stability of the lever arm, two knife edges were fixed at some distance from each other instead of a single knife edge in the centre of the lever arm in the previous machine. The base of this machine had a rectangular area removed to facilitate access to the oven which was constructed to fit beneath this area. The base of the machine was fixed on an asbestos block in which a small volume (90 mm x 50 mm x 25 mm) was removed. This cavity accommodated heating elements, thermocouples and several specimens to be tested at high temperatures. The manipulation of the specimens inside the oven could be made through a hole in one side which could be closed by a small asbestos block. The top of the oven was also closed with an asbestos plate which had a circular hole

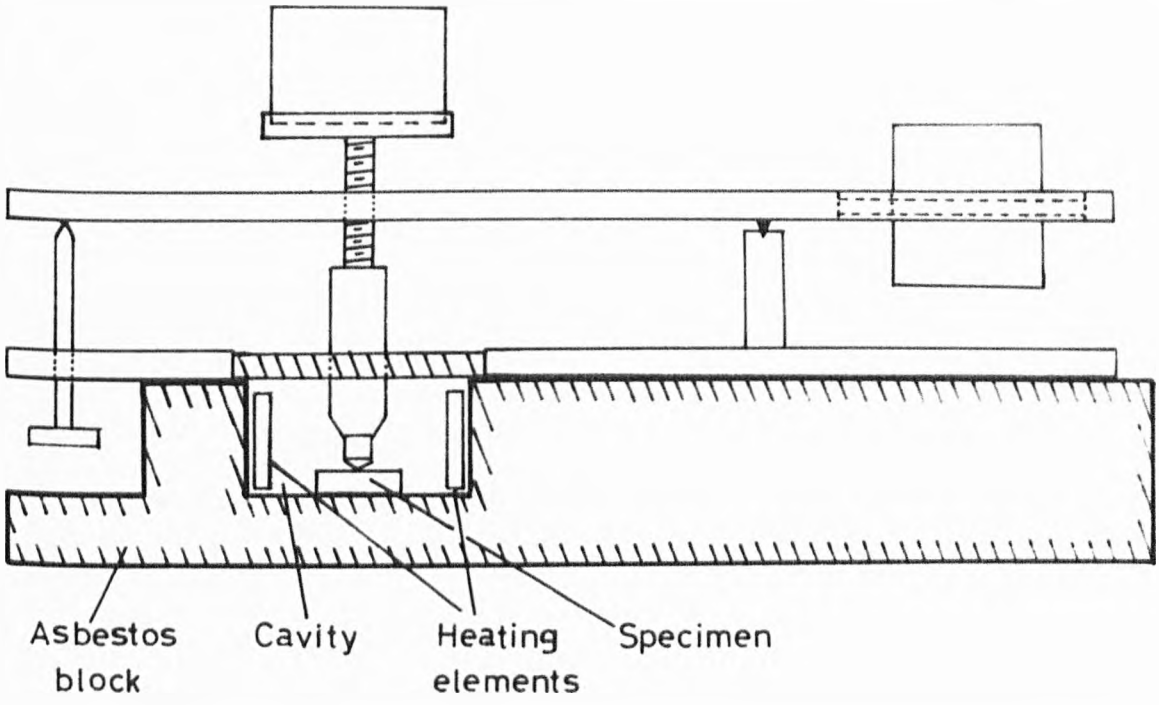

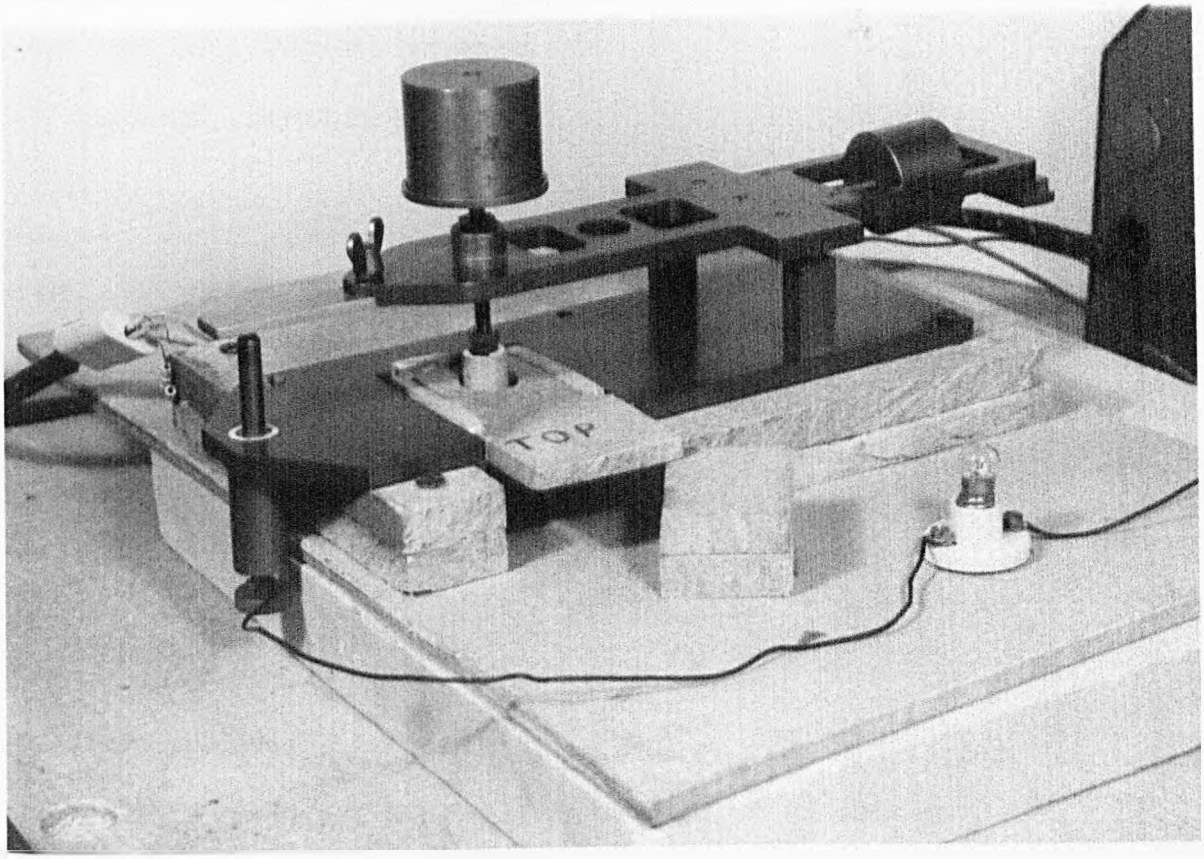

Figure 2.4. (a) Diagramatic representation and (b) photograph of the high temperature hardness tester designed by the author.

cut in the middle to allow the indenter holder to move freely up and down.

The available diamond pyramid indenters consist of a shaped diamond crystal which is fixed onto a small steel rod which in turn is tightly fitted into a cylindrical hole in the end of a shaped steel block. To reduce heat losses by conduction from the heated indenter to the other parts of the machine through the steel block the latter was replaced by a holder specially made from machinable ceramic.

Heating of the oven was achieved by two 65-Watt soldering iron heating elements. The temperature was controlled to within $\pm$ 2 K of the set temperature by a Transitrol (type 994) temperature controller (ETHER LTD). The thermocouple was placed near the position of the specimen. A second thermocouple could be inserted, through the side opening of the oven.

2.3 Materials and specimen preparation

In the main series of experiments the following materials were used:

1) Soda-lime-silica glass in two forms: a) Float glass and b) microscope slides.
2) Borosilicate glass: Pyrex (7740).
3) Aluminosilicate glass: E-glass.
4) Fused silica: Vitreosil.

The compositions and manufacturers of these glasses are shown in table 2.1. Specimens of Soda-lime-silica glass, Pyrex, and Vitreosil up to 6 mm thick were cut as blocks ~ 20 mm x 20 mm from the larger glass plates obtained from the manufactures.

E-glass was in the form of spheres, 20 mm in diameter,

Table 2.1

Nominal composition of glasses

	Float[1]	Microscope slides[2]	E-glass[1]	Pyrex[3]	Silica[4]
SiO_2	72.7	72.3	54.0	80.5	99.9
Na_2O	12.9	13.4	<0.5	3.8	TRACE QUANTITIES
K_2O	0.6	0.6	<0.5	0.4	
CaO	9.0	7.3	17.5	-	
MgO	3.1	4.3	4.5	-	
B_2O_3	-	-	8.5	12.9	
Al_2O_3	1.0	1.7	15.0	2.2	
Others	0.7	0.4	-	0.2	

(1) Pilkington Bros Ltd.
(2) Chance Propper Ltd.
(3) Corning Glass Works.
(4) Thermal Syndicate Ltd.

from which thin slabs, approximately 5 mm thick, were cut with a diamond-impregnated wheel. The slabs were subsequently polished using a metallographic polishing machine and diamond pastes up to ~1 μm grain size to obtain a mirror smooth surfaces.

In the case of soda-lime-silica glasses, specimens were annealed in an air oven at 813 K for one hour and subsequently cooled to room temperature at approximately 2 K min^{-1}.

Two types of Float glass surface were used:

a) Natural, as - received surface and

b) Fracture surface.

For the preparation of fracture surfaces the technique described by Gunasekera (1970) was adopted. In brief, blocks of Float glass 20 mm x 20 mm x 6 mm were slotted parallel to the natural surfaces with a diamond-impregnated wheel as shown in figure 2.5. By inserting a wedge inside the slot and applying a small force the glass blocks could be cleaved easily producing two triangular-shaped fracture surfaces, which were mirror smooth, although not flat and parallel to the natural surface of the specimen over the entire area. Indentations were made in different places on the fracture surfaces, but only those whose shape was close to the square were measured. This cleavage technique enabled pristine surfaces to be produced while the entire specimen was submerged in a dried liquid environment, so that atmospheric contamination of the fresh fracture surfaces was completely eliminated.

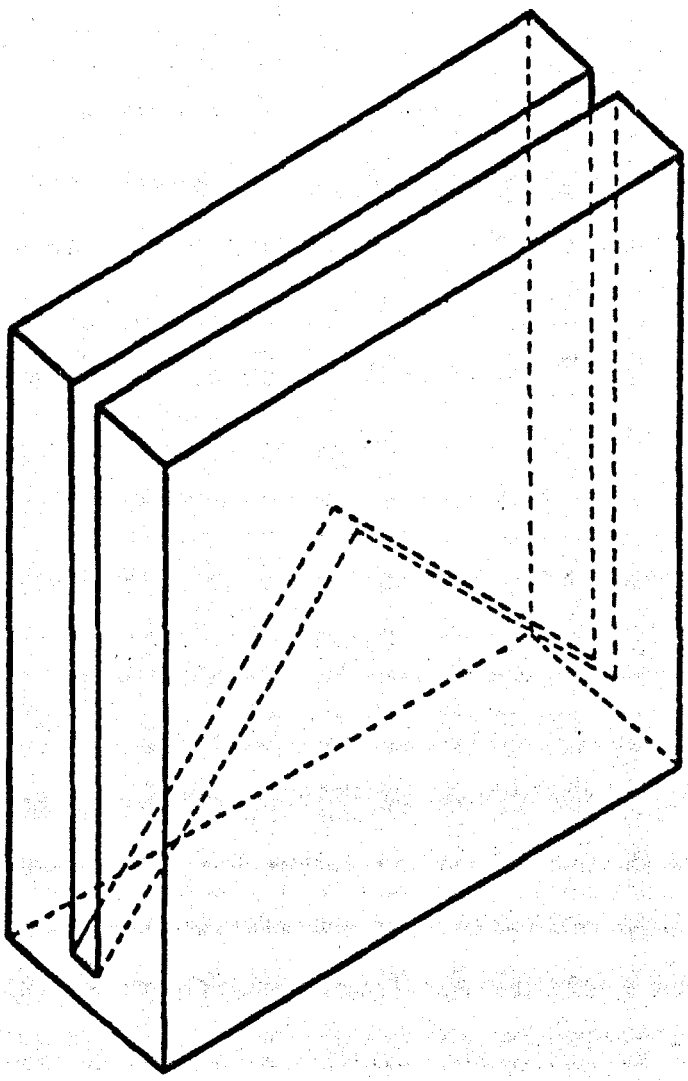

Figure 2.5 Shape of the swallow-tail cut glass blocks used to produce smooth fracture surfaces.

2.4 Experimental procedure

In all the indentation experiments described hereafter the contact of the diamond indenter with the specimen was made at a very slow rate estimated to be between 1 and 10 μms^{-1}. The loading time covered the range from 1s to 10^6s (12 days). The timing was started immediately after the contact-indicating lamp went off. For the shortest loading time, nominally 1s, the load was applied at the normal slow rate until the full load was supported by the specimen and this was followed by an immediate unloading. Obviously the loading time could not be exactly one second but because a logarithmic time scale was used, small deviations of the loading time from one second are not important.

The loads used for these experiments ranged from 1 N to 50 N. But in a large number of indentation tests the load was standardized at 2.94 N.

After completion of an indentation test, the specimen was removed from the machine and the diagonals of the indentation were measured in the Vickers projection microscope using a 60X objective lens and a 10X filar micrometer eyepiece. In reflected light large clear images of the indentations were obtained and the corners were well defined, figure 1.3. Particularly when heavy loads were used (>5 N) occasional indentations were surrounded by cracks which occured the indentation corners either by intersecting with the indentations near their corners or by reflecting light into the image, figures 1.3, 2.6. No attempt was made to measure the diagonals of such indentations.

Each of the hardness numbers presented in this thesis was calculated by using the average diagonal length of at least

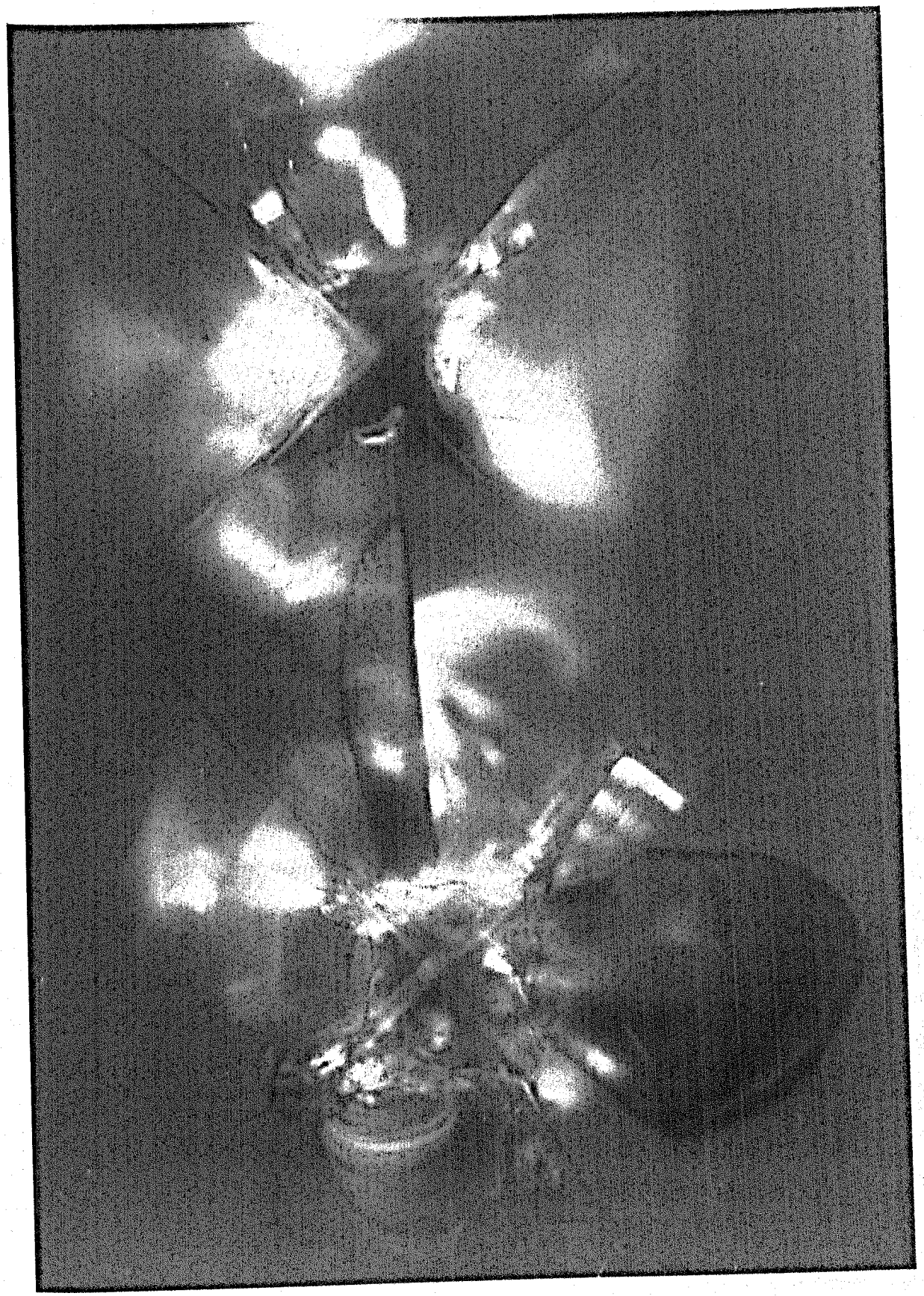

Figure 2.6. Vickers indentations in Float glass exhibiting severe cracking. (Indenter load 5N, mag. x 1340).

8 indentations carried out under the same experimental conditions.

A number of indentation tests were carried out at room temperature in different environments following strictly the procedure described by Gunasekera (1970). The hardness machine (the one constructed and used by Gunasekera himself) was fixed on the stage of the projection microscope, figure 2.3, and the indentation size was observed and measured continuously through the microscope without removing the load. Good visibility of the indentations which in fact were the area of the diamond indenter in contact with the glass surface was achieved by observing in dark field illumination. Nevertheless, because observations were made through the thickness of the specimen which in this case was 6 mm, low power objective lens (22X) had to be used for the experiments in air, and an even lower power objective lens (13X) for the experiments conducted under a liquid due to the additional thickness of the container.

The shortest loading time for these experiments was 20s and the longest 10^5s. Loads up to 5 N were used.

2.5 Experiments in different environments

Indentation tests were carried out in a variety of liquid environments. These were: liquid paraffin, siliconeoil, Dimethyl sulphoxide, alcohols, toluene, water and liquid nitrogen. All but the alcohols of the organic liquids were dried over freshly drawn sodium wire or new molecular sieve (Union Carbide, aluminium calcium silicate molecular sieve, type 5A). An amount of drying agent was always added to the test liquid during the indentation experiments. Three containers were constructed, two made of

glass plates pasted together with epoxy resin and one made from a single block of brass by milling a cavity 20 mm deep and 30 mm diameter. In the case of indentation tests under liquid nitrogen the brass container was surrounded by foam polystyrene to reduce heat losses from the container. The specimen was inserted in the liquid nitrogen and the indenter was slowly lowered until it was fully immersed in the liquid. Liquid nitrogen was supplied occasionally to the container so that the specimen and the diamond indenter were always submerged in the liquid nitrogen. The indenter was further lowered to touch the specimen only after the liquid nitrogen had stopped boiling vigorously.

A number of experiments were carried out under extremely dry conditions. Specimens were kept for several days in a jar containing molecular sieve. The jar was placed in a glove bag flushed with helium gas previously passed through a coiled pipe immersed in a liquid nitrogen trap. All the necessary equipment (hardness tester, weights, container etc.) were also placed inside the glove bag. An amount of freshly activated colour-indicating silica gel and sodium hydroxide pellets were always present inside the glove bag. For the indentation test a specimen was removed from the jar with the molecular sieve and placed in the brass container which also contained molecular sieve.

No attempt was made to measure the water content of this environment but careful experimental techniques followed thoughout these experiments ensured that this environment was the driest used in the present study.

It is worth noting that because the gas introduced into

the glove bag was already dry*, "water loading" of the molecular sieve is expected to be very small. Assuming that the water content of the molecular sieve is 2% and using data supplied by the manufacturer**, it is found that the partial pressure of water vapour at room temperature in the gas in equilibrium with the molecular sieve is $\sim 3 \times 10^{-4}$ Nm^{-2} which corresponds to 10^{-3}% relative humidity. This value however must be regarded as a theoretical one; in practice it must be expected that this value can be approached only near the molecular sieve pellets. It is worth mentioning that the drying action of the molecular sieve was seen when wet colour-indicating silica gel, which is coloured pink, placed near molecular sieve pellets its colour turned gradually into dark blue, i.e. the colour of this type of silica gel after a reactivation process.

2.6 Experiments at high temperatures

Temperatures up to 823 K were used at 50 K or 150 K intervals. Several specimens to be indented at high temperature were inserted into the oven and after some time, long enough to heat the specimen up to the set temperature, the normal indentation procedure was followed. After completion of the loading time the specimen was removed from the oven and allowed to cool down to room temperature while another specimen already heated was placed beneath the indenter ready for indentation; new specimens were then added to the oven to heat up. At 423 K and for loading times up to 20s up to three indentations were made on each specimen.

---

* In J.H.Robertson (1963), it is reported that nitrogen gas so produced contains one molecule of H_2O per cubic metre of gas.

** "Union Carbide" molecular sieves for selective adsorption. Third edition, B.D.H Laboratory chemicals division, Poole, England.

In all other cases one indentation only was made on each glass block, which was removed immediately after unloading. This procedure was followed in order to avoid keeping an indentation at high temperatures for a long time after removal of the indenter, a situation which might effect the size of the indentation as will be discussed in a later chapter.

For these experiments it was important to know the actual temperature at the site of the indentation and also whether the temperature remains constant during a long time test. For these reasons a control specimen was constructed in the following way: A small glass block was heated above its softening point in a Bunsen burner and then a thermocouple whose tip had been mechanically flattened was pressed into the soft glass surface. This glass block with the thermocouple stuck on its surface was placed inside the oven underneath the indenter and temperature reading were taken with a galvanometer while the oven was heated at different temperatures. It was found that these readings were up to 3 K lower than the temperature indicated by the Transitrol controller. When the flattened thermocouple was indented in the usual way, the temperature indicated by the galvanometer was found to reduce by approximately 10 K. This reduction in the temperature reading which was almost instantaneous was found to be independent of the actual temperature, of the indenter load and of the duration of loading. Indentations of the thermocouple were also made at room temperature but no change of the galvanometer reading could be detected so the effect observed at elevated temperatures was probably due to a temperature difference between the indenter and the specimen. In view of these observations it was thought that a more realistic indication

of the temperature can be taken by subtracting 10 K from the temperature displayed by the Transitrol controller.

CHAPTER 3

RESULTS AND PRELIMINARY DISCUSSION

3.1 Introduction

In the present chapter the results on the indentation creep behaviour of different glasses under different experimental conditions are presented.

The Vickers hardness number, H_v, was calculated using equation (1.2) but in a more convenient form:

$$H_v = \frac{1.85\ P}{d^2} \qquad (3.1)$$

where the load, P, is expressed in Newtons and the average diagonal length, d, in metres.

Most of the results are shown in the form of graphs where the hardness values, H_v, are plotted against the logarithm of loading time, t - indentation creep curves. Where practicable several indentation creep curves are plotted on the same graph so that direct comparison of the indentation creep behaviour of the same glass under different experimental conditions is possible.

In the appendix I all the experimental results are presented in a tabulated form.

Whenever it was judged that a set of experimental points

could be represented by a straight line, the line of regression of H_v on logt was computed.

Also in the present chapter, results of the indentation creep behaviour of glasses reported by previous authors are reviewed and compared with the results of the present study. As has been stated in the general introduction of this thesis very little agreement, if any, exists between the results reported by various authors.

3.2 Reproducibility of the results

On each graph an error bar is printed representing the typical magnitude of the total scatter of the results which rarely exceeded the range of ± 0.1 GNm^{-2}. This value is within the range of scatter reported by previous authors for indentation experiments.

In the course of the present study no systematic differences were observed in the results obtained from different soda-lime-silica glass surfaces or by using different hardness machines and experimental procedures. The two natural surfaces (top and bottom) of Float glass are known to be slightly different in chemical composition (e.g. Sieger, 1975)*. Early experiments in this study showed that both natural surfaces of Float glass and also natural surfaces of soda-lime-silica microscope slides have identical hardness and indentation creep behaviour over a wide range of load used.

---

* Obviously the composition differences are due to the manufacturing process, Float process, in which one side of the production ribbon is in contact with melted tin whereas the other surface is exposed to a hot reducing gas atmosphere.

Several results obtained from each machine under various experimental conditions are shown in table 3.1. Hardness values obtained by direct measurement of the indentation diagonals from below while the indenter was in contact with the specimen under load appear to be slightly lower than those obtained by measuring the diagonals after the load was removed and the specimen inverted. In the former case the dispersion of the results about the mean was found to be twice as much (± 0.2 GNm^{-2}) as the typical value. Results obtained from fracture surfaces also showed a higher (X 2) dispersion than the usual.

In any case, the differences observed in the hardness values were within the experimental error of the measurements.

Finally the variation of Vickers hardness with load in the range 1 - 50N at different loading times and environments was found to be within the experimental error observed in this study, figure 3.1.

In view of these results it does not seem necessary to report the particular hardness tester used and the applied load for each experimental point shown on the graphs which follow.

3.3 Results

Figure 3.2 shows the indentation creep curves for different glass compositions obtained in air, on natural surfaces in normal laboratory conditions (temperature ~295 K and relative humidity ~ 60%).

In figure 3.3 indentation creep data for soda-lime-silica and aluminosilicate glasses are presented, for both natural and cleaved surfaces in a variety of environments. It is noted that

Table 3.1

Comparison of Vickers hardness of Float glass obtained from different hardness machines under different experimental conditions

Design of Hardness tester	Conditions					
	20s			10^5s		
	air	water	dry	air	water	dry
Cooke Troughton and Simms Ltd.	5.35	-	-	4.65	-	-
Gunasekera's[1]	5.35	5.29	5.40	4.65	4.72	-
Gunasekera's[2]	5.25	5.22	5.33[3]	4.60	-	4.68[3]
This author's	5.35	5.26	5.45	4.70	4.75	4.80

(1) Measurement of the diagonal length was made after removing the indenter.

(2) Measurement of the diagonal length was made while the indenter was still in contact with specimen under load, figure 2.3.

(3) Results obtained from indentations in cleaved surfaces.

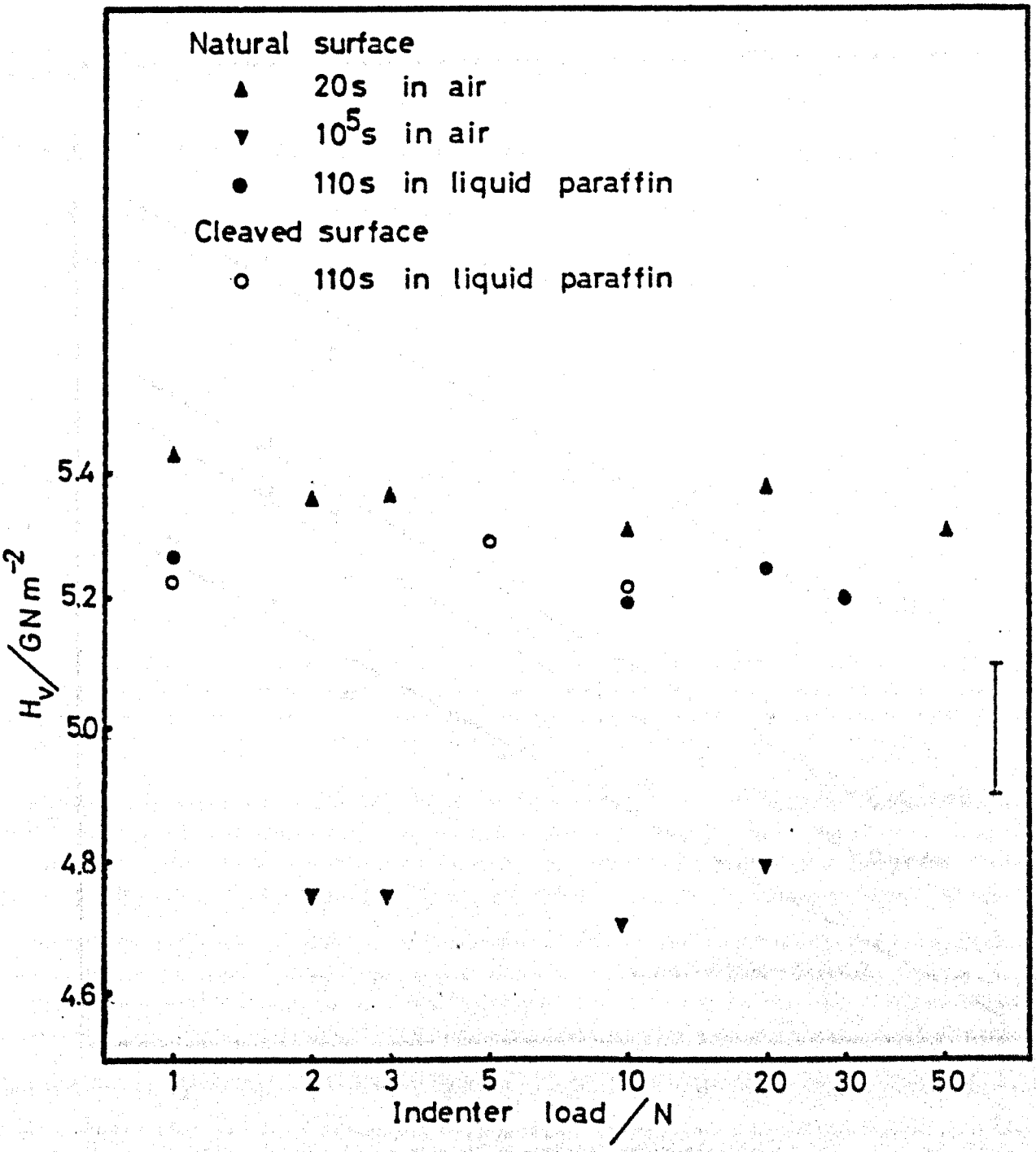

Figure 3.1 Vickers hardness versus indenter load (logarithmic scale) for Float glass. (The bar indicates typical total scatter).

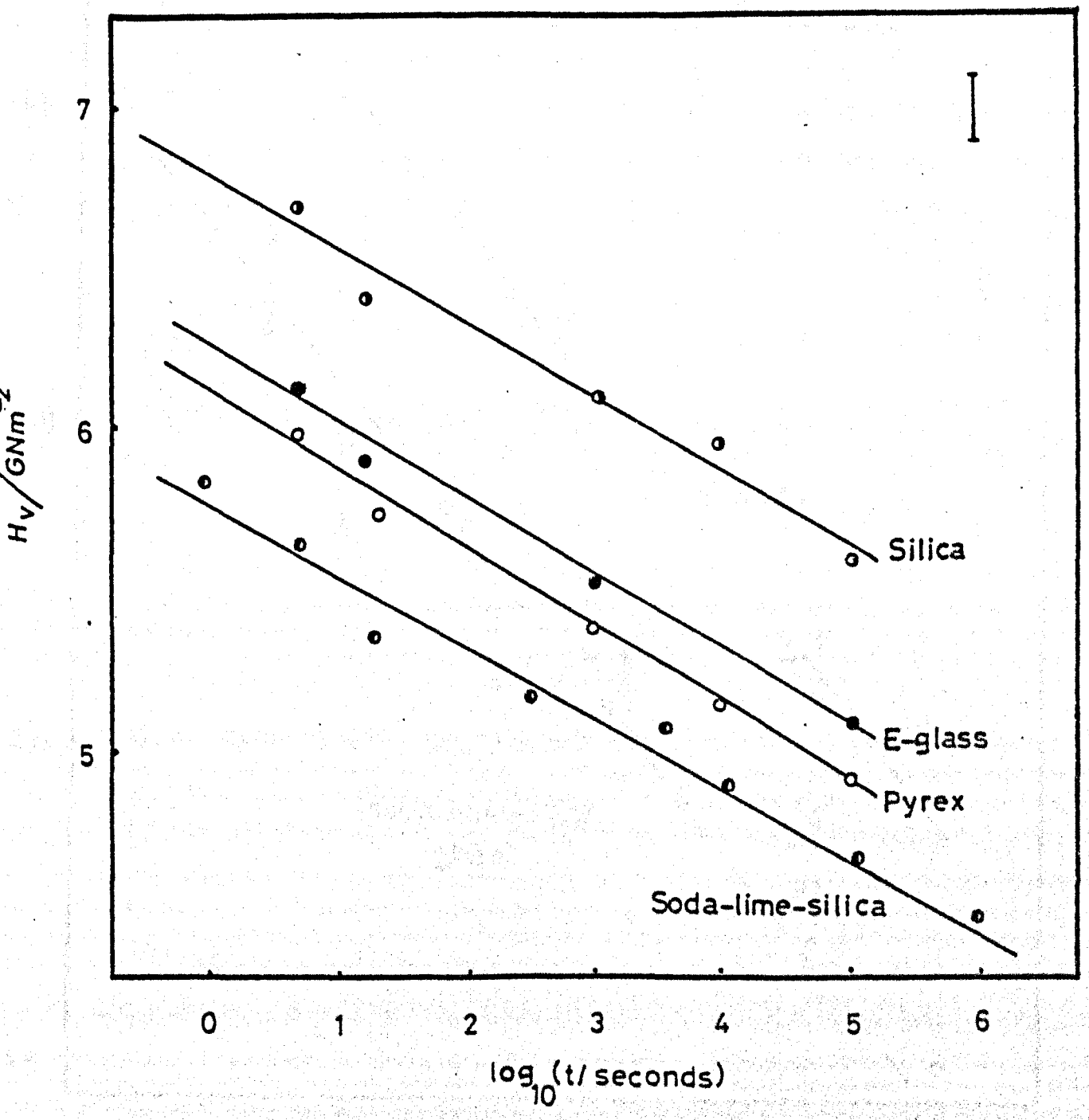

Figure 3.2 Indentation creep curves for different glasses in air at room temperature. (The bar indicates typical total scatter).

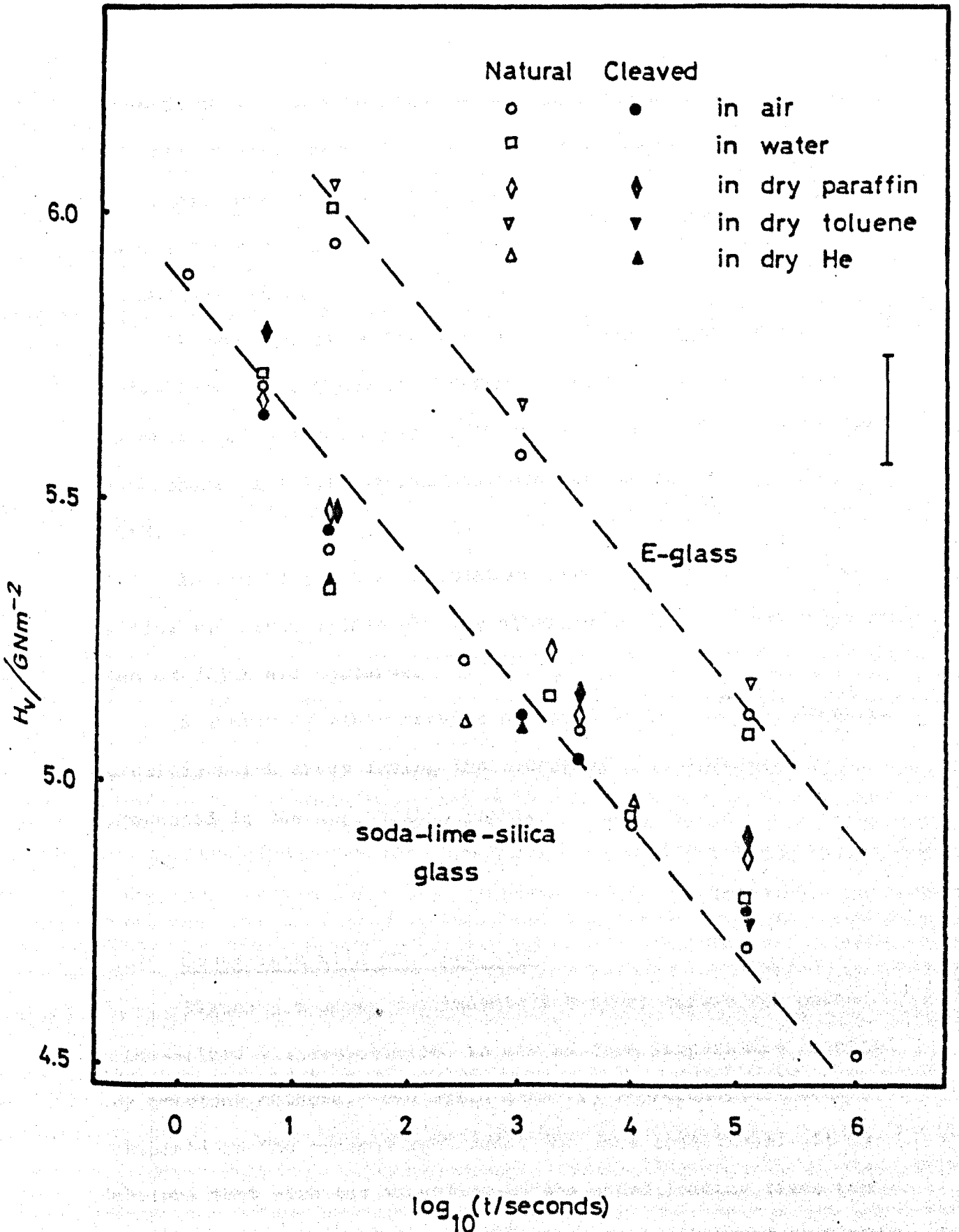

Figure 3.3 Indentation creep results obtained from natural and cleaved surfaces of Float and E-glass at room temperature. (The bar indicates typical total scatter).

several points on this graph have been obtained under the special dry conditions described in the previous chapter. The dashed lines represent the best fit lines for all the experimental points for each glass i.e. assuming that the observed differences in hardness in different environments are not significant.

Figure 3.4 shows the indentation creep behaviour for soda-lime-silica glass at different temperatures; with the exception of the top curve which was obtained in liquid nitrogen atmosphere, all the experiments were carried out in "laboratory air".

In figure 3.5 the indentation creep curves for soda-lime-silica and borosilicate glasses obtained in air at room temperature and at 773 K are compared.

A number of other results produced to investigate specific problems which arose during the course of the study will be presented in the appropriate place.

3.4 Comparison with previous work

Figure 3.6 shows the indentation creep curves for soda-lime-silica glasses obtained in air at room temperature reported by previous authors. The solid line (I) represents the results obtained in the present work under the same conditions. It is obvious that with the exception of the short loading times (up to approximately 30 s) the indentation creep behaviour observed by the different research groups is completely different. The bottom curve (V) is due to Gunasekera (1970) and extends from 0.5×10^{-3} second up to 10^{5} seconds. The short time hardness results (up to 5 seconds) were obtained with an electromagnetically

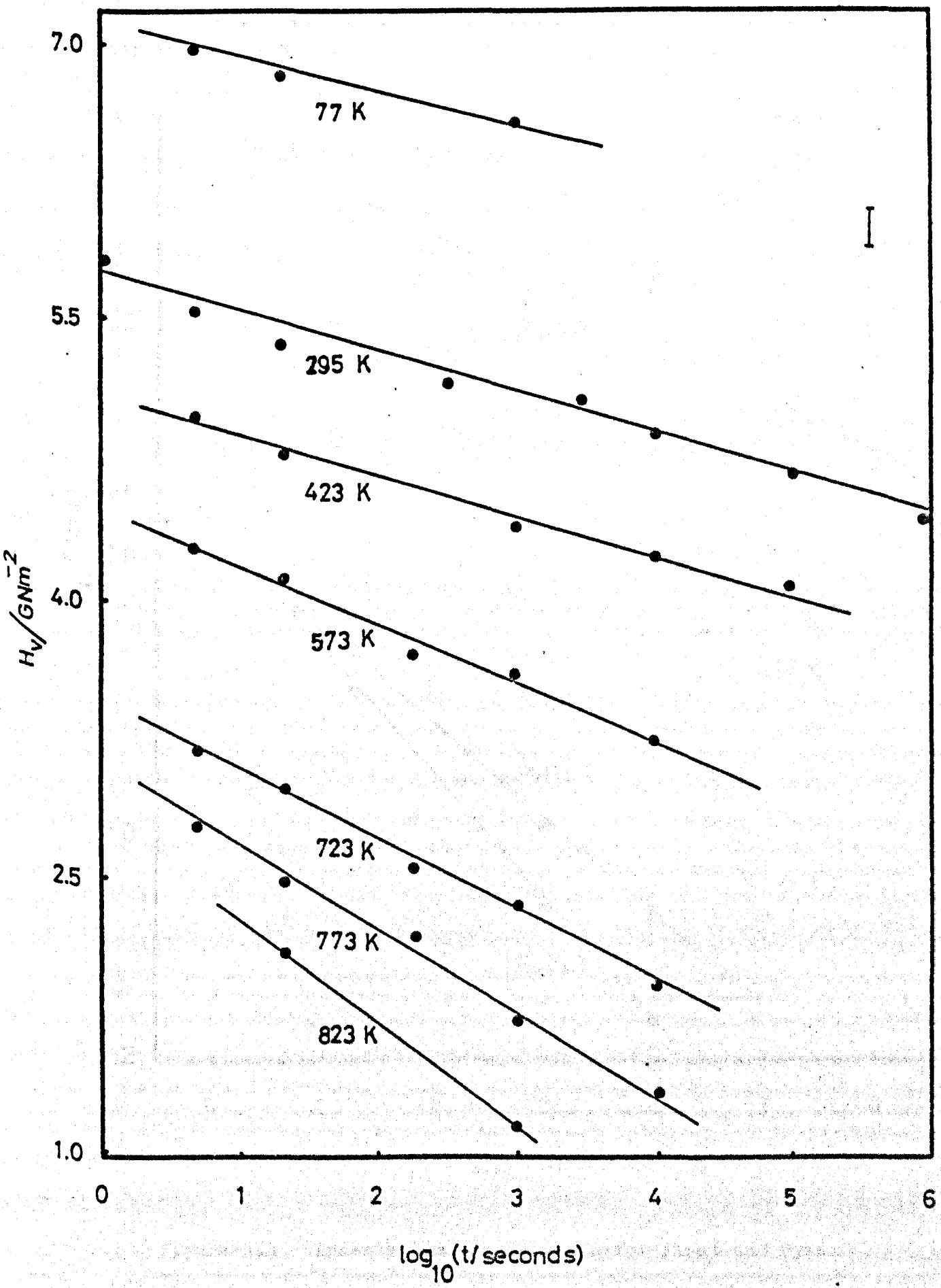

Figure 3.4 Indentation creep curves for Float glass at different temperatures. (The bar indicates typical total scatter).

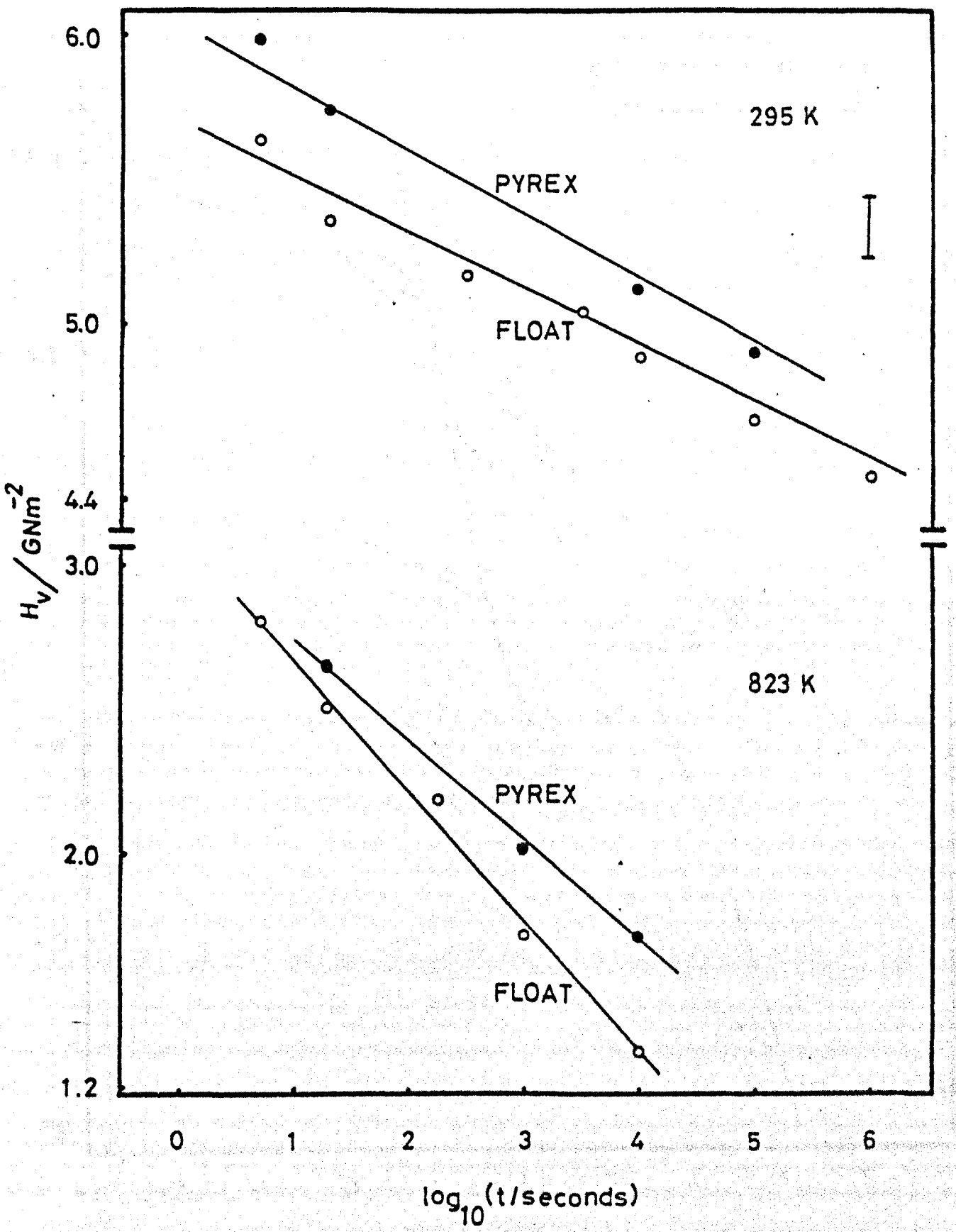

Figure 3.5 Indentation creep curves for Float and Pyrex glasses at different temperatures in air. (The bar indicates typical total scatter).

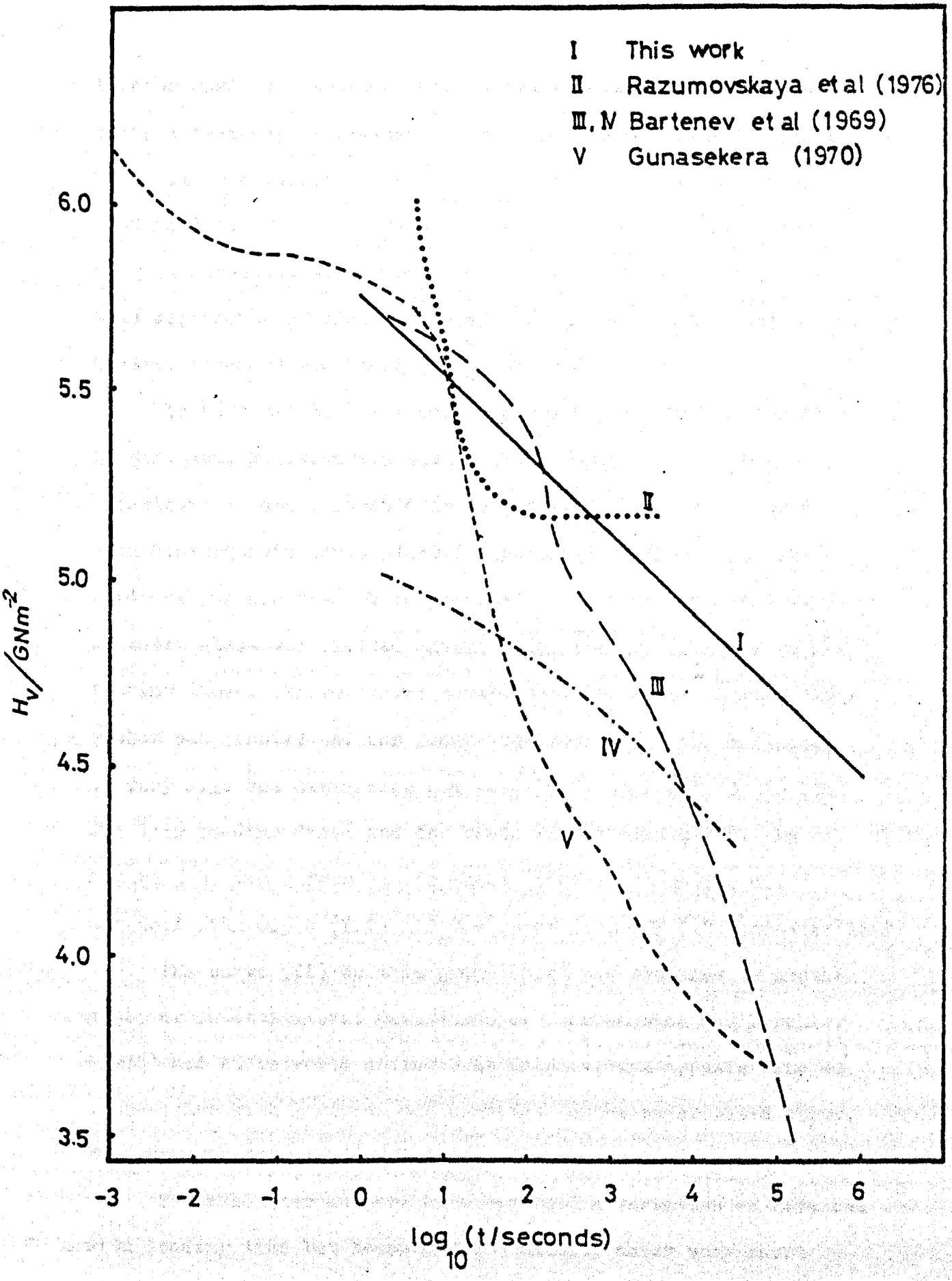

Figure 3.6 Comparison of the indentation creep curves for soda-lime-silica glass at room temperature in air.

loading hardness machine. Gunasekera's indentation creep curve shows a tendency to flatten off at times longer than 10^4 seconds. This author's results when converted to flow stresses versus loading time, following Marsh's conversion method, was found in good agreement with results published by Marsh (1964) on the time dependence of flow stress of soda glass (Marsh, 1964, however extended the loading time up to 10^3s).

In contrast to Gunasekera's results, the results reported by Bartenev, Razumovskaya and Sanditov (1969) show a different behaviour: a rather steep drop in hardness at the time range when Gunasekera's curve started showing saturation. In fact, Bartenev and his co-workers produced a graph in which the hardness of sheet glass was plotted against the indenter load for various loading times. These curves showed that for short loading times (below one minute) and for loads less than 0.5 N the hardness is very high but diminishes and becomes independent of the load for long loading times and for loads larger than 0.5 N. In figure 3.6, two curves due to these authors are shown, one obtained with 0.5 N (III) and the other with 2 N (IV) indenter load.

The curve (II) on this graph (3.6) was obtained by another group of investigators: Razumovskaya, Turchinovich and Dorzhiev (1976) and it is worth noting that Razumovskaya appears also as a co-author with Bartenev and Sanditov in the paper cited above. This case is discussed in the next chapter of the present thesis.

Several other authors have reported a variation of hardness with loading time but because these results cover very short ranges of loading time they are reported separately in table 3.2; some results from the present work are included for comparison.

Figure 3.7 shows the indentation creep behaviour of soda-

Table 3.2

Comparison of Vickers hardness values in GNm^{-2} as a function of loading time in air

Type of glass	Loading time in seconds					
	1-2	5	15-20	30	60	200
Soda-lime-silica						
(1)	5.83	5.63	5.35	-	-	5.20
(2)	-	-	5.35	-	-	-
(3)	-	-	5.33	-	-	5.12
(4)	5.97	5.44	5.44	5.44	-	-
Borosilicate crown (BK 7) (5)	6.00	-	5.56	5.38	5.38	-

(1) This work for Float glass and microscope slides.

(2),(3) Data from Pilkington Bros Ltd. for Float and Optical soda-lime-silica glass respectively.

(4) Ainsworth (1954).

(5) Komeni, Kawate and Obora (1963).

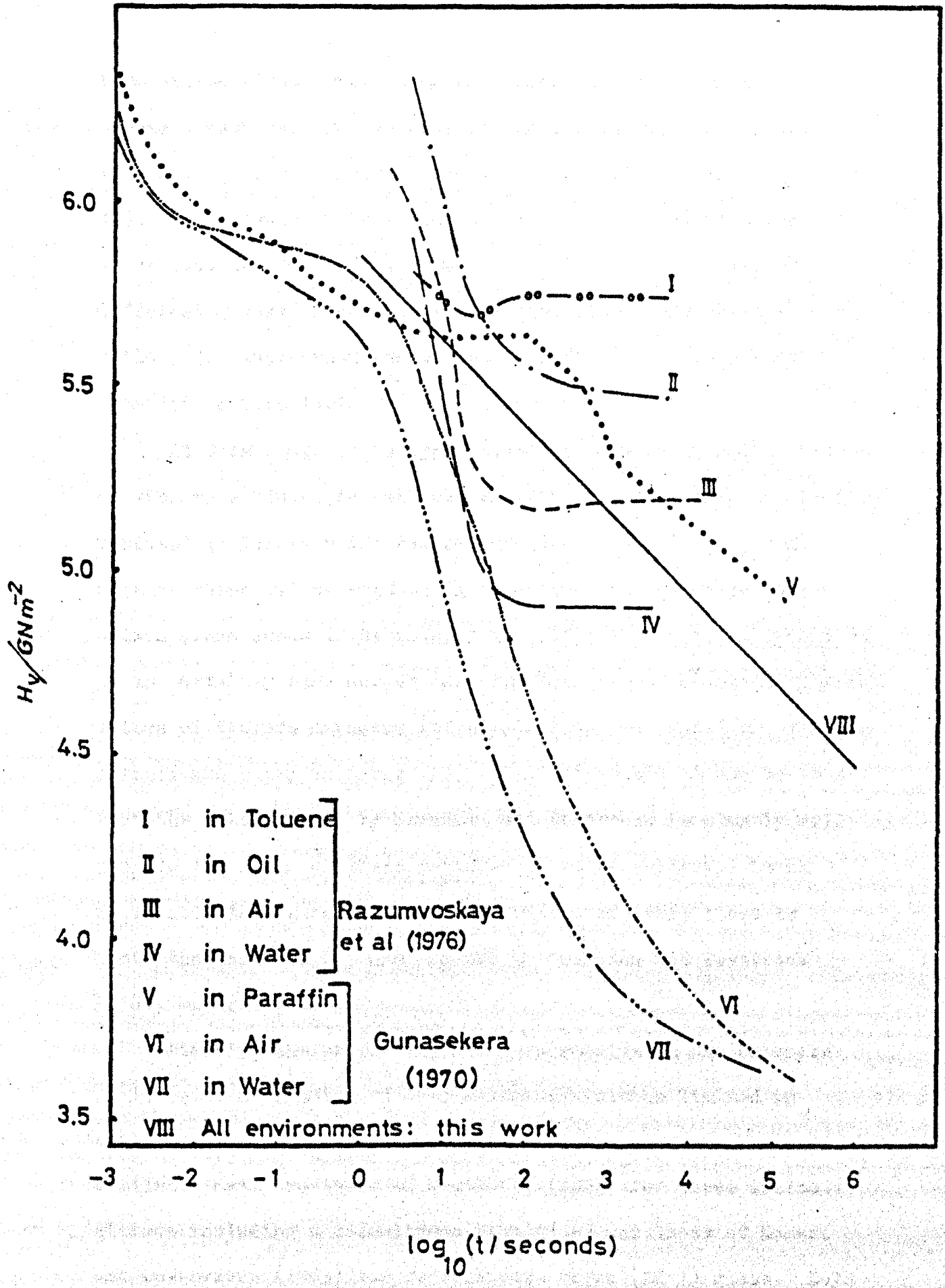

Figure 3.7 Comparison of the indentation creep curves of soda-lime-silica glass in different environments.

lime-silica glass observed under different environments by previous authors. The results of the present work are shown with a solid line which represents the results plotted in figure 3.3. It is again evident that there is widespread disagreement. Other results on the environment sensitivity of hardness of different glasses reported by previous authors are shown in table 3.3. Representative values from figure 3.7 have been inserted in this table for comparison.

At this stage it is appropriate to comment upon the values of Vickers hardness for silica glass in air and dry environment reported by Hanneman and Westbrook (1968). In the author's opinion these values must be in error for the following reason: Silica glass seems to be amongst the hardest of silicate glasses; it is certainly much harder than typical soda-lime-silica glasses. Values of Vickers hardness for silica glass as quoted by previous authors are shown in table 3.4. From this table it can be seen that the value quoted by Hanneman and Westbrook is clearly well outside the range of those reported by other authors. It is noticeable that some of the latter values are very close or above the value of 7.1 GNm^{-2} found by Hanneman and Westbrook in dry environment.

Finally, the previously reported results on the hardness of glass as a function of temperature are rather limited in number and do not include indentation creep results. The only available data are those of Westbrook (1960) for three silicate glasses including a soda-lime-silica glass and those of Komeni and co-workers (1963) for borosilicate crown (BK 7) glass. Both sets of results are difficult to compare with those of the present

Table 3.3

Comparison of the Vickers hardness (in GNm^{-2}) for several glasses under different conditions

Investigator	Type of glass	Loading time/ seconds	Conditions		
			Air	Water	Dry
This work	Float	20	5.35	5.27	5.43
"	E-glass	20	5.89	5.94	5.99
Gunasekera 1970	Float	20	5.25	4.69	5.73
Razumovskaya Turchinovich and Dorzhiev 1976	Soda-lime-silica	10	5.70	5.50	5.70(1) 6.06(2)
Komeni Kawate and Obora 1963	BK 7	30	5.38	5.29	5.49
Hanneman and Westbrook 1968	Fused silica 93.4% SiO_2	15	5.39	-	7.10
		15	4.31	-	5.53

(1) In Toluene.

(2) In Spindle oil.

Table 3.4

Comparison of the Vickers hardness for silica glass in air for loading time 15s

Investigator	Load/N	Vickers hardness/GNm^{-2}
Hanneman and Westbrook 1968	up to 2	5.39
This work	up to 3	6.37
Ainsworth 1954	up to 1	6.96
Prod'homme 1968	up to 3	6.07 - 7.35
Neely and Mackenzie 1968	up to 10	6.22 - 6.51
Lawn and Evans 1977	up to 100	6.2
Hagan 1979	unspecified	6.2

work because Westbrook carried out his experiments under continuously increasing temperature (up to 523 K) and 15 s loading time and his results showed a large scatter. For example at 373 K hardness values showed a spread of ± 0.5 GNm^{-2} ! On the other hand, Komeni's results were obtained under controlled gaseous atmosphere and for 2 s loading time.

As far as the results in liquid nitrogen are concerned, Marsh (1964) reported that the hardness of glass under liquid nitrogen is independent of loading time and that it is at least twice as high as the value at room temperature. Table 3.5 summarizes the results obtained by three authors on the hardness of glass at liquid nitrogen atmosphere (77 K). The extremely high values of hardness of soda and silica glasses observed by Marsh are probably products of the experimental techniques he adopted: He reported that for these experiments in liquid nitrogen "the apparatus was re-designed" and that a tungsten carbide pyramid was used. When the standard machine with diamond indenter was used to indent glass kept under liquid nitrogen until a thin layer of liquid nitrogen was left over the glass surface, the hardness values obtained were not significantly different from those observed at room temperature.

Table 3.5

Comparison of the Vickers hardness (in GNm^{-2}) of two glasses tested under liquid nitrogen for 15 - 20 seconds loading time.

Investigation	Soda-lime-silica glass	Silica glass
This work	6.81	-
Westbrook (1960)	6.95	6.86
Marsh* (1964)	10.78	19.40

* The type of glass used by Marsh was quoted as soda-glass and the indenter was a 136° - tungsten carbide pyramid.

CHAPTER 4

DISCUSSION

4.1 Introduction

In this chapter several ideas expressed in the past to explain the indentation process are reviewed briefly and this is followed by a consideration of several factors which might be responsible for the disagreement between the indentation creep behaviour observed by various authors. But it should not be anticipated that this sort of discussion can lead to a positive identification of the source(s) of error or confussion.

It is shown then that all the indentation creep results reported in this thesis can be described by a "universal" indentation creep curve from which several interesting points emerge. Finally the consequences of the present results on the existing quantitative model relating the flow and fracture of glass are discussed and the need for further work is underlined.

4.2 Brief survey of important ideas concerning the hardness and flow of glass

Some material related to the above heading has already been presented in the chapter one of the present thesis. The

forthcoming discussion will be concerned only with the basic principles and the implications of several ideas expressed by previous authors; details of the development of these ideas will be omitted.

The fact that indentation tests on glass surfaces produce plastic indents similar to those observed on hard metals led some authors to propose that glass undergoes plastic deformation, (Taylor, 1950; Ainsworth, 1954).

Ainsworth attempted to correlate the Vickers hardness number with the flow stress of glass by means of a conversion factor derived by simple geometrical considerations and which turned out to be equal to that observed for metals: $\frac{H_v}{Y} = 3$. Marsh (1964) pointed out that this procedure yielded values of flow stress below the maximum breaking strength of glass and proposed that the ratio H_v/Y for highly elastic materials is a function of the ratio E/Y (where E is Young's modulus). Relating the indentation process to an expansion of a hemispherical cavity under internal pressure, he derived the ratio H_v/Y for materials with different ratios of E/Y. Experimental results from a variety of materials (i.e. values of H_v and Y) verified the values of H_v/Y obtained theoretically. This procedure yielded a value for glasses of $H_v/Y \simeq 1.6$ (by interpolation in figure 1.4). This analysis provided yield stresses (from the measured values of H_v) for glass in close agreement with the observed breaking stresses for several glasses, loading times and temperatures. On the basis of his observations he proposed that time sensitive fracture phenomena in glass can be explained in terms of the time dependence of flow stress derived from indentation tests.

Surprisingly, Marsh did not consider the possible effect

of loading time and temperature on the experimental values of H_v/Y for the other materials he tested and the plastic deformation of which is readily observable, that is, it was not examined whether the graphs in figures 1.4 and 1.5 can be used for any loading time and temperature.

An alternative explanation of the observed indentations in glass has been proposed by Douglas (1958). According to this author the flow of glass under an indenter is due to cold viscous flow enhanced by the indenter pressure.

He pointed out that the pressure under the indenter at the beginning of the penetration is extremely large: the total load divided by a minute area of contact. This high pressure, in Douglas' opinion, reduces the viscosity of glass; as the indenter sinks into the glass the mean pressure reduces until it reaches a constant value at which the viscosity returns to its normal value.

From theoretical considerations of the probability of a particle crossing the energy barrier associated with neighbouring particles under the action of the external stresses, Douglas derived an approximate equation for the viscosity of glass as a function of the applied shear stress. It was shown then that the extremely high values of shear stress during the initial penetration of the indenter (i.e. when the total load is supported by a minute area of contact) can result in a substantial reduction of the viscosity of glass. Whereas, when the value of shear stress is relatively low, (~ 5 GNm^{-2}), i.e. when the penetration ceases, the viscosity, n, of the glass returns to its normal value, n_o. Thus Douglas claimed to have demonstrated that the formation of indentations in glass is due to cold viscous

flow: the value of shear stress at which $n = n_o$ (~ 5 GNm^{-2}) is of the same order of magnitude as that observed experimentally in hardness tests.

However the indentation creep of glass observed by various authors does not seem to be readily explicable in terms of Douglas' approach from which it is rather implied that indentation creep must not happen at long loading times above 5 or 10s (i.e. after "completion" of the penetration) because the value of the shear stress has already reached a level at which $n = n_o$ and therefore is not capable of affecting further the viscosity of the glass as the loading time increases. But, most importantly, the viscous deformation as envisaged by Douglas can not account for the temperature dependence of H_v observed in the present work. The change of viscosity , n, over the (high) temperature range used in this work for indentation tests (573 - 823 K) is at least 5 orders of magnitude, whereas the hardness, H_v, changes by approximately a factor of 2 over the same temperature range. Moreover it is found that the present data do not fit an Arrhenius-type relationship ($\ln H_v$ versus $\frac{1}{T}$), an essential feature of the relation between lnn and 1/T. Douglas' idea however that the high level of shear stress at the beginning of the penetration is responsible for the formation of permanent indentations remains a plausible one.

That glass undergoes densification under an indenter has been the subject of debate for some years now. According to Hillig (1963), Ernsberger (1968), Neely and Mackenzie (1968), and Peter (1970) the refractive index of glass beneath a diamond pyramid indentation is higher than the normal refractive index of the glass. This feature was often observed in fused silica

glass but according to Ernsberger (1968) when indentations were carried out in Pyrex and in soda-lime-silica glass "the results are qualitatively the same". The essential characteristic of densification is that volume decreases under the indenter. It has been reported that the "disappeared" volume is recovered partially upon annealing the indentations at temperatures below the transition range of the glass (Hillig, 1963; Bartenev, Razumovskaya and Sanditov, 1968).

Densification of glass under high compressive stresses was known, mainly, from the work of Bridgman and Simon (1953) and Cohen and Roy (1961). In general, it was found that in inorganic oxide glasses the relative increase in density is smaller, the higher the proportion of network modifiers in the glass. Density increases up to 15% have been reported. Densification was found to occur however above a "critical" value of pressure. Sakka and Mackenzie (1969) reviewing the effects of high pressure on glass reported that different investigators observed different threshold values of the pressure for densification. They speculated that this variation could be due to the shear stresses present during compression tests arising from the pressure transmitting system and which enhance densification (and therefore reduce the threshold value of pressure for densification). The observed threshold values of pressure for densification were between 2 and 10 GNm^{-2}. It can be seen that these values are of the same order of magnitude as the flow stress obtained from the previously mentioned approaches (plastic flow and cold viscous flow). The possible effect of loading time upon the threshold value of pressure for densification in high pressure apparatus has not been studied (to the author's knowledge) so

that the possibility that the indentation creep observed in practice is due to a time-dependent "flow stress" for densification cannot be examined.

Yamane and Mackenzie have derived an equation for the calculation of Vickers hardness of a glass from its chemical composition. The derivation of the equation was based on certain considerations of the nature of deformation under the indenter, which finally resulted in expressing Vickers hardness number in terms of the "average single bond strength", a, Young's modulus, E, and the ionic volume fraction V of the glass:

$$H_v = 0.051\left(\frac{a}{0.462 + 0.09V - V^2}\right)^{1/2} E$$

Using this equation they calculated the Vickers hardness numbers for 47 different glasses which included complex silicate as well as non-silicate inorganic glasses. The values obtained were in excellent agreement with published values for H_v in the literature. (The latter values were obtained apparently at 15-20 seconds loading time). However, despite the fact that the agreement of the predicted and the experimental values of H_v was remarkable, the equation does not seem to account for indentation creep phenomena. This would have been possible only if the ionic volume fraction V, or/and the average bond strength or/and Young's modulus were functions of time. To the author's knowledge there exists no evidence suggesting the time sensitivity of these quantities for oxide glasses at room temperature.

Finally, Imaoka and Yasui (1976) have applied the finite element method for the analysis of the Vickers indentation in elastic-plastic materials and particularly in glass. These

authors were able to calculate the relationship between hardness H_v and flow stress Y for materials with different ratios of E/Y. In their calculation the criterion for yield was that of von-Mises but no assumption for the stress distribution beneath the indenter was necessary. When the results obtained were plotted in the form adopted by Marsh (1964), figure 1.4, and also by Hirst and Howse (1968), reasonable agreement was found with the experimental results of these authors. However the shapes of Vickers indenation in glass obtained from the finite element analysis were not in agreement with the shapes observed in practice.

Refering to previous reports that glass can undergo densification under the action of high hydrostatic pressure, Imaoka and Yasui argued that the yield criterion applied to glass must take into account the hydrostatic component of the applied stress. For this reason they repeated the calculation using the Mohr-Coulomb yield criterion which includes a term accounting for the hydrostatic stress components. Several other factors such as "the densification factor", "the stress hardening rate" and "the piling-up factor" were considered in their calculation. They claimed that the new calculation provided indentation shapes in agreement with those observed in practice, whereas the quantitative agreement between their predictions and the results of Marsh (1964) and Hirst and Howse (1968) was not affected at all. The contribution of densification to total deformation for silicate glasses was estimated to be up to 45%.

The significance of the findings of Imaok and Yasui's study cannot be fully appreciated at the present time, but it was indicated strongly that hardness is not related simply to the yield stress but is a more complex function of the mechanical properties of the material.

From the foregoing discussion it is obvious that the various theories proposed to explain the nature of deformation of glass have been based on empirical observations or on oversimplified mathematical treatments. Most of the evidence on which the interpretation of the deformation mode is based is rather ambiguous. For example the results of experiments conducted by Bridgman and Simon (1953) in high pressure apparatus have been taken by Marsh (1964) as evidence of plastic flow of glass whereas Ernsberger (1968) and others regarded the same results as strong evidence of densification. Moreover none of the proposed ideas seem to predict indentation creep which has been observed by almost all the investigators in the field. In view of this deficiency it does not appear profitable to discuss whether the ideas expressed for the deformation of glass can be applied to macroscopic fracture phenomena (crack propagation and static fatigue) even in a qualitative or speculative sense.

Unfortunately it is very rarely acknowledged in the literature that there is lack of fundamental understanding of the deformation process in silicate glasses. Some authors did not hesitate to invoke the concept of dislocations in these materials (Levengood and Vong, 1960; Levengood, 1966; Gilman, 1975). Levengood in particular claimed to have seen dislocations in silicate glass*.

It should be recognized that the mode(s) of deformation of glass during indentation is very complicated even for the simplest of silicate glasses, the fused silica glass. The kind of deformation that may predominate is probably dictated by the

* Tichane and Wilson (1964), also have reported seeing features reminiscent of dislocations, but they argued that the patterns observed were artifacts associated with the technique used (chemical etching).

atomic bonding in the glass but major differences would not be expected between the deformation mode(s) in silica and in other silicate glasses with high SiO_2 content; however this expectation is not in accord with claims made recently in the literature.

On the other hand the present work has shown that the indentation creep behaviour (the variation of H_v with logt) of four different silicate glasses is approximately the same, figure 3.2. Whether this can be regarded as evidence that all the examined glasses undergo the same type of deformation is subject to debate.

4.3 Discussion of the indentation creep of glass reported by different investigators

The severity of the discrepancies between the results of different investigators on the indentation creep behaviour of glass is evident from figures 3.6 and 3.7. Attention is drawn particularly to the discrepancy existing between the results of the present study and those obtained by Gunasekera (1970) working in this same laboratory. In summary, the present work has shown that the Vickers hardness of several glasses, including Float glass, decreases linearly with log(loading time) and that the rate of decrease is independent of the test environment. This behaviour is in direct conflict with the results of Gunasekera who found that the rate of decrease of H_v with logt in Float glass is strongly dependent upon the test environment. Specifically he found that in moist environments the rate of decrease of H_v with logt is significantly greater than in a water-free environment. On the

basis of his results Gunasekera argued that stress-enhanced diffusion of water under the indenter resulting in softening of the subsurface layers is probably responsible for this effect.

It is interesting to note on figure 3.7 that the environment independent indentation creep behaviour of soda-lime-silica glass observed in the present study corresponds closely to that observed by Gunasekera in dry environment. This fact can be explained, at least in principle, if it is assumed that the samples used in the present study somehow inhibited the glass softening process from taking place. For example, if a layer of modified glass existed on the surface of the glass used which inhibited or perhaps delayed the diffusion of water into the glass, the surface of the glass under test would respond to the indentation process as if the surrounding medium was water-free. Layers of modified glass on soda-lime-silica glass surfaces have been detected after a long-time aging in moist environmets, heat treatment at high temperatures, special treatments with chemical substances etc*. Frozen thermal stresses may also exist in these glasses. But there is no a priori reason to believe that any of the above mentioned features would inhibit the stress-diffusion of water.

The results of special experiments carried out in the present study eliminated the possibility that any of these features were responsible for the effect (or rather lack of effect) observed. These experiments included indentation tests in two different soda-lime-silica glasses (Float glass and microscope slides) which have vertually the same chemical composition but are manufactured by different processes. "Old"

---

* The properties of glass surfaces in this context are review by Holland,1965; Ergsberger, 1972; Doremus, 1973.

and "new" specimens from these glasses were tested "as found" or after annealing. Also, fracture surfaces of Float glass were produced and tested in air and under extremely dry conditions. For the main series of experiments three hardness testing machines were used and three different main experimental procedures. (One of these machines was used in two different procedures).

These experiments were carried out over a period of one year but after an interval of a further year most of the experiments were repeated following the same and whenever possible modified experimental procedures. In all cases the reproducibility of the results was excellent; the total scatter of the results from tests carried out for a fixed loading time but under different experimental conditions, machines, loads, environments, never exceeded $\pm 4\%$ and was usually $\pm 2\%$.

The present author gained additional confidence in his own results when he was able to reproduce indentation creep results for PMMA in air reported by McQuillin (1974) from this laboratory.

Particular attention is drawn to the following fact: Gunasekera (1970) carried out his experiments on 6 mm thick Float glass; these specimens had been preserved in a laboratory drawer since then. These specimens were retested by the present author on both natural surfaces and also on freshly produced fracture surfaces following the experimental procedure and using the same instruments, lenses etc, specified by Gunasekera. In all cases the results were identical to those found in the course of the present study; the more rapid indentation creep reported by Gunasekera to occur in moist environments could not be reproduced.

It is also appropriate to mention here another remarkable case in which seriously inconsistent indentation creep results were reported from the same laboratory (V.I Lenin Moscow Pedagogical Institute) by two research groups* with I.V.Razumovskaya being a co-author in both studies. These two studies were performed apparently on the same soda-lime-silica glass (although the exact composition was not given in either paper), and with the same load, 0.5 N, and with identical hardness testers, (PMT-3). (Figure 3.6 curves II and III).

It is possible however that some of the glasses used by earlier authors had a "defective" surface, that is, surface layers of modified glass with different hardness from the bulk glass. Holland (1964) for instance has reported that "a soda-lime microscope slide some 10 years old had a surface film of 600 Å (0.06 μm) thick with about a quarter of the hardness of the substrate glass". The question is not however whether a surface layer has a different hardness than the bulk glass but whether it has different indentation creep behaviour and most importantly whether its thickness is comparable with the depth of the indentations. The depth of Vickers indentations in a glass with a typical hardness number of 5.5 GNm^{-2} produced with loads of 0.5 N and 5 N are 1.8 μm and 5.9 μm respectively. It is therefore rather unlikely that such layers (if any) could have played a decisive role in the indentation process.

If the effect of glass properties is to be considered unlikely as a possible source of the discrepancy between the results of the various authors, then some other effect must be responsible. In the forthcoming discussion the possibility that

* G.M.Bartenev, I.V.Razumovskaya and D.S.Sanditov (1969). I.V.Razumovskaya, L.M.Turchinovich and D.B.Dorzhiev (1976).

operational errors, vibration and other effects can influence the indentation process is examined. This discussion includes an account of curious observations reported by earlier authors in connection with the indentation process in general.

4.4 Discussion of possible sources of error.

a) Operational error.

There is a number of factors that may, in principle, influence the results from indentation tests. These are the quality and the geometry of the indenter, the position of the weight above the indenter which determines the value of the load applied to the indenter, the quality of the image of the indentations and the calibration of the optical system used for measuring the indentation diagonals.

But it can be readily appreciated that such factors can result only in systematic errors (i.e. the indentation creep curve will be shifted parallel to the H_v axis) or in an increase in the total scatter of the results for each experimental point. The slope or the shape of the indentation creep curve cannot be affected. As can be seen in figure 3.6 the discrepancy between the indentation creep curves of different investigators is in the shape of the curves.

b) Vibration effects.

It is possible that vibrations produced by various appliances in research laboratories or in the surrounding environment may affect especially the indentation creep process. Such vibrations would most likely be of randomly varying frequency and amplitude (i.e. noise) and would affect the magnitude of the applied load

but also would result in local (frictional) heating of the material in contact with the vibrating indenter. It seems most likely that this would result in decreasing the hardness, and the longer the loading time under these conditions the larger would be the effect on the hardness. In fact several indentations produced after long loading times ($\sim$ 3 days) were found to be surrounded by a large number of cracks which obscured the corners of the indentations. This phenomenon might be due to instantaneous shocks produced by a pass of a heavy vehicle or to a door slam. An attempt deliberately to produce shocks to the hardness tester resulted in the same phenomena: severe cracking around the indentation.

Vibrations have been thought in the past to cause significant reduction in the hardness number. Tabor (1954) reported that vibrations produced by the illuminating system of the hardness tester affected the hardness of a fully annealed single crystal of aluminium. He used a Cooke, Toughton and Simms hardness tester fitted to a Vickers projection microscope (a system identical to that used in the present study) which carried a mercury vapour lamp and a carbon arc. When indentations were carried out with both illuminating sources switched off the value of hardness was found to be $\sim$ 0.2 GNm^{-2}. However values as low as 0.04 GNm^{-2} and 0.1 GNm^{-2} were obtained when the carbon arc and the vapour lamp respectively were switched on. Although Tabor suspected that the illumination system caused vibrations which resulted in reducing the hardness of aluminium, there exists a large literature on the effect of light, both visible and infrared, on the hardness of a wide range of materials including semiconductors (Ge, Si, InSb, GaAs, GaP, PbS), semimetals (Bi, Sb),

ionic crystals (NaCl, LiF, KCl) and Ti. For most of these materials, an electric potential applied between the specimen and the indenter was also found to effect the hardness number. (These phenomena have been referred to as photomechanical and electromechanical effects respectively; see for example Leighly and Oglesbee, 1973; Varchenya, Upit and Manika, 1973). Specifically it has been reported that light or electric field (or both) decrease the hardness number of the materials and that for certain values of the intensity of light or electric field the hardness number reaches saturation. The final reduction in hardness can be by 20% of the "dark value".. The combined effect of loading time and light (or electric field) has not been studied yet. Presumably, the possibility that the source of light or of the electric field might have produced vibrations so that the observed reductions in hardness were due to the vibration of the indenter and not to the light or potential cannot be ruled out. Alternatively, local heating produced by illuminating the surface with intense light could cause reduction in hardness.

In this study the effect of visible light on the indentation creep in glass was investigated by illuminating the indentation site with incident light from the illuminating system of the Vickers projection microscope (tungsten-halogen lamp) during the loading time. Several indentations were made while the lamp was operated at its maximum output. The experiment was repeated with the light off. In both cases the results obtained were identical to those found in the course of the present study under (usually) moderate illuminating conditions.

The rate of loading can also be discussed as a possible source of the discrepancy observed. Most of the investigators

involved with the hardness testing on glass reported that slow rates of loading up to 20 μms^{-1} were used. Ainsworth (1954) and Brearley (Gunasekera, 1970) reported that high rates of loading result in larger indentations and hence lower hardness numbers. No effect of rapid loading on long time indentation hardness is reported. In any case it must be expected that indentations produced by rapid loading would not show creep phenomena because the load is applied to a larger area than that which would have been produced after a long loading time at normal (slow) loading rates.

In connection with the environment dependence of the hardness of glass the following curious phenomena reported by earlier authors are worth mentioning.

Westbrook and his co-workers (e.g. Westbrook and Jorgensen, 1965; Hanneman and Westbrook, 1968) investigated the influence of the test environment ("wet" and "dry") on the indentation creep of some non-metallic materials. In their experiments, dry surfaces were prepared by heat-treating the samples at 573 K in a dry argon atmosphere and subsequently quenching in water-free toluene. For the materials treated in this way, the hardness was found to be independent of the loading time whereas samples tested in air, showed indentation creep. Some of their results are shown in figure 4.1. For Al_2O_3 in particular they showed that by increasing the penetration above 1 μm (by increasing the indenter load) the environment effect on the hardness disappears. They also reported that when mixtures of DMSO and toluene were used as test environments, the hardness of LiF for a given loading time was higher than that observed in "water-free" toluene.

In view of their observations Westbrook and his co-workers

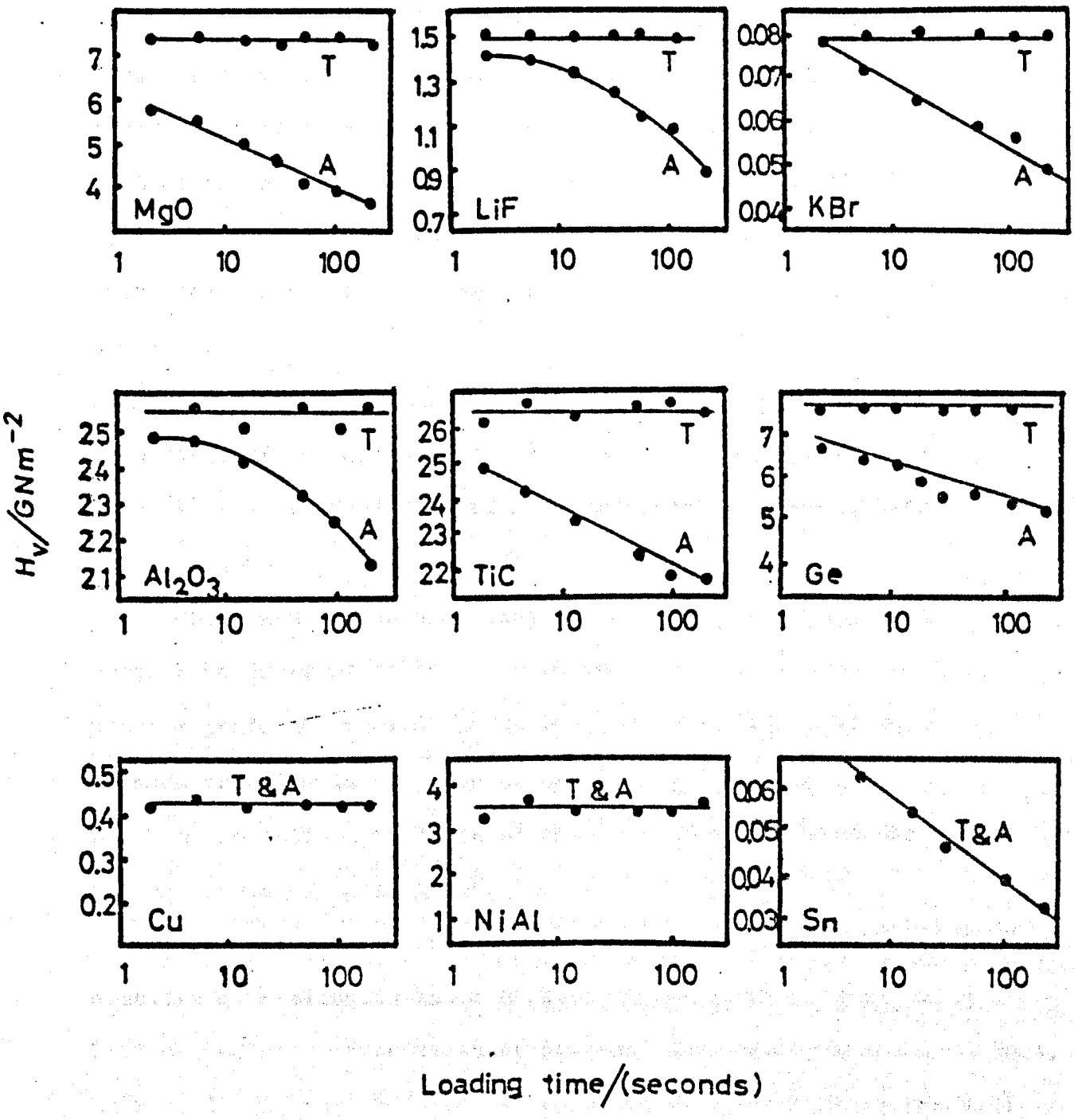

Figure 4.1 Time dependence of hardness H_v of various solids in air A, and under toluene, T. After Westbrook and Jorgersen (1965).

proposed that most of those phenomena can be explained on the basis of lubrication-friction effects induced by adsorption. Bowden and Tabor (1964) (and others) have shown that the coefficient of friction can be altered appreciably by adsorption, so that the slow decrease in hardness with time observed by Westbrook in air could be due to the time taken for water molecules or OH^- ions to reach and lubricate the newly formed surfaces.

Other curious phenomena related to the environment dependence of the hardness of glass and other materials have been reported by Westwood and his associates (Westwood, Parr and Latanision, 1972; Westwood and MacMillan, 1973).

These authors used an unorthodox method to measure the surface hardness of solids: the pendulum sclerometer method in which a pendulum pivoted on the test material with a Vickers diamond indenter is set into oscillation and the pendulum hardness is defined in terms of the logarithmic attenuation in the amplitude of oscillation.

The environments used by these authors were water, toluene, a series of n-alcohols and a series of n-alkanes. The pendulum hardness of glass fracture surfaces produced under these environments as reported by Westwood and his colleagues is shown in figure 4.2b. A sharp increase in the pendulum hardness was observed in both the alcohols and the hydrocarbons for chain length $n = 7$ whilst in water and in toluene the pendulum hardness was similar to that for alcohols with $n < 4$. This latter observation was particularly emphasized by Westwood and his co-workers who claimed to have demonstrated that the water content measured in the environments used could not account for the variation of hardness observed

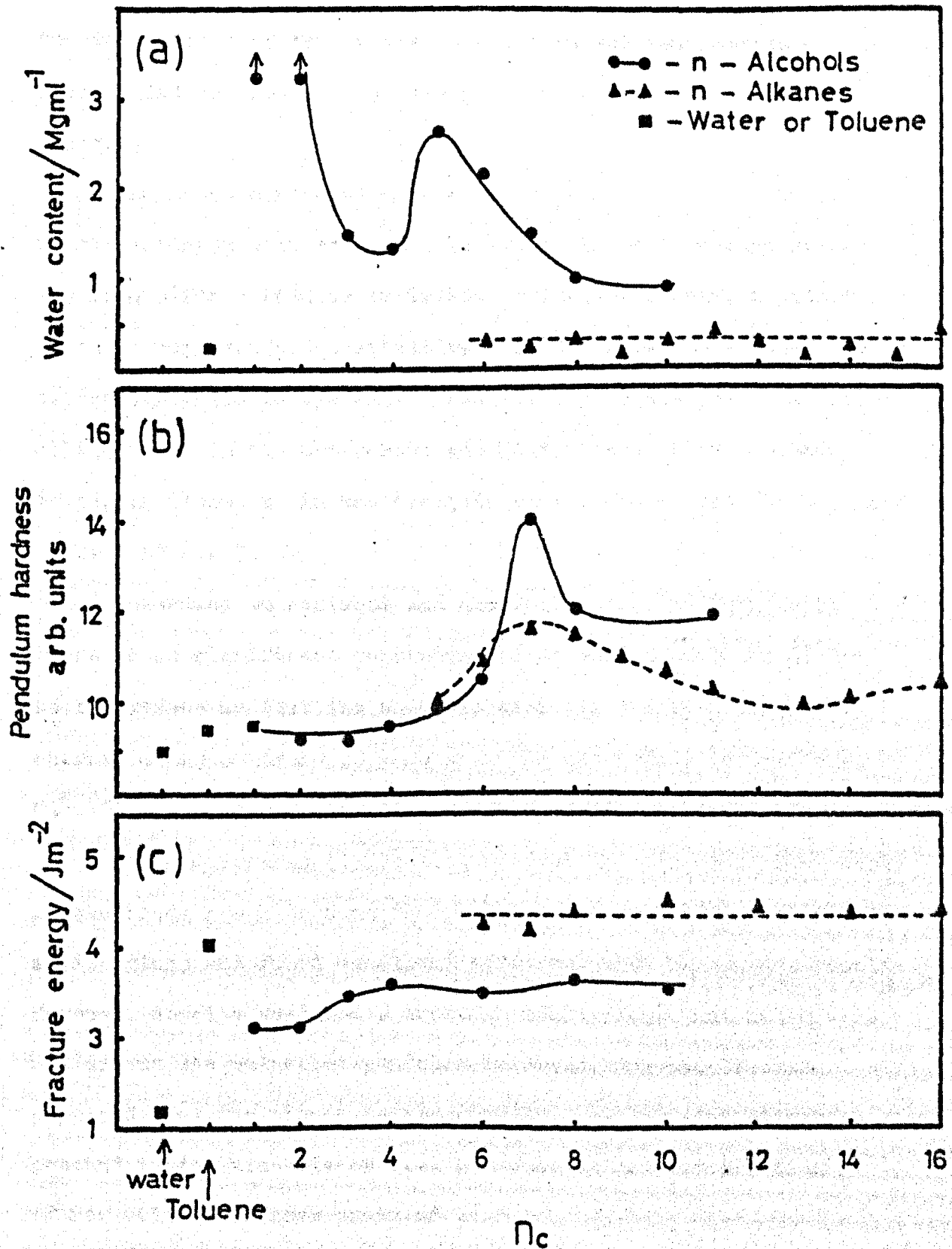

Figure 4.2 Variation with environmental composition of

a) water content of test environment

b) Pendulum hardness of soda-lime-silica glass

c) Fracture energy of soda-lime-silica glass determined by the double-cantilever technique. After Westwood et al (1972).

under these liquids, figure 4.2a. It was also shown that the fracture energy of this glass measured in the same series of liquids did not follow the same pattern as the pendulum hardness, figure 4.2c.

The above mentioned authors proposed that the variation of the hardness with the chain length could be connected with the adsorption - induced variation of surface charge, a phenomenon which is represented quantitatively by the zeta (ζ) - potential of the solid-liquid system*. When the ζ-potential of soda-lime-silica glass in the n-alcohols was plotted against the number of carbon atoms, n, in the alcohols it was shown that the ζ-potential is zero at n = 7.

According to Westwood and his colleagues, at ζ-potential = 0 there is no significant concentration of surface charges at the solid surface so that the material exhibits the bulk hardness, whereas at $J > 0$ or $J < 0$ ions from the subsurface layers (e.g. Na^+, OH^-) concentrate near the surface causing a local softening.

Fox and Freeman (1979) also studied the effect of n-alcohols in the range n = 5 to 8 on the pendulum hardness of soda-lime-silica glass and found excellent agreement with Westwood's results. However, despite Westwood's emphatic declaration that water does not affect the values of pendulum hardness, Fox and Freeman proposed that the phenomena observed are due to water either present in the alcohols or "... produced by catalytic action of new silica surfaces produced ..."

In the present study the effect of n-alcohols with n = 5 to 8 on the Vickers hardness of Float glass was investigated. The results showed that the Vickers hardness of Float glass

* The ζ-potential describes the electric field associated with the charge carriers in the near-surface regions of the solid and is influenced by the presence of liquids.

is unaffected by these environments.

In the preceding discussion, no attempt has been made to cover all the aspects of hardness testing in which curious and conflicting experimental evidence has been reported by earlier authors, but in view of what has been presented so far it must be obvious that the identification of factors which led to the production of the conflicting results is almost impossible. The only speculative conclusion that one can be led to, is that several complex factors present during the indentation tests (including material preparation and measuring procedures) under specific conditions were not suspected or their influence was not thought to be critical for these tests and therefore were not reported.

It must be made clear at this point that the present author is unable to identify or even to speculate further on the nature of these "complex factors" which led to the production of such conflicting results.

However, the question of which results represent the indentation creep behaviour of glass remains to be answered. It may be argued that in view of the serious descrepancies existing between the results published by the various authors, none of the existing results are reliable. Nonetheless the extensive experimental evidence obtained in the present study can justify the author's claim that the results reported herein represent the real behaviour of the materials tested. But before this is unambiguously established further work by independent investigators is clearly needed.

4.5 Discussion of the present results

In this section it will be shown that all the indentation creep results reported in this study can be described by a simple expression relating the Vickers hardness with a temperature-compensated time parameter.

As shown from figure 3.4 the indentation creep behaviour of Float glass can be represented by an equation of the form

$$H_v = A + B \ln t \qquad (4.1)$$

where A and B are constants for constant temperature.

Alternatively, the indentation creep results can be represented by plotting values of H_v against test temperature for different loading times. Figure 4.3 shows that to a good approximation the indentation creep results fall on a series of straight lines suggesting that H_v can be represented as

$$H_v = C + DT \qquad (4.2)$$

where C is a constant approximately independent of the loading time and D is a time dependent parameter.

It is possible, in principle, to combine equations (4.1) and (4.2) so that H_v can be expressed as a function both of temperature and of loading time i.e.

$$H_v = C + B' \sigma(T,t) \qquad (4.3)$$

where B' is a constant and the function $\sigma(T,t)$ should contain the product T ln t. It will be shown below that the exact form of $\sigma(T,t)$ can be derived empirically from the experimental data available.

It is found in practice that the slopes of the H_v vs T lines

(figure 4.3), for different loading times vary linearly with lnt, that is,

$$D = D' + D'' \ln t \qquad (4.4)$$

where D' and D'' are constants.

Table 4.1 shows the values of D(calculated by the method of least squares from the data of figure 4.3), the corresponding value of t and lnt and the temperature range ΔT over which H_v was measured at t = constant.

Table 4.1

Values of the slopes D, load duration t, lnt and temperature range ΔT

$D \times 10^3/GNm^{-2}\,K^{-1}$	t/s	lnt	ΔT/K
-5.94	5	1.6	77-773
-6.12	20	3.0	77-823
-7.07	10^3	6.9	77-823
-7.39	10^4	9.2	295-773

So that equation (4.2) can be written as

$$H_v = C + T(D' + D'' \ln t) \qquad (4.5)$$

or,

$$H_v = C + B' T(\ln t + C') \qquad (4.6)$$

where $B' = D''$ and $C' = \frac{D'}{D''}$ and can be calculated from the data of table 4.1. This procedure provided that $C' = 28$ and by letting $C = H_{vo}$ the hardness of soda-lime-silica glass can be expressed as

$$H_v = H_{vo} + B' T(\ln t + 28) \qquad (4.7)$$

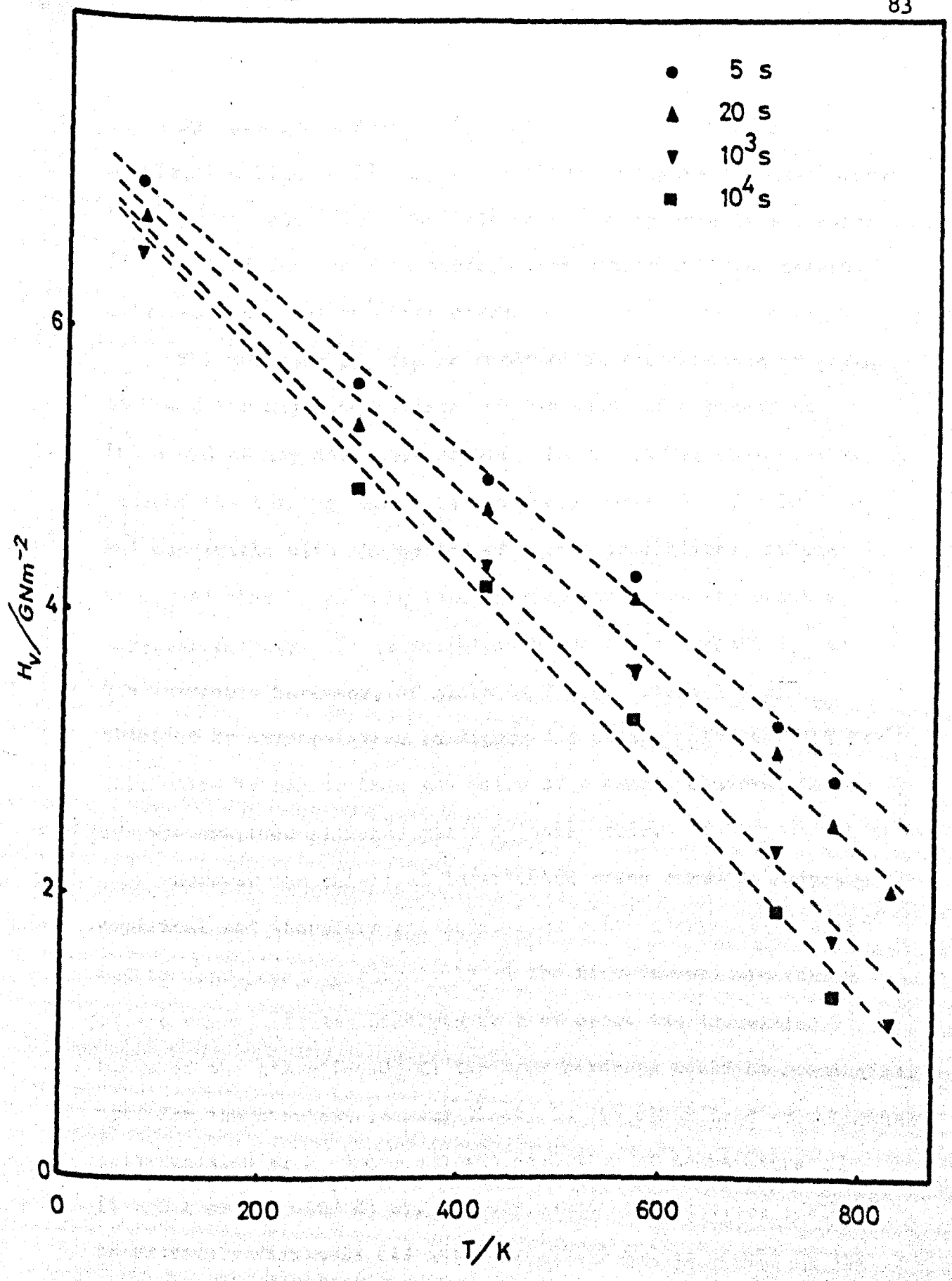

Figure 4.3 Vickers hardness as a function of temperature for different loading times.

By plotting values of H_v against the corresponding value of $\sigma(T,t) = T(\ln t + 28)$ the curve shown in figure 4.4 is obtained. It is worth noting that the indentation creep results for Pyrex (figure 3.6) fall on this curve, which can,arguably,be called universal indentation creep curve.

The constant H_{vo} can be regarded as the hardness of glass at $T = 0$ for any loading time, or the value of hardness at $\ln t = -28$ at any test temperature. In the latter case however because the loading time t is extremely small, $t = 7 \times 10^{-13}$ s, and comparable with the period of atomic oscilations, it can be argued that H_v at this loading time would not represent a physical reality. It is therefore plausible to regard H_{vo} as the intrinsic hardness, of glass at $T = 0$. The value of H_{vo} obtained by extrapolation in figure 4.4 is approximately 7.5 GNm^{-2}. This value is higher than any value of hardness observed in any of the examined silicate glass in this study.

However the universal indentation creep curve is entirely empirical and therefore predictions made by extrapolation would not be appropriate particularly at the high-temperature region of the curve. At temperatures near or above the transition range of the glass ($\sim 10^3$ K) the term hardness would be meaningless even for the shortest loading time. On the other hand experimental determination of H_v under extreme condition of temperature ($T \simeq 0$ K or, $T \sim 10^3$ K) or, at very short loading times would be extremely difficult (if not impossible) and so should be the verification of the predicted values. The usefulness of the universal indentation creep curve should be confined only to predicting the Vickers hardness of a glass at a given temperature and at a given loading time. Further experimental work is

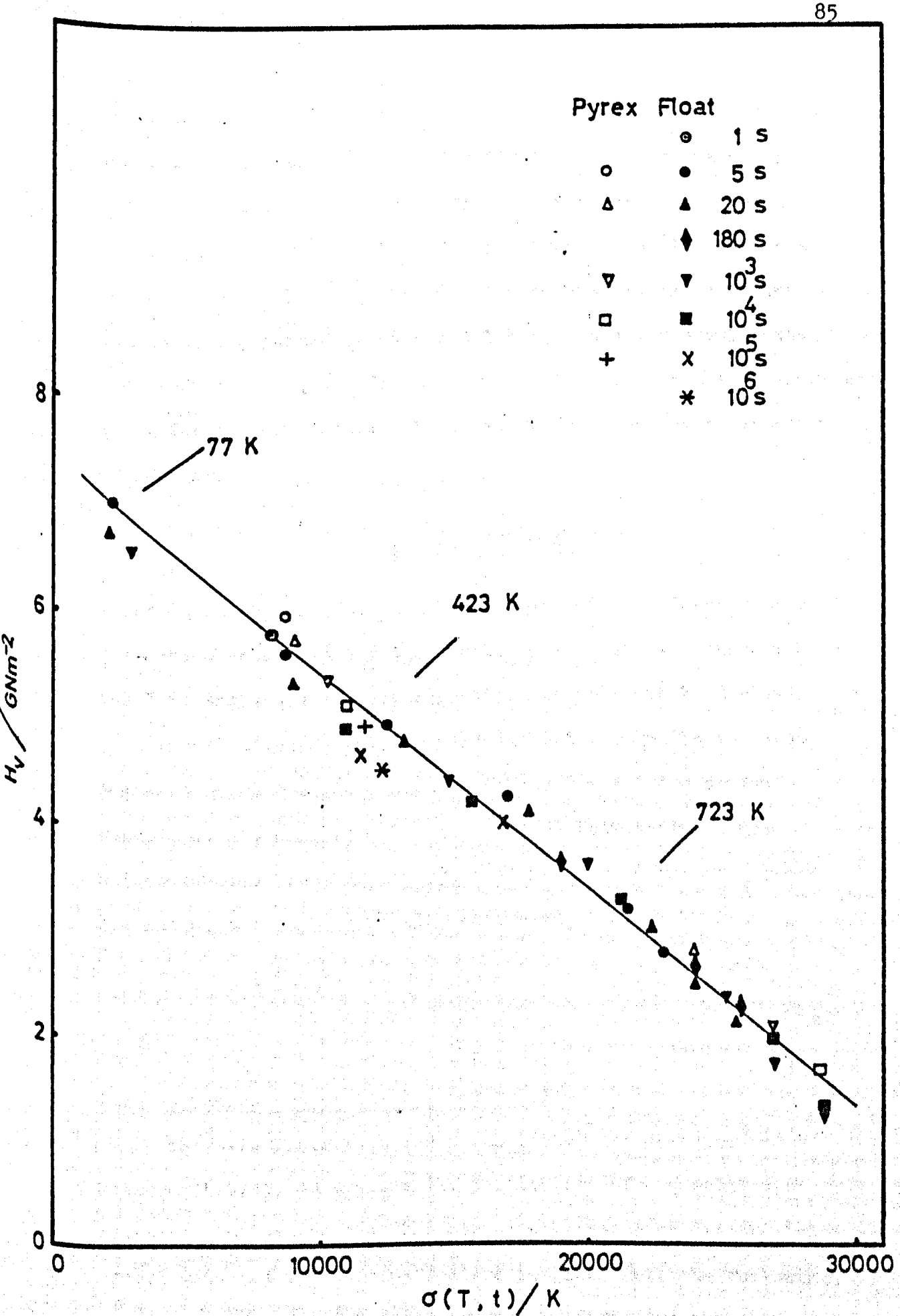

Figure 4.4 The Universal indentation creep curve: Plotting H_v against $\sigma(T,t) = T(\ln t + 28)$.

certainly needed to define the range of glass compositions for which the curve can be applied. Additional experimental data may also lead to another form for the universal indentation creep equation from which useful conclusions for the nature of deformation involved in the indentation process may be drawn. It has been reported (Bowden and Tabor, 1964) for example that some soft metals (e.g. Indium) exhibit indentation creep behaviour at different temperatures which can be described by an equation of the form

$$H_B = f(t \exp - \frac{E}{RT})$$

where H_B is the Brinell hardness number, t is the loading time, T is the absolute temperature, R the universal gas constant and E is the activation energy which was found to be the same as the activation energy for self-diffusion over the relevant temperature range. As discussed in section 4.2 the present results do not exhibit a linear relation between $\ln H_v$ and $\frac{1}{T}$ (for constant loading times), that is, the indentation creep did not appear to be thermally activated.

4.6 Consequences of the present results

The main facts that led Marsh (1964) and Weidmann and Holloway (1974b) to examine the possibility of a quantitative relationship between the flow stress obtained from indentation experiments and fracture parameters in glass were the following: The fracture energy for crack extension is found to be much larger than the theoretically estimated surface free energy;

the hardness and the strength (of both pristine and precracked glass specimens)are found to decrease with the duration of loading (static-fatigue); slow crack growth is observed at rates which are stress and environment dependent.

According to Marsh (1964) there exists a zone of plastically deformed material at the tip of a loaded crack in glass the size of which can be characterized by a length R. This zone expands dissipating elastic strain energy from the specimen until it reaches a critical size, R_c, at which bond rupture "is more favourable" than further flow. This is the criterion which provides a limit to plastic flow and it is a fundamental consideration for crack propagation. This idea was further quantitatively developed by Weidmann and Holloway (1974b). These authors were able by using general equations of continuum fracture mechanics to derive an equation for the speed of an advancing crack in terms of the rate of change of flow stress at the crack tip:

$$V = \left[\frac{\partial R}{\partial t}\right]_{\text{critical size}} = \left[\frac{K^2}{\pi Y}\ \frac{\partial}{\partial t}\ \left(\frac{1}{Y}\right)\right]_{\text{critical size}} \qquad (4.8)$$

where K is the stress intensity factor.

Values of the flow stress, Y, and the rate of change of Y with loading time in different environments were obtained from the hardness indentation creep experiments of Gunasekera (1970), It was found possible to express the flow stress as a function of time as:

$$\frac{1}{Y} = A \ln(Bt) \qquad (4.9)$$

where A and B are constants dependent upon the test environment. Assuming that the time scale for plastic flow at the crack tip

is identical to that for plastic flow under the indenter, and, inserting equation (4.9) into equation (4.8) the crack velocity was finally expressed as

$$V = \frac{KAB}{\pi} (2\pi R_c)^{\frac{1}{2}} \exp - \frac{(2\pi R_c)^{\frac{1}{2}}}{KA} \qquad (4.10)$$

It was found in practice that lnV is approximately a linear function of K^{-1} in both wet and dry environments. From the slope of lnV vs K^{-1} lines the values of R_c were computed and found to be $R_c = 5$ nm in wet and 25 nm in dry environments. However when values of R_c were calculated from the intercepts of the lnV vs K^{-1} lines they were found absurdly large ($R_c \sim 10^3$ to 10^{22} metres). This discrepancy between the predicted values of R_c could be overcome by adjusting B in equation (4.9), and this was equivalent to displacing the $\frac{1}{Y}$ vs lnt lines but not changing their slopes. If the shift is confined to $\frac{1}{Y}$ axis the physical implication of the required adjustment is that the tensile flow stress at the crack tip for any given load duration is lower (by a factor of 1/2) than that deduced from indentation experiments. Alternatively, if the shift is confined to (lnt) axis the implication is that plastic flow at the crack tip takes place on a time scale which is approximately 150 times longer than under an indenter in all environments.

As far as static fatigue phenomena are concerned, Weidmann and Holloway proposed that the time to failure of a pristine glass sample is the time taken for the flow stress to reach the level of the applied stress, σ, at a local irregularity in the atomic configuration, (provided that the applied stress, σ, is smaller than the instantaneous strength of glass). Therefore the time to failure can be given from the equation (4.9) as

$$t_f = \frac{1}{B} \exp\left(\frac{1}{A\sigma}\right) \qquad (4.11)$$

The times to failure predicted from equation (4.11) were found in good agreement with experimental results from static-fatigue experiments on pristine soda-lime-silica samples reported by previous authors, (provided that the adjustment of the constant B is taken into account).

For "as-received" or abraded soda-lime-silica glass specimens they proposed that the fatigue life-time is the time taken for an existing surface crack to reach a critical length at which catastrophic failure would occur, and which can be obtained by integration of the expression for the crack velocity. Again, the prediction was found compatible with experimental observations on the fatigue life-time of damaged specimens of soda-lime-silica glass.

Of the theories proposed for establishing a quantitative base for the mechanisms involved in fracture and static fatigue behaviour of soda-lime-silica glass, that of Weidmann and Holloway seems to be the most comprehensive one. It succeded in accounting for static-fatigue phenomena of both damaged and pristine glass specimens and also for the environment sensitivity of these phenomena. The apparent success of this theory dictated that further research is required to define the range of glass compositions and temperatures to which it can be applied. The present work undertook this task. But failure to reproduce the results on which the theory was based not only made the extension of the theory impossible, but called into question the validity of the model.

The main feature of the discrepancy is the environment

insensitivity of hardness observed in the present study, and this eliminates any possibility of modifying the theory. It must be made clear however that the present results affected only the inter-relationships between the flow stress and the rate of crack propagation in different environments. The quantitative interrelationships between crack propagation and static fatigue for pre-cracked glass specimens in wet and dry environments remains apparently unaffected.

It should be pointed out strongly that

a) If the results of the present study do represent the flow behaviour of soda-lime-silica glass, and if the flow process observed under an indenter corresponds to the flow process occurring in tension and at the crack tip region then Marsh's (1964) and Weidmann and Holloway's (1974b) hypothesis that fracture occurs when the applied stress reaches the flow stress must be rejected, and some other explanation must be sought for the problems associated with the high value of fracture surface energy, slow crack growth, environment dependence of fracture characteristics etc.

b) If Marsh's (1964) and particularly Gunasekera's (1970) results represent the flow behaviour of soda-lime-silica glass then there is still need for establishing that the flow process under the indenter corresponds to the flow process under tensile stresses at the tip of a crack or in fracture in tension. It is recalled that the adjustments that had to be made in Weidmann and Holloway's model in order to obtain consistent results implied that the time scale for plastic flow in fracture phenomena is not identical to that for plastic flow under an indenter, or, that the flow in fracture occurs at a stress level much smaller

($\times \frac{1}{2}$) than the fracture stress. These implications however were in sharp contrast with Marsh's original ideas which seem to have strong experimental support.

That glass can undergo a limited amount of plastic deformation during fracture cannot be ruled out, but there are grounds for questioning whether the flow behaviour under an indenter, and in tensile fracture of pristine samples or at the tip of a propagating crack are to be expected to be comparable even in a qualitative sense. This argument can be substantiated in the following way.

Consider a hemispherical zone around a Vickers indentation in the way adopted by Marsh (1964) as the basic form of the expanding cavity under internal pressure, H_v. The centre of the sphere is thought to be at the tip of the indentation and its diameter is slightly bigger than the indentation diagonal. Within this zone the material is plastically deformed and the boundary between this zone and the bulk material represents the elastic-plastic boundary at which the level of the shear stress induced by the indenter reaches the yield stress of the material. In fact, observations in sectioned indentations (along a diagonal) reveal a kind of intersecting pattern of lines (similar to the flow lines depicted in early theoretical models of the deformation beneath an indenter) which form a hemispherical zone around the indentation, figure 4.5*. If it is assumed that the area covered by these lines represents the extent of the plastically deformed material then it can be seen that the radius of the zone is approximately equal to half the length of the diagonal. Following Marsh's ideas, the

* Similar pictures have been published by Peter (1970) and Arora, Marshall, Lawn and Swain (1979).

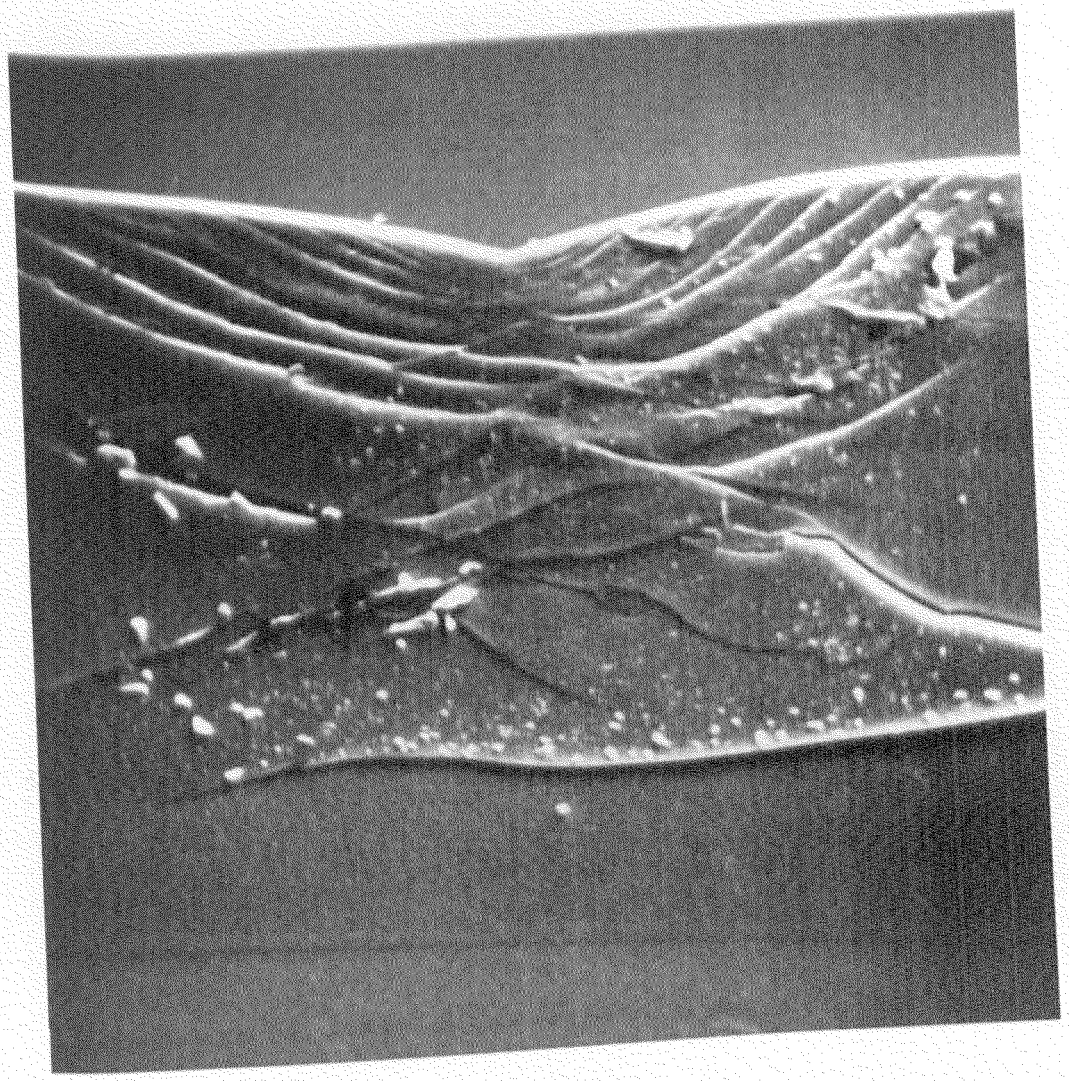

Figure 4.5. Scanning electron micrograph of a section through a Vickers indentation in Float glass (mag. x 2000).

expansion of the spherical zone with load duration (i.e. indentation creep) must be due to the reduction with time of the yield stress of the material at this elastic-plastic boundary*. If the surrounding environment, water molecules in particular, affects the flow stress of the material then it must be concluded that water molecules must reach the elastic-plastic boundary around the indentation (perhaps through a stress-enhanced diffusion process). This implies that the larger the indentation and hence the larger the radius of the plastically deformed zone the more difficult it will be for water molecules to reach the boundary, but on the other hand the stress is independent of the size of indentation, that is, independent of the applied load. This implies in turn that environmental effects should be more conspicuous when small indentations are produced. Such a phenomenon however has never been observed except in Westbrook and Jorgensen's (1968) work in which the environment sensitivity of the Vickers hardness for Al_2O_3 disappeared gradually when the load on the indenter was increased to produce indentations more than 1 μm deep. For indentations in glass with a typical hardness of 5.5 GNm^{-2} produced with 0.50 N and 10.00 N the semidiagonal length is 6.5 μm and 29 μm respectively. Penetration of water molecules to depths of this order is highly improbable.

In the above simple argument densification of material within the plastic zone was not considered. Clearly, the presence of a densified region beneath the indentation will inhibit diffusion of atmospheric species into the bulk of the material.

---

* Local softening of the near-the-surface region of glass in contact with the indenter may also result in indentation creep, as discussed for instance by Westbrook and his colleagues, (see section 4.3). But then such an effect would be irrelevant to the plastic flow hypothesis proposed for glass.

Marsh himself stated:

"... The water in glass is believed to be chemically bound by a type of hydrolysis... Thus water acts as a type of network modifier in softening the glass.

"This water can either come from the atmosphere or be drawn from the "built-in" water present in all glasses. In bulk fracture measurements, atmospheric water predominates except in very dry atmospheres (Mould, 1961), but it can be readily shown than in fibre strength and hardness measurements the different diffusion conditions mean that "built-in" water is much more important. This is fully supported by experiments and is more fully discussed in Marsh (1964c)".

Surprisingly, this paper, Marsh (1964c) has never been published.

Considering now the plastic flow at the tip of a loaded crack in glass it can be readily appreciated that the stress field at this region is entirely different from that under an indenter. The main difference is that there are not compressive stresses at the crack tip region. Also the size of the plastic zone around the crack tip must be extremely small and essentially independent of the specimen and of the crack (or loading) configurations. If the length of the plastic zone is about 5 nm (a value derived in Weidmann and Holloway's model) it seems possible that "water" can diffuse into distances of this order and influence the flow process at the boundary of this plastic zone. That is, environment sensitive plastic flow is more likely to occur at the crack tip than beneath an indenter.

With the above simple reasoning it was desired to underline the fact that although glass may undergo a limited amount of

plastic deformation, the hardness test is not suitable for quantifying the flow behaviour under tensile loading conditions; it was argued in particular that the environment insensitivity of the hardness of glass anticipated by Marsh himself and observed in the present study can be physically justified.

4.7 Concluding remarks

The principal aim of the present work was to examine quantitatively the correlation between the indentation creep behaviour of several glasses at different temperatures and other fracture parameters exhibiting time dependent properties (slow crack growth and static fatigue). This would have been in effect an attempt to extend and possibly to define the limitations of the theory proposed by Weidmann and Holloway. However, the original expectations have not been fulfilled: the earlier results from indentation creep tests of soda-lime-silica glass at room temperature on which the model was based could not be reproduced.

It was shown that conflicting experimental results on the indentation hardness and its variation with load, time or temperature for various materials, and for glass in particular, are not rare in the literature, but the reasons for this are far from obvious. Attempts to identify the factor(s) responsible particularly for the "internal" conflict - meaning the results obtained by Gunasekera and by the present author in this laboratory - failed to provide any sensible solution to this problem.

It is the author's scientific belief which arose after laborious and sometimes distressing investigation that the

results of the present study do in fact represent the "true" indentation behaviour of the silicate glasses examined.

Certainly the factors which led to the conflicting experimental evidence reported by the various authors have yet to be identified, although this seemed to be an extremely difficult task and would remain a subject of scientific curiosity even after the true indentation behaviour of the material is unambiguously established by several independent investigators.

In the context of the present results it was argued that the Vickers indentation test is not suitable for studying plastic flow phenomena in glass. Even a qualitative correlation between indentation creep and slow crack growth or static-fatigue seemed unattainable. It was argued that the different stress distributions and different sizes of plastic zone involved in indentation and fracture processes are the basic obstacles for such a correlation.

Apart from the obvious, and indeed urgent, need of experimental work to establish the true indentation behaviour of glass there seem to be a range of problems to be solved associated with the plastic flow of glass. The present work does not question at all the hypothesis that glass undergoes plastic flow, but it should be emphasized that no experiment has been devised as yet to demonstrate and quantify this important property of glass and that the so called evidence of plastic flow in glass are inferential and therefore weak.

It is hoped that the electron microscopy will be able in the near future to establish whether a very small plastic zone exists at the crack tip in glass, (possibly, by detecting deformation features similar to those found in other materials in larger extent). Electron microscopy may also be able to detect and

measure the crack tip radius if it exists. When detection and measurement of these characteristics of plastic deformation become realities, the calculation of the flow stress will become feasible through equations of continuum mechanics. But if electron microscopy succeeds in detecting such submicroscopic features in glass - of the order of a few nm - then it would probably also be able to provide vital information about the structure of this material. In this event, it may be found that some of the silicate glasses are not continua over regions the size of which is comparable with that of the plastic zone and therefore the application of equations of continuum mechanics would not be straightforward.

Some techniques used to examine compositional changes and diffusion phenomena in glass may be of great value in examining some aspects of the deformation of glass. Radioactive tracer experiments would probably be the most suitable for this kind of investigation. Specifically, examination of subsurface layers of glass underneath large indentations in a glass which contains a radioactive ion (e.g. ^{22}Na) can reveal whether densification has occurred. (By comparing the intensities of γ-rays of ^{22}Na from regions beneath the indentation and from the surrounding glass). Similarly, whether diffusion of water under the indenter pressure takes place can be verified in common glass which was indented in a T_2O or DTO atmosphere (Details on radioactive tracer experiments are given by Frischat, 1972).

In this final sentence of the first part of the present thesis the author wishes to express his appreciation to his supervisor, Dr. D.G.Holloway, for his unbiased attitude and

continuous encouragement during carrying out and writing of this work which apparently questioned the validity of a theory in which he was so much involved.

PART II

CRACK HEALING IN GLASS

CHAPTER 5

THE MEANING OF CRACK HEALING

5.1 Introduction

Despite the large amount of experimental work carried out on crack propagation and generally in the fracture of solids, very little attention has been given to the reverse process: crack closure or the apparent healing of fractures. Perhaps this is due to the fact that while fracture has been a recurring, everyday experience, the welding of fracture surfaces in non-living material is not a commonly observed phenomenon.

Knowledge of fracture was entirely empirical until the beginning of the 20th century. At that time, Griffith (1920) put forward some ideas in which, at least implicity, both crack propagation and crack closure in an elastic solid were considered. Griffith's theory of fracture was based on a simple and very well-known thermodynamic principle: the conservation of energy: crack propagation proceeds by conversion of elastic energy, U, in the body containing the crack, into surface free energy, T, of the fracture surfaces; thus, the surface energy of the newly created surfaces must be equal or less than the release of elastic energy from the body. This is the Griffith's energy-balance criterion for crack propagation in an elastic solid and can be

expressed

$$-\frac{\partial U}{\partial A} \geqslant \frac{\partial T}{\partial A} \qquad (5.1)$$

where A, is the area of the crack surface.

From this argument it is implied that if,

$$-\frac{\partial U}{\partial A} < \frac{\partial T}{\partial A} \qquad (5.2)$$

surface energy is recovered and the crack might be expected to close up.

Griffith's energy-balance criterion, equation (5.1), although applicable only to ideal brittle materials, has been modified and extended to embrace real materials exhibiting different degrees of brittleness (Irwin, 1947; Orowan, 1948). In real materials an energy dissipating process occurs at or near the crack tip as it advances but an energy criterion can still be a sufficient condition for crack propagation. The released elastic strain energy must in this case provide both the free surface energy and the energy lost, P, in the dissipating process: i.e. the term T in equation (5.1) is replaced by $T + P = \gamma$ where γ is the fracture surface energy of the real solid.

However, the reversibility of cracks as originally envisioned by Griffith is rarely observed, it has remained a theoretical concept, which might be expected strictly to apply only to ideally brittle materials.

As discussed later, there are practical reasons why crack closure and recovery of the surface energy are not common phenomena even with highly brittle materials for which P is very small. These include the effects of topographical features

produced during crack propagation and the environmental contamination of the freshly produced fracture surfaces.

Crack propagation in semibrittle materials is accompanied by plastic deformation around the crack tip, which often results in the formation of surface irregularities. When the externally applied load is removed, the relaxing elastic field around the crack tends to bring the fracture surfaces of the crack into contact. But contact is made only at the tip of the highest irregularities and for all practical purposes the crack remains open.

In very brittle materials, even though crack propagation may produce smooth fracture surfaces over small areas, usually it also produces surface steps, striations and fracture debris which can wedge open the opposing fracture surfaces so that closure is improbable.

It is possible, with some materials and under suitable test conditions to form smooth fracture surfaces over relatively large areas and also to avoid the formation (or the presence on the fracture surfaces) of fracture debris. Then crack closure can take place although the adsorption of environmental species such as O_2, H_2O or CO_2 onto the fresh fracture surfaces may inhibit significant bonding between the surfaces: although closed and possibly invisible, such cracks would therefore probably not be load bearing.

Nevertheless, in practice it is observed that closed cracks in certain materials exhibit load bearing properties: i.e. a finite load is required to reopen the closed cracks.

5.2 Aims of the present study

The closure and the load bearing properties of closed cracks in selected materials have been studied by a very small number of investigators and only superficially. As will be seen in the forthcoming paragraphs, the few published reports in this field indicate that crack closure can take place under certain conditions but the extent to which the closed cracks would support an applied load has not been examined in any detail. Such published results as there are, are qualitative and rather inconclusive.

The objectives of the present investigation were to examine the closure and the load bearing properties of closed cracks in glassy materials. The influence of several factors such as time, temperature and environment upon these characteristics is also investigated. Knowledge of the behaviour of closed cracks in solids may not be entirely esoteric; it may contribute to our understanding of the fracture and the strength of materials. For instance, it is of interest to know how a closed or an invisible crack affects the strength of a particular specimen. Does a closed crack remain a potential weakness in the solid or does it assume the mechanical properties of the bulk structure? But the potential of the present study is even wider. The study of crack closure and crack repropagation may perhaps offer a novel way of studying adhesion between solids; the initial fracture produces clean matched surfaces which require no further preparation such as polishing, drying etc.

It is often mentioned in the literature (e.g. Holland, 1964; Weyl, 1975) that freshly prepared glass bottles and fibres stick together when they are placed in contact at temperatures

several hundred degrees below the softening temperature of the glass. Laboratory glass-blowing provides frequent examples of low temperature adhesion between glass articles. When a piece of glass tubing is blown out special care is taken so that the bubble does not touch the wall of the tube or other near by tube. If accidental contact occurs it is highly likely that strong adhesion will take place, even though the surfaces are quite cool. It is hoped that an investigation of the adhesion of fresh glass surfaces might shed light on these striking phenomena.

5.3 Observations by earlier investigators

Despite the previously mentioned closure prevention mechanisms often met with in practice, crack closure has been observed by various investigators in a limited selection of very brittle materials. Some of these authors also attempted to investigate the load bearing character of the closed cracks.

Historically, Obreimoff (1930) appears to be the first author to report phenomena on crack closure and on crack repropagation. He observed that cleavage cracks in mica crystals close readily when the applied forces on the crystal are removed, and also that the closed cracks were load bearing. Cleavage test, were carried out to measure the energy required to propagate cracks both in laboratory air and in a vacuum of 10^{-4} Nm^{-2}. This energy was 0.375 Jm^{-2} in air and 5 Jm^{-2} in vacuum*.

The energy per unit area to re-open a closed crack in air was found to be less than 0.375 Jm^{-2} but no actual value

* An arithmetical error appears in Obreimoff's original calculation of cleavage energy, which gave values four times too big. The correction was made by Orowan (1944).

was given. On the other hand the energy to re-open closed cracks in vacuum was found to be the same as that required to reopen a closed crack in air.

More recent experiments on crack closure in mica crystals have been carried out by Bailey (1957, 1961) and Bryant (1962). Bailey found that the energy required to reopen a closed crack in air was about 0.25 Jm^{-2} while the energy for cleaving a virgin crystal in air was found to be 0.31 Jm^{-2}.

Bryant found that in air the energy for re-opening a closed crack was 0.15 Jm^{-2} that is, half of that required for cleavage of a virgin mica crystal. But in ultra high vacuum, 10^{-11} Nm^{-2}, he found the cleavage energy was about 10 Jm^{-2} while the energy to re-open the closed crack was approximately 9 Jm^{-2}.

Other materials in which crack closure has been observed include alkali halides crystals (Forty and Forwood, 1963), Germanium (Haneman, Roots and Grand, 1964) and inorganic glasses. Several authors have reported that occasionally cracks in glass specimens disappear when the externally applied load is released.

For example Finkel and Kutnik (1962) observed that small cracks in soda-lime-silica glass plates can propagate and close repeatedly as a bending moment is applied and removed, respectively. They also reported that using high speed cinematography, they had observed that some cracks formed by hitting a glass plate with a striker, disappeared a small fraction of a second after being formed.

Outwater and Gerry (1967) reported that unloaded cracks in glass became invisible "until the glass was restrained".

Varner and Frechette (1972)observed that cracks induced by water quenching hot glass specimens, frequently closed up

partially. As a force was applied to the specimen the closed portion of the glass could be seen to reopen readily, until the "true" crack tip was reached.

Cheesman and Lawn (1970) reported a quantitative investigation on what they called"crack healing in glass"where crack closure and the load bearing properties of closed cracks were examined; in their experiments, however, crack closure occurred only after the cracks had been subjected to a compressive load or to a heat treatment and even then reproducible results were not obtained.

Wiederhorn and Townsend (1970) have also reported a quantitative investigation on "crack healing in soda-lime-silica glass". They observed that for "spontaneously formed" and closed cracks the fracture energy is up to 80% of the fracture surface energy of virgin glass, whereas for cracks held open to the ambient atmosphere for some time before unloading and closure, the fracture surface energy was only up to 20% of the fracture surface energy of virgin glass.

However, as will be discussed later in this thesis, the experimental procedures used by Cheesman and Lawn (1970) and by Wiederhorn and Townsend (1970) can be criticized seriously so that the validity and significance of their results are questionable.

Finally, Weidmann (1973) reported that cracks produced in a controlled manner in soda-lime-silica glass close upon unloading, and also that the closed cracks were load bearing; several qualitative observations on closed cracks were reported by this author.

5.4 Definitions

In the reports cited above the terms "crack healing" and "crack re-healing" were used to describe both the closure of a crack and its load-bearing character. The terms have also been used by Outwater and Gerry (1967) to describe the disappearance of cracks in epoxy resin specimens after heating the specimens at temperatures above the softening temperature of the resin. Evans (1977) used the term "crack healing" to describe the closure of cracks in alumina specimens heat-treated at temperatures above 1473 K.

There are, in principle, a number of different phenomena associated with unloaded cracks and it will be convenient here to define several different terms which will be used in this part of the present thesis to distinguish between these phenomena.

Crack closure: disappearance of a crack on unloading the specimen. This usually occurs over a part of the total length of a crack near the original position of the crack tip.

Apparent crack healing: state of a closed crack in which it exhibits some load-bearing character i.e. some kind of bonding must exist between the fracture surfaces.

Genuine crack healing : state in which part or all of the crack has recovered the normal structure and properties of the original bulk material. Thus, this term will signify, at least over part of the area, re-making of the original chemical bonding characteristic of the particular material. It is perhaps unlikely often to be found in practice because of the interference caused by adsorption of environmental species onto freshly formed fracture surfaces.

Before turning to more detailed consideration of experimental

procedures, it is worth pointing out that crack closure in glass in particular, is a quite common phenomenon though not always obvious. Closed cracks may be found in many glass articles which have been accidentally or otherwise broken. The photograph in figure 5.1 shows a broken glass panel found in a university building. Apparently the glass panel was broken by impact; several radial cracks have closed over many centimetres. Some of these cracks contain large and small pockets of air, trapped during the rapid closure which followed the original violent crack propagation. Surface traces can also be seen along the closed portions of these cracks.

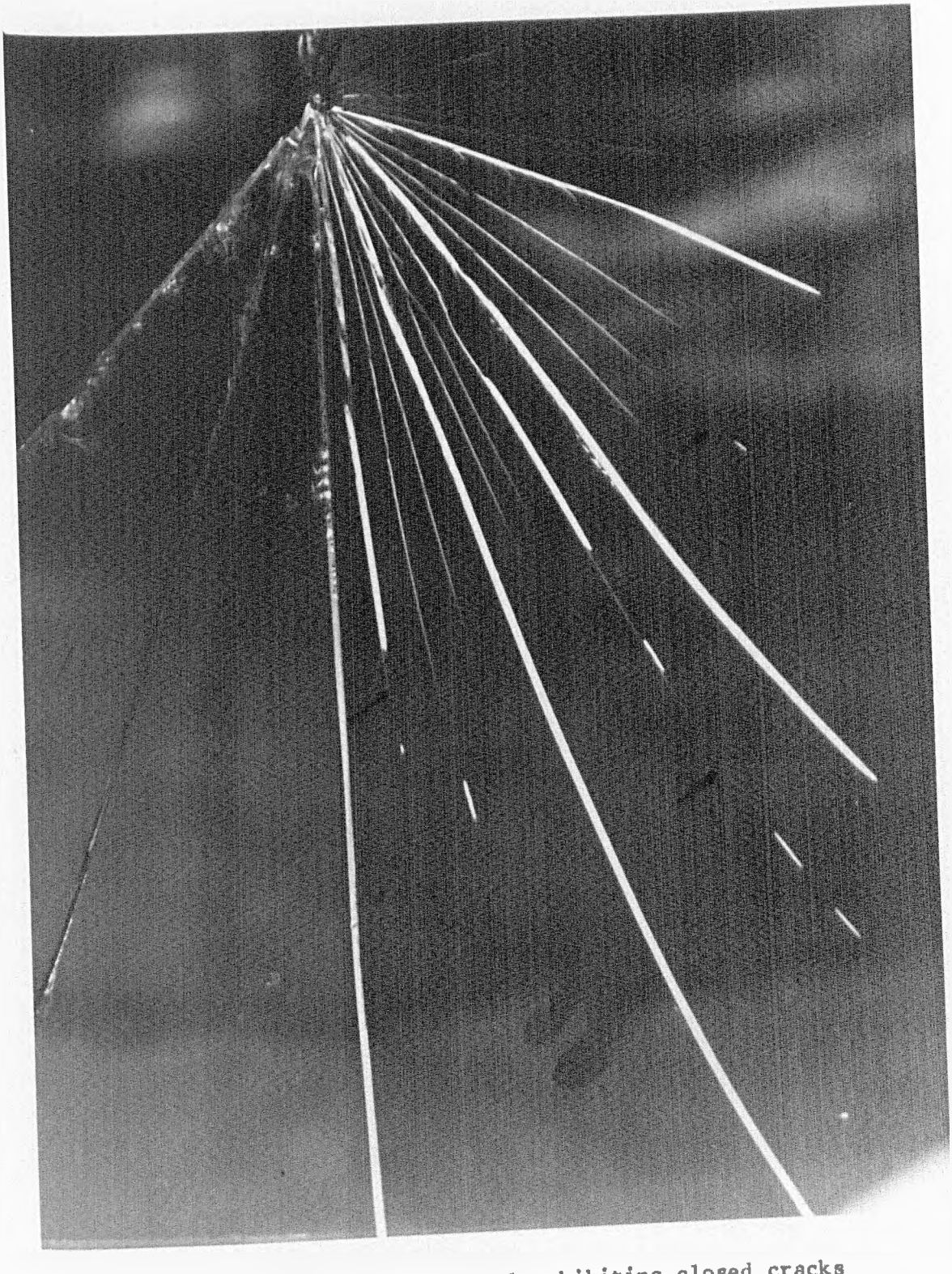

Figure 5.1. A fractured glass panel exhibiting closed cracks (indicated by the arrows).

CHAPTER 6

EXPERIMENTAL: APPARATUS AND MEASUREMENTS

6.1 Introduction

Despite the small number of published studies on crack closure and apparent crack healing, a number of different techniques have been used by the various investigators. In this chapter these techniques are described briefly and their suitability for crack closure and apparent healing studies is discussed. Also the experimental techniques and apparatus used in the present investigation are reported in detail.

Most of the experimental methods adopted by previous investigators are mechanical methods in which a specimen containing a small crack is loaded in a system designed for fracture mechanics studies of crack propagation. The crack is forced to extent by an applied load. A load is applied to the specimen which results in a stress concentration at the tip of the crack. At some critical value of the stress intensity at the crack tip the crack extents. The crack is stable when small increments of the stress intensity at the tip of the crack cause small increments of the length of the crack. However, at crack lengths large compared with the dimensions of the test piece, the crack becomes unstable; small increments of the stress intensity

at the crack tip cause large crack extensions and the crack propagates catastrophically. In crack closure studies the applied load is withdrawn before the crack runs through the specimen. The energy required for the original extension of the crack can be determined from the magnitude of the applied stress or strain, the geometry and the elastic constants of the test specimen. If the crack closes on unloading, the closed crack can be forced to re-open by reloading the specimen. The energy expended per unit area of crack surface can be determined, for this second re-opening to compare with that for the original crack propagation.

6.2 Techniques used by earlier authors

Obreimoff (1930) in his pioneering study on crack closure used a simple cleavage technique, figure 6.1. Thin sheets of mica were cleaved from thicker ones by advancing a glass wedge. When the splitting wedge was retracted, the mica sheets came in contact, (the cleavage crack closed). On re-advancing of the splitting wedge the cleavage crack appeared to open again.

Bailey (1957, 1961) in her experiment with mica used a slightly different cleavage technique, figure 6.2a. Mica specimens of uniform thickness were split into two sheets of equal thickness by applying the forces, f, at one end of the specimen. This method is now usually called the double-cantilever beam (DCB) technique. A cleavage crack could be made to advance or retreat by increasing or decreasing, respectively, the forces, f.

Linger (1967), studying the fracture of glass in double-cantilever beam specimens, figure 6.2b, attempted to investigate

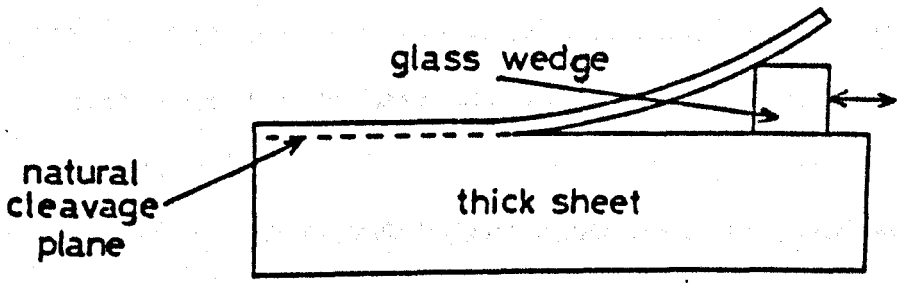

Figure 6.1 Specimen configuration for cleavage in mica crystals, Obreimoff (1930).

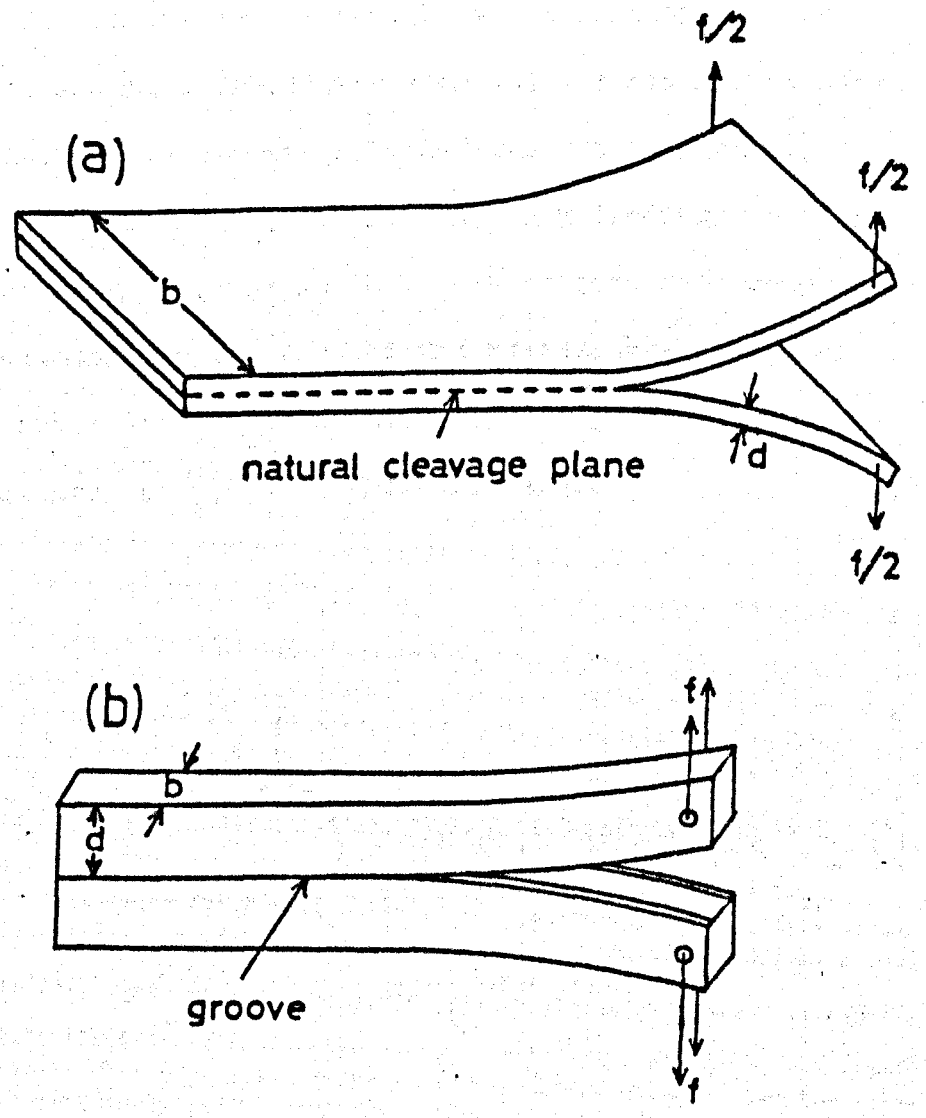

Figure 6.2 Double-cantilever beam specimen configuration used for cleavage (a) of mica crystals, Bailey (1961)
(b) of glass, Linger (1967), Wiederhorn and Townsend (1970).

the possibility of crack closure in glass in this loading configuration. However, he only rarely obtained crack closure and this apparently discouraged any attempts to examine the phenomenon in detail.

Wiederhorn and Townsend (1970) also used the double-cantilever technique to study the load-bearing capacity of closed cracks in soda-lime-silica glass but the closed cracks were introduced by hand manipulation of the specimens before they were loaded in the double-cantilever beam machine.

Cheesman and Lawn (1970) investigated the closure of cone cracks in glass formed beneath a loaded spherical indenter, figure 6.3. The cone cracks did not show any tendency to close when they were unloaded, unless they were subjected to compressive load or to heat-treatment. Some of the treated cracks showed load-bearing properties. The results obtained in these investigations are discussed in a later chapter.

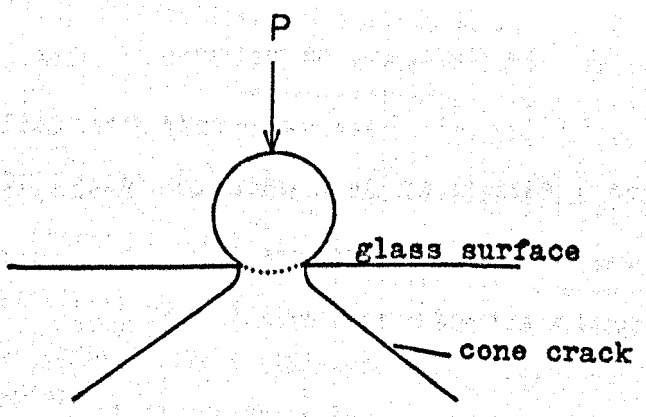

Figure 6.3 Illustration of a cone crack formed beneath a loaded spherical indenter.

The information available from these earlier investigations suggests that certain techniques are really not suitable for studying crack closure and apparent or genuine healing in glass. Although the double-cantilever cleavage technique has proved suitable for such a study in the sheet structure of mica which provided an inherent stability during crack closure, it apparently was not satisfactory for glass. It is believed that small lateral displacements of the two arms of a double-cantilever beam specimen in which $b < d$ (figure 6.2b) is responsible for the unreliable closure of cracks in specimens of this configuration. In the case of the mica it was practicable to produce specimens with $b \gg d$ which resulted in excellent elastic resistance to shearing displacement of crack surfaces. Wiederhorn and Townsend's use of special tricks to produce closed cracks may have been inspired by the difficulty of producing reliable crack closure in the double-cantilever cleavage configuration.

The cone cracks have also been proved unsuitable for crack closure studies. The failure of cone cracks to close as the load was withdrawn, according to Cheesman and Lawn, is primarily due to mechanical effects; the fracture surfaces of a cone crack exhibit topographical features such as hackle lines, cleavage steps, striations etc, and any small lateral displacement of the fracture surfaces will prevent precise matching of the opposing fracture surfaces.

A technique which has been used successfully for crack propagation studies in glass and other materials but has not been used in a systematic way hitherto to investigate crack closure, is the double-torsion technique (see for example Weidmann and Holloway, 1974a).

Preliminary experiments early in the course of the present study suggested that crack closure could reliably and regularly be produced in glass using this configuration. The double-torsion technique was therefore adopted and new apparatus was constructed for the main series of experiments. Before describing the refined double-torsion loading machine a brief account of the mechanics of the double-torsion technique is given.

6.3 Mechanics of the double-torsion technique

The double-torsion technique was first introduced by Outwater and Gerry (1966). Since then many investigations in which this technique was used, have been reported in the literature of fracture mechanics (see for example Kies and Clark, 1969; Evans, 1972; Weidmann and Holloway, 1974a).

The test specimen used in this procedure is a simple rectangular plate. The two halves of the plate are subjected to equal and opposite torques applied by means of a four-point loading system at one end of the plate. The crack propagates along the mid-plane parallel to the length of the specimen, figure 6.4.

The strain energy release rate (the energy per unit area of the crack surface) during crack propagation can be derived relatively simply:

The total work, W, done on a linearly elastic specimen in producing an angular deflection, Θ, between the torsion arms is

$$W = \frac{M\Theta}{2} \qquad (6.1a)$$

or,

$$W = \frac{M^2 C}{2} \qquad (6.1b)$$

where C is the compliance of the specimen and M is the applied torque.

In this case

$$M = fm \tag{6.2}$$

where f is the force at each loading point and m is the distance between the two loading points in one arm of the specimen, figure 6.4.

The work done by the torque, M, is stored as elastic strain energy, U, in the specimen.

The strain energy release rate, G, is defined as

$$G = -\left(\frac{\partial U}{\partial A}\right)_{\theta} \tag{6.3}$$

where A = bL, b is the thickness of the specimen and L is the crack length.

Equations (6.1a) and (6.3) give

$$G = \frac{M^2}{2b}\frac{dC}{dL} \tag{6.4}$$

If it is assumed that each torsion arm of a cracked specimen can be modelled by a rectangular beam whose length is equal to the crack length, L, and a torque is applied at one end of the beam whilst the other end remains fixed, the torque, M, is given by (Timoshenko and Goodier, 1970)

$$M = \frac{1}{3}\frac{\theta}{2}\frac{\mu b^3 \omega}{L}\left(1 - 0.63\,\frac{b}{\omega}\right) \tag{6.5}$$

where μ is the elastic shear modulus of the test material and ω is the width of each rectangular beam.

Because $C = \frac{\theta}{M}$, equation (6.5) can be written as

$$C = \frac{6L}{\mu b^3 \omega\left(1 - 0.63\,\frac{b}{\omega}\right)} \tag{6.6}$$

Substituting equation (6.2) and (6.6) into (6.4) we obtain

$$G = \frac{3f^2m^2}{\mu b^4\omega(1 - 0.64\,\frac{b}{\omega})} \qquad (6.7)$$

It is worth noting in equation (6.7) that G is independent of the crack length, L, for a constant applied force, f.

Equation (6.7) can also be expressed in terms of the angular displacement, θ; from equations (6.2), (6.5) and (6.7) it is found that

$$G = \frac{\mu\theta^2b^2\omega(1 - 0.63\,\frac{b}{\omega})}{12L^2} \qquad (6.8)$$

However, these equations have been derived using linear elasticity theory, and also (tacitly) assuming that the crack front is a straight line, perpendicular to the direction of propagation, figure 6.4. The actual shape of a crack in a double-torsion specimen is that shown in figures 6.5 and 6.7.

Thus, it might be expected that the above expressions would serve, at best, only as approximations to the conditions in practice.

Nevertheless, Weidmann and Holloway (1974a) showed that there is a range of crack lengths where the compliance is indeed proportional to $1/L^2$, as implied by equation (6.6). Also over approximately the same region, the crack velocity is constant independent of crack length for a constant applied force. This region was found to be the middle region of the specimen length, extending from about one quarter to about three quarters of the specimen length.

The peculiar shape of the crack front does not seem to have any significant effect, at least on the expressions for G, provided that measurements of crack length and/or crack velocity are taken in the middle region of the specimen. It is worth

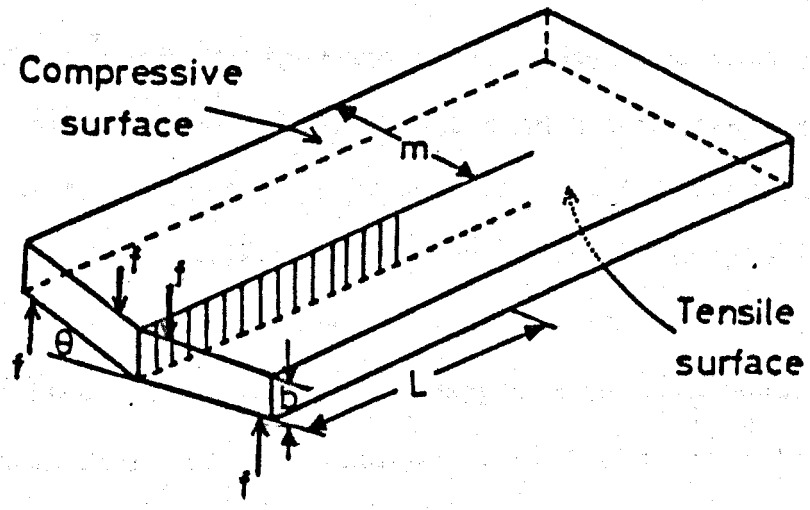

Figure 6.4 The double-torsion specimen and loading configuration.

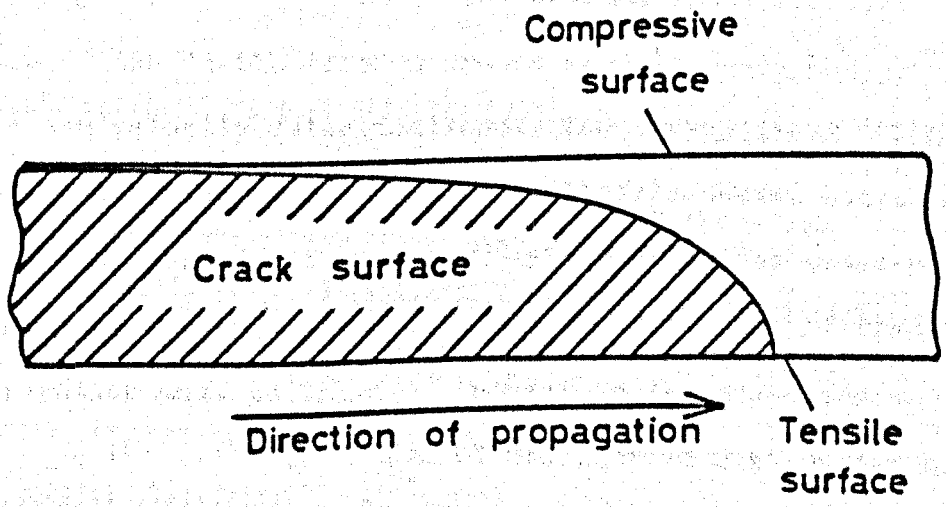

Figure 6.5 Illustrating the shape of the crack front in double-torsion.

noting that excellent agreement exists between the results on slow crack propagation (crack velocity versus strain energy release rate) in soda-lime-silica glass published by different investigators who used completely different loading configurations. Namely, of Schönert, Umhauer and Klemm (1969) who used simple tension; of Wiederhorn (1971), who used the double-cantilever cleavage technique and that of Weidmann and Holloway (1974a), who used the double-torsion technique. In the simple tension and double-cantilever cleavage techniques the crack front is virtually linear during crack propagation in constrast to the curved crack front in the double-torsion technique. In all the techniques crack lengths and/or crack length increments are measured at the surface of the specimen, (the tensile one in the case of the double-torsion technique). Because it is found that the crack velocity is a sensitive function of the strain energy release rate, any influence of the shape of crack front on the slow crack propagation characteristics would have yielded different results when different techniques were used.

By constrast, Evans (1972) has argued that the peculiar shape of the double-torsion cracks must be taken into account in crack velocity determinations. The above author depicted the shape of the crack front as a slightly curved line, figure 6.6. He used a value for the ratio $\frac{\Delta a}{b}$ about five, for glass and alumina specimens, and argued that the direction of crack propagation must be taken normal to the crack front. According to Evans the optically measured crack speed must be reduced by a factor of

$$\frac{b}{\sqrt{(\Delta a)^2 + b^2}} \qquad (6.9)$$

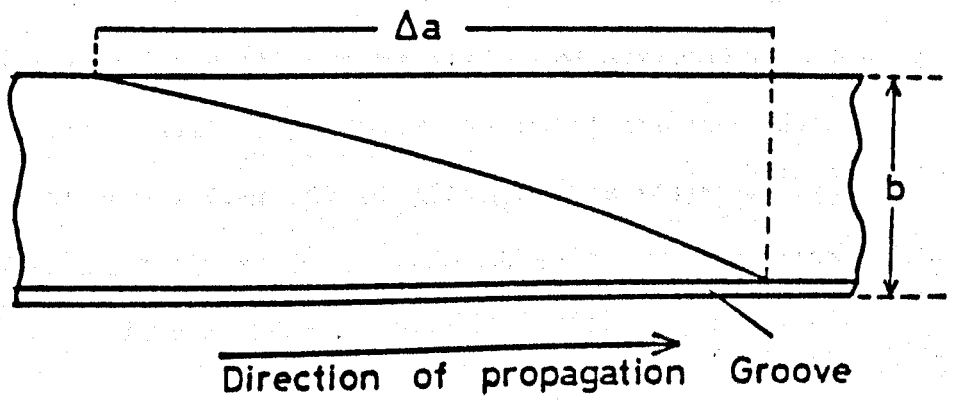

Figure 6.6 Illustration of the double-torsion crack front as depicted by Evans (1972).

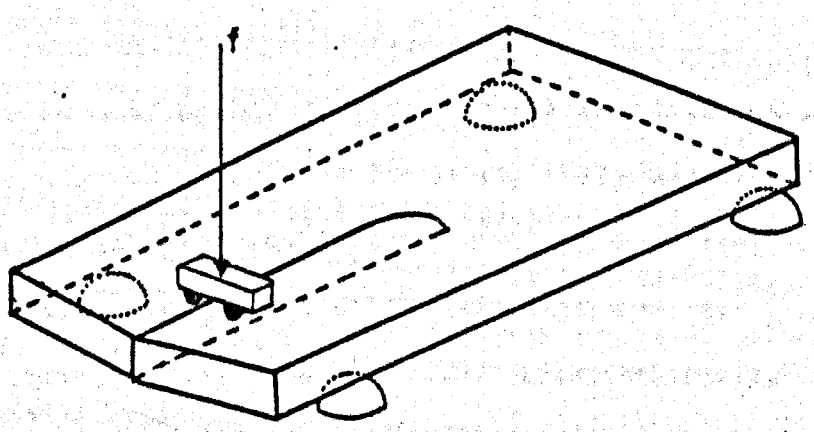

Figure 6.7 Illustration of the principle of operation of the original double-torsion machine (Outwater and Gerry, 1966).

(see figure 6.6)

Evans' depiction of the crack front and the value of $\frac{\Delta a}{b} = 5$ does not correspond to the shape observed by previous and present members of this laboratory, including the present author. The line of the crack front reaches the tensile surface of the specimen nearly at a right angle and approaches the compressive one almost asymptotically until the underlying glass, which is now a fine rib of glass, breaks (figure 6.5). The ratio $\frac{\Delta a}{b}$ is found to be considerably larger than that quoted by Evans.

6.4 The double-torsion machine

The original double-torsion machine described by Outwater and Gerry (1966) is illustrated in figure 6.7. Four steel hemispheres, fixed on a horizontal base, support the specimen. The end of the specimen in which a crack had been initiated before mounting, is loaded through two other hemispheres at one end of its top surface. A scratch or a groove on the bottom surface of the specimen guides the crack to propagate along the midplane of the specimen.

This simple form of double-torsion machine is still being used in some laboratories (Young and Beaumont, 1977) but a modified system of double-torsion loading has been developed and used in this laboratory. This system was developed by Weidmann and Holloway (1974a) from a machine which originally had been designed and used for four-point bending tests on glass rods by Brearley, Hastilow and Holloway (1962) in this laboratory.

The description given below of the loading system follows

that given by Weidmann and Holloway (1974a).

The principle of the method is illustrated in figure 6.8a. A torque is applied to the specimen, C, through two pairs of steel pins, A and B, one of which, A, is mounted on an arm which can rotate about an axis midway between the two pairs. The shaft of this rotatable arm is connected to a pulley, P. Rotation of this pulley under the action of the force, F, causes the pins, A, to exert a torque on one half of the specimen. This applied torque is balanced by that generated in the other half of the specimen by the reaction of the fixed pins, B.

Each pair of pins is mounted on a separate small rectangular block, D and E, figure 6.8b, so that the line joining the centre of the pins in each pair can be rotated through a small angle and then clamped rigidly by means of the lateral screws, S, shown in figure 6.8c. This rotation of the blocks enables specimens of different thickness to be tested in the machine.

A specimen mounted in the machine can be loaded either by applying a constant force (dead load) to the end of a cord attached to the periphery of the pulley, or by applying a known constant deflection between the two halves of the specimen. This can be achieved by means of a micrometer screw which is threaded through a small block fastened to the basal plate of the machine and which can thrust against the end of the moving arm.

As well as offering versatile loading this double-torsion system enables a specimen to be loaded while it is vertical in the machine. This particular facility was used by Weidmann and Holloway (1974a) and by the present author in order to study the characteristics of crack propagation in glass specimens

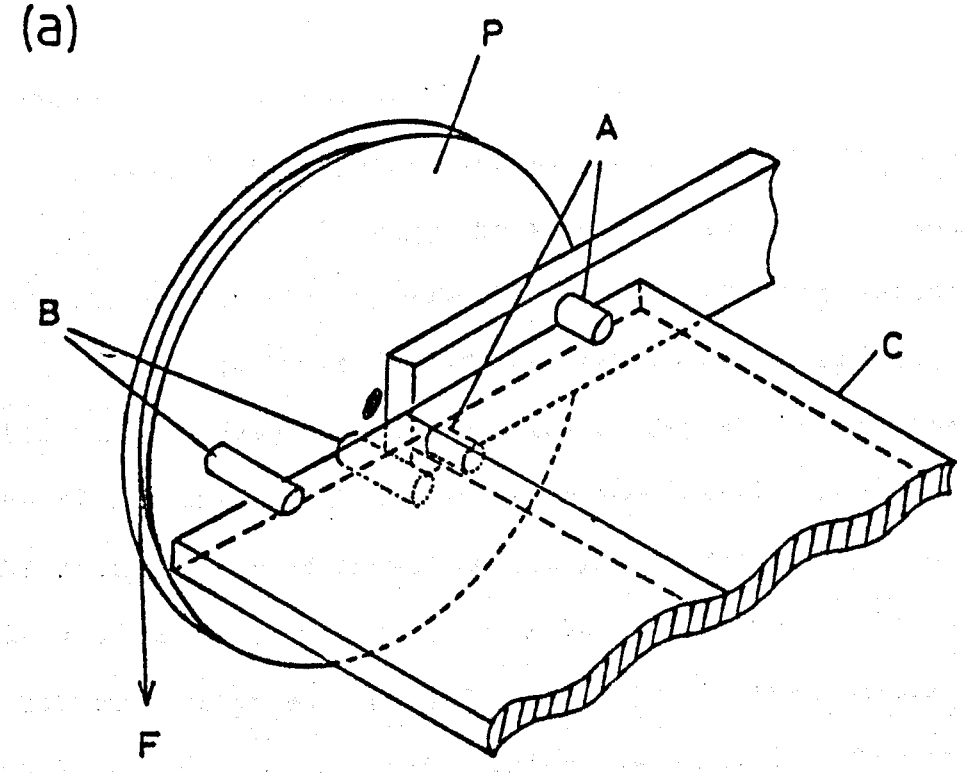

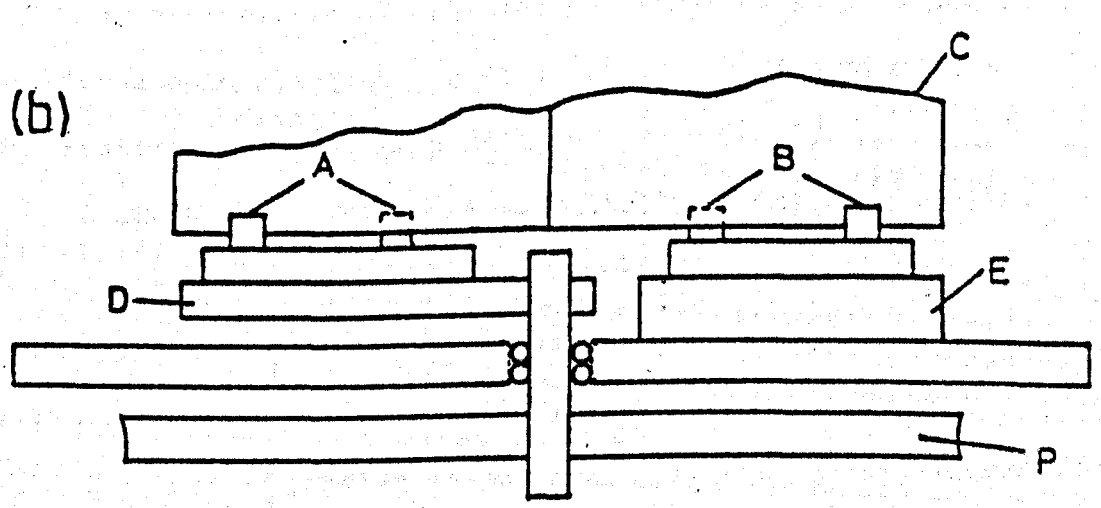

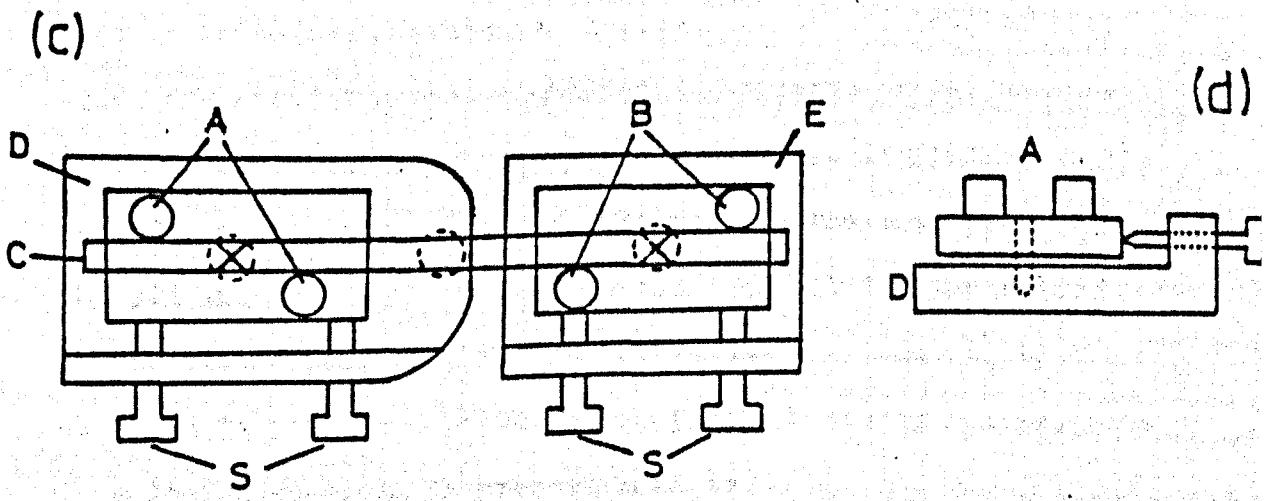

Figure 6.8 The double-torsion machine

(a) illustrating the principle of the loading system

(b) vertical section of the machine, (c) plan view of pins and

immersed in a variety of liquid environments.

Part of the experimental work described in the present thesis was performed using the already existing double-torsion machines constructed as described in the previous paragraphs.

In the early stages of the present investigation the phenomena of crack closure and the load-bearing capacity of the closed cracks was studied in soda-lime-silica glass. However, the desirability of expanding the investigation to cover other glasses and other materials soon became apparent. The early experiments also suggested that it might be instructive to observe crack closing and re-opening under the optical microscope. The cost and availability of selected materials as well as the need for microscopic observations dictated the construction of a much smaller double-torsion machine.

A new machine, which is essentially a miniature version of that used by Weidmann and Holloway (1974a) was therefore designed, figure 6.9. It is capable of accommodating specimens up to a thickness of 2.5 mm with a width of only ~ 25 mm.

The biggest problem in the design of such a small-sized machine is to avoid excessive deflections of the loading pins which are among the most highly stressed parts of the machine.

Simple elasticity theory shows that the deflection at the end of each loading pin is proportional to the load applied on the pin and to L^3/r^4 where L is the length and r the radius of the cylindrical pin, figure 6.10. But the load required on each pin to produce a given value of strain energy release rate in a loaded specimen is proportional to

$$f \propto \frac{b^2 \omega^{1/2}}{m} \qquad (6.10)$$

(see equation (6.7)).

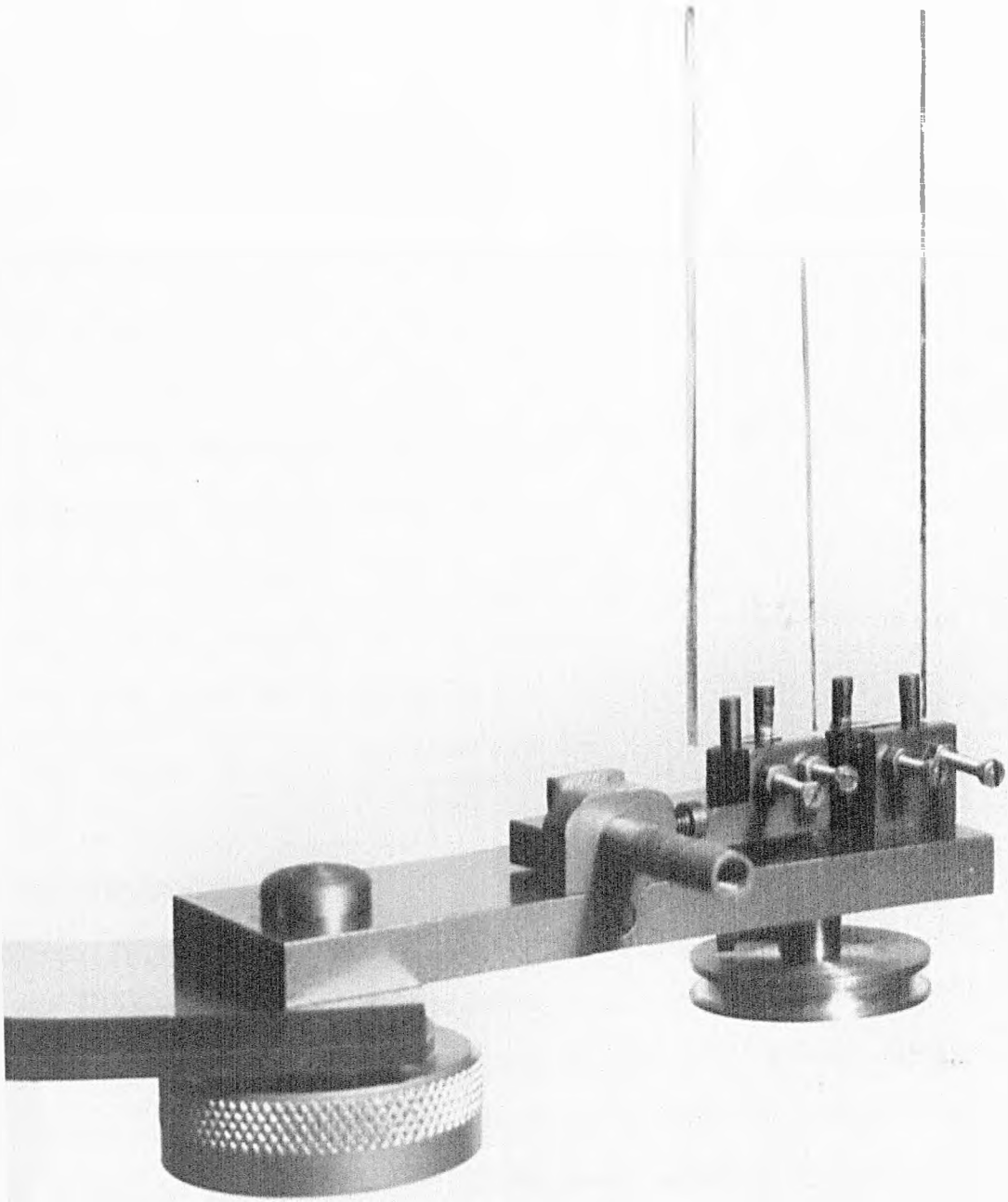

Figure 6.9 The miniature double-torsion machine designed by the author (mag. x 1.3)

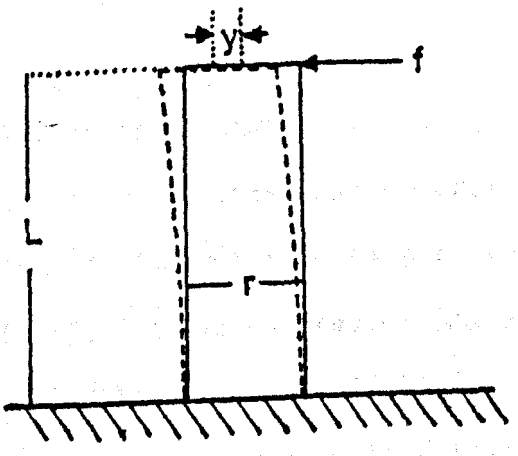

Figure 6.10. Illustration of a loading pin deflected by the force f.

Thus the deflection at the end of each pin for a given value of G, is proportional to

$$y \propto \frac{b^2 \omega 1/2_L 3}{mr^4} \qquad (6.11a)$$

The complete expression for the deflection y, is

$$y = \frac{4G\mu(1 - 0.63\,\frac{b}{\omega})}{3E\pi} \cdot \frac{b^2 \omega 1/2_L 3}{mr^4} \qquad (6.11b)$$

where E is Young's modulus of the material the pin is made of, steel in the present case. If it is attempted to scale down the dimensions of the components of the double-torsion machine and also the dimensions of the specimen by the same (small) factor, for instance 4, then, as can be seen from expression (6.11a) the deflection, y, in the small machine would be the same as that in the original machine (within a factor of two). This scaling down however, was not practicable in the present case; for practical purposes the thickness of the specimen and the length of the pin had to be reduced by a factor of approximately 3 and all the other dimensions shown in expression (6.11a) had to be scaled down by a factor of approximately 6.

This scaling down of the dimensions resulted in a value of y, ten times larger than that in the original machine.

Nevertheless, in the large double-torsion machine the maximum deflection at the end of each pin when the machine was operating at a very high load (corresponding to $G = 10\ Jm^{-2}$) was about 2×10^{-8} m (from equation (6.11b)). Thus the maximum deflection of the pins in the small-sized machine is about 2×10^{-7} m, which is also very small and it is thought to be a safe value for the reliable operation of the miniature machine.

In addition to the above difficulties, the accurate parallelism of the loading pins was discovered to be very important for the reliable operation of the machine. In the early stages of operation of the machine, curved cracks which often failed to close when they were unloaded and erratic experimental results (crack velocity versus G) were obtained. This difficulty was presumably due to loading of the specimen with three loading pins before the forth pin came in contact with the specimen. Such an awkward loading configuration would seriously perturb the stress distribution at the crack tip and hence the orientation of the crack during crack propagation. When the parallelism of the pins was corrected, the production of specimens with long straight cracks, which could close readily when the load was released, was a matter of routine.

The miniature double-torsion machine was equiped with all the facilities of the large machine so that both loading methods (constant load or constant deflection) could be used. In addition, its small size enabled the present investigator to carry out experiments in a vacuum chamber and in other controlled environments. The use of a large test machine which naturally required a large-

sized specimen would have been extremely difficult for the performance of experiments of this nature.

A separate, simple piece of apparatus was developed to facilitate optical observations with the Vickers projection microscope. The device is in effect a versatile stage to which a miniature double-torsion machine can be attached. A specimen is mounted in the device on its side: that is, it has the direction of its width perpendicular to the microscope table. This arrangement enables the crack plane to be examined microscopically while the crack is under load.

Using suitable illumination, interference fringes formed by reflection from the crack walls could be studied. These observations, however, required that the specimen be adjusted so that the crack plane can be made accurately perpendicular to the axis of illumination. The special mounting stage was designed to facilitate such adjustment.

6.5 Double-torsion machine stage-mounting device

The photograph of figure 6.11 gives a general view of the mounting device which was constructed in mild steel, in the Department's workshop to the author's design.

The double-torsion machine is attached to a vertical pillar on the frame F, clamped to a base plate, P, which can be mounted on the stage of the Vickers projection microscope. The double-torsion machine is attached to the pillar by means of the screw, A, and can be rotated about the axis of this screw by adjustment of screws B and C.

The frame, F, has three feet on its underside which rest

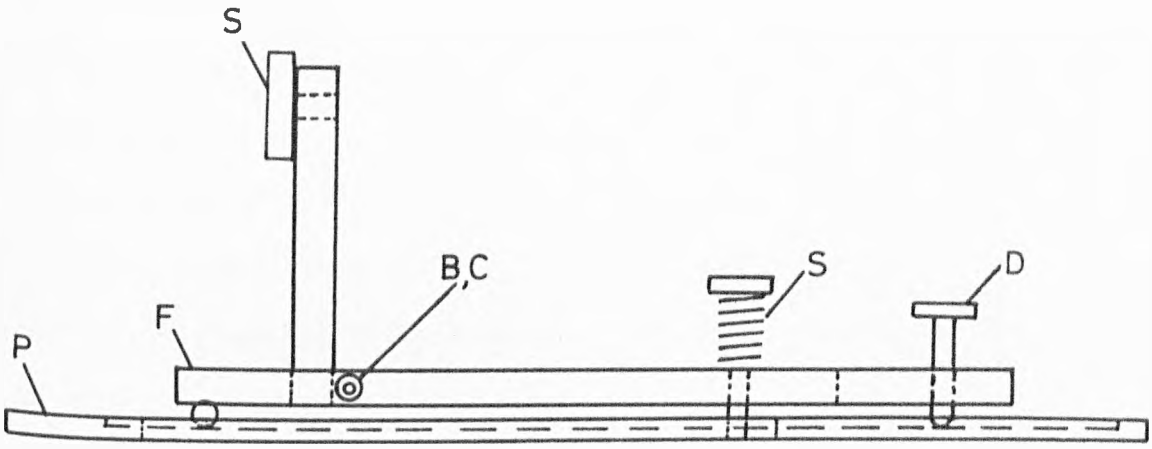

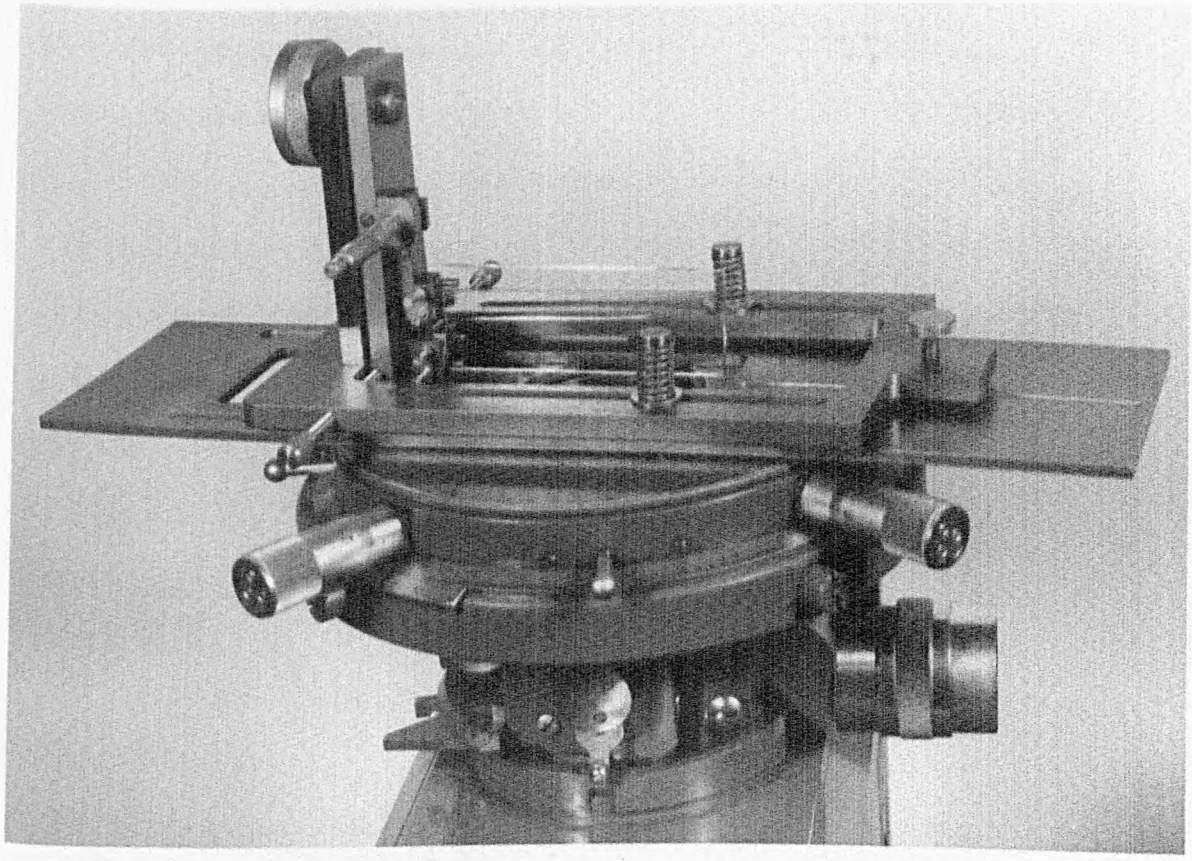

Figure 6.11 (a) Diagramatic representation and (b) photograph of the double-torsion machine stage-mounting device designed by the author.

in parallel grooves in the base plate, P; one of these feet can be adjusted via the screw, D, so as to adjust the frame about a horizontal axis and the whole frame can slide horizontally in the grooves of the base plate.

In order to keep the frame in position while the double-torsion machine is manipulated, the frame has two long slots parallel to the underlying grooves and it is loaded via a pair of springs, S, the axes of which pass through the slots and are firmly fixed to the base plate. A large hole in the central area of the base plate allows the specimen to be observed when the device is mounted on the stage of the inverted projection microscope.

By sliding the frame, F, along the plate, P, the desired area of the crack plane can be brought into the field of view. Then, by manipulating the screws B and C, in combination with the screw D, the plane of the crack can be made precisely perpendicular to the axis of illumination. The two transverse movements of the microscope stage as well as the independent rotation about the optical axis of the objective lens, increase the manoeuvrability of the system.

6.6 Materials

The materials used in the present investigation were the following

i) Soda-lime-silica glass as:

   a) Float glass (Pilkington Bros Ltd)

   b) Microscope slides; (Chance Propper Ltd).

ii) Borosilicate glass; Pyrex (7740, Corning Ltd).

iii) Silica glass (Thermal Syndicate Ltd) as

a) fused silica: Vitreosil 066 and

b) synthetic silica: Spectrosil B

The nominal compositions of the above glasses as quoted by the manufacturers are given in table 2.1.

iv) Epoxy resin; Araldite CT200 with curing agent HT 901 (CIBA - GEIGY).

This epoxy resin composition was chosen for its glassy nature and its transparency. Although it is widely used as a photoelastic model material due to its excellent optical sensitivity (high stress optical coefficient) it is used in some laboratories as a model material for studying fundamental phenomena regarding the fracture behaviour of composite materials. Systematic research by Griffiths (1968) in this laboratory showed that Araldite CT 200 with low hardnener content (5 parts per hundred by weight (5 pph)) has a very low fracture energy ($\sim 1\ Jm^{-2}$) and exhibits fracture characteristics similar to that of silicate glasses. In the present study it was used either as pure CT 200 or with up to 5 pph hardener.

The above selected materials gave not only a wide range of glass compositions, but also an organic system which phenomenologically behaves like the oxide glasses but differs entirely from them in chemical nature.

6.7 Specimen preparation

Specimens of Float glass were cut to suitable size from larger plates, according to the size of the testing machine to be used.

Specimens of Pyrex glass were already available in our laboratory as the arms of double-cantilever beam specimens which have previously been cleaved (Linger 1967). These arms were cut and ground to suitable size for the small-sized double-torsion machine, and then polished to transparency.

Specimens of Vitreosil were cut to suit a small-sized double-torsion machine and then polished to transparency. Specimens of Spectrosil were purchased in a finished form.

Specimens of epoxy resin were cast in specially made moulds of silicone rubber (Silicoset 151, I.C.I Ltd).

The required amount of epoxy resin was heated in an electric oven at 413 K and then hardener was added to give a mixture containing 3 or 5 pph hardener. The mixture was stirred until all the hardener had dissolved. The resin was then poured into the preheated moulds and cured for 4 hours at 413 K and then allowed to cool down to room temperature. The epoxy resin does not stick to the flexible silicone rubber moulds, so that the removal of the specimens was quite simple. These specimens were virtually free of frozen strains (when examined between crossed polaroid sheets) and hence post curing (annealing) of the specimens was not necessary.

In addition to partially hardened epoxy resin specimens a number of unhardened resin specimens were prepared following the same procedure but without adding the hardener.

A short crack was initiated in all the specimens to be tested in the double-torsion machines. A fine scratch about 15 mm long was scribed by a diamond glass cutter along the midline of one face of each specimen and from one end. A small crack then was introduced by tapping over this scratch on the

face of the specimen opposite the scratch.

Crack initiation in glass specimens became a straight forward procedure, whereas the extreme brittleness of the epoxy resin materials resulted in only a small percentage of the prepared specimens reaching the testing machine. Most of them were destroyed during the crack initiation stages.

The quality of the short scratch was found to influence to some extent the closure characteristics of the cracks. The finer the scratch the longer was the region over which the crack closed when the load was released. This was probably due to the fact that a "crude" scratch produces multiple lateral cracking around the scratch so that when the crack is induced the glass around the scratch flakes off and glass particles fall into the crack wedging it open.

Finally, some of the Float glass specimens were annealed at 813 K in an air oven for approximately an hour and then slowly cooled ($\sim$ 2 K/min) to room temperature. But no difference in the crack propagation-closure characteristics could be detected between annealed and as-received specimens.

6.8 Experimental procedure

In the following paragraphs, the main experimental techniques which were employed in the present study are described and the present chapter ends with a description of two additional methods which were used to demonstrate and study qualitatively the load-bearing properties of closed cracks. Other techniques used in attempts to answer specific questions which arose during the investigation are reported in a later chapter.

Specimens having had a crack initiated as described above were mounted in one of the double-torsion machines and the crack was propagated from the initiated crack. In the preliminary experiments, specimens were mounted vertically so that the cracks were propagating downwards, but, for most of these specimens, the cracks closed over very short lengths at the crack tip. The failure of these cracks to close when the load was removed was attributed to particles, particularly fracture debris produced either during scratching or during subsequent crack propagation, falling into the crack and wedging it. For most of the experimental work, therefore, specimens were mounted vertically but the load was applied at the bottom end so that the cracks were propagated upwards. With this configuration the majority of the cracks closed over an appreciable length when they were unloaded. In many cases the cracks closed up to the end of the diamond scratch when the applied load was completely withdrawn.

The standard procedure followed in this investigation was to extend the crack slowly until it had run about three quarters of the specimen's length. The load then was gradually reduced until the crack closed. The load was then re-applied gradually until the crack appeared to repropagate.

The speed at which the crack appeared to repropagate or to close was determined for various loads by measuring the distance covered by the crack tip in a known time. The crack tip was observed through the telescope of a cathetometer which was fitted with both a vernier and a micrometer so that crack length increments could be measured accurately. To facilitate location of the position of the crack tip, the crack plane was

illuminated using a microscope lamp of variable light intensity, so that light was total internally reflected from the walls of the open crack*.

For crack velocities higher than 10^{-4} ms^{-1}, determination of the crack velocity was made by measuring the relative position of the crack tip on a sequence of frames of a cine-film of the crack motion taken with a Vinten 16 mm scientific camera.

6.9 Aging and heat-treatment of closed cracks

Crack repropagation tests were performed either within 5 minutes after the crack had closed, or after allowing the closed crack to age for various, much longer times. For aging times up to three days, the specimens were left mounted on the machines. For longer than this, the specimens were removed from the testing machine and were replaced for further testing after completion of a specified aging period.

In order to investigate the effect of heat-treatment of closed cracks upon the repropagation characteristics, specimens with closed cracks were heat-treated in air in an electric oven. Temperatures of heat-treatment ranged from 313 K to about 1023 K. The selected temperature was controlled to within ± 2 K. The specimens were always inserted into the oven at room temperature, the duration of heat-treatment after the temperature had reached the set level was standardized at 30 minutes. Slow rates (approximately 2 K/min) of heating and cooling were used.

---

* This arrangement led to the discovery of a faint reflection from the region of the closed portion of the crack. This particular phenomenon is described in the next chapter.

6.10 Experiments in different environments

Experiments on crack closure and repropagation were carried out in air, water, various organic liquids and gases, and in vacuum.

The majority of the experiments reported in this thesis were performed in air. No attempts were made to control either the temperature or the humidity, but the normal laboratory conditions provided a reasonably constant temperature at around 295 K and relative humidity between 50% and 70%.

In experiments in different liquids the double-torsion machine was inverted so that the specimen could be mounted below it and the initial crack propagated vertically downwards. The double-torsion machine was supported over a glass vessel containing the liquid so that the specimen could be immersed in the liquid up to the loading points.

The chosen liquids were water (tap and distilled), dimethylsulfoxide (DMSO) and paraffin. DMSO and paraffin were dried over molecular sieve, Union carbide type 5A (B.D.H. Ltd) and freshly drawn sodium wire respectively.

In some tests the cracks were unloaded while the specimens were immersed in the liquid and then were taken out of the liquid to dry and subsequently be treated before further repropagation tests.

For the tests in gaseous environments, inflatable glove bags were used. The double-torsion machine with the specimens and all the necessary accessories (weights, stands, etc) were inserted in the glove bag. The gas to be introduced inside the glove bag was first passed through a coiled pipe immersed in a liquid nitrogen trap. Amounts of freshly activated silica gel,

molecular sieve and sodium hydroxide were also introduced into the bag. The outlet of the glove bag was left open for about one hour while the gas inlet was open. In order to allow the system to reach equilibrium the experiments commenced at least an hour after sealing the glove bag. Test were carried out in this way in helium and nitrogen gas.

For the experiments in vacuum, a commercial coating unit (Speedivac 12E3, Edwards High Vacuum Ltd) was used. A small-sized double-torsion machine was clamped to one of the built-in stands of the vacuum chamber. Manipulation of the machine, that is, the loading-unloading procedure was achieved by means of a simple two-gear system attached to the built-in vacuum-sealed shaft. The latter allowed rotary mechanical motion to be transmitted from outside into the vacuum chamber. The system was calibrated so that for a measured rotation of the external drum (which rotates the vacuum-sealed shaft) the induced deflection between the two halves of the specimen could be calculated. The cover of the chamber was a bell-shaped transparent Pyrex glass which enabled direct optical observation of the specimen inside the chamber. During the measurements the backing, rotary pump was switched off in order to reduce vibration. The pressure achieved with this system was about 10^{-3} Nm^{-2}.

6.11 Optical techniques

Two optical techniques were used to study qualitatively the load bearing properties of closed cracks in the tested materials.

The first method was based on observations of the photoelastic

stress pattern at the tip of a crack when the crack was observed between crossed polaroid sheets. As the load applied to the specimen was increased, the photoelastic stress pattern at the crack tip spread out until the crack propagated. When the applied load was gradually reduced, the photoelastic stress pattern appeared to "shrink" and then to move backwards, that is, the crack was closing. On complete unloading, a small portion of the crack remained open and a residual photoelastic stress pattern could be seen at the tip of this open portion of the crack. On re-loading the closed crack, the photoelastic stress pattern could be seen to spread and eventually to move forwards, that is, the crack was repropagating along its closed portion.

The second optical method was based on observations of interference phenomena produced at the open portion of the crack. By suitable specimen arrangement and illumination (using the double-torsion machine stage-mounting device) a pattern of Fizeau fringes could be observed at the gap of the open crack. As the load was applied progressively the spacing between fringes decreased until the whole fringe pattern started moving forwards. This sequence of phenomena could be seen in reverse order when the load was progressively withdrawn: the moving fringe pattern stopped, the inter-fringe distance increased and eventually the whole fringe pattern moved backwards.

These two optical methods were used to demonstrate not only the load-bearing character of closed cracks but also the particular feature that cracks in glass can close against an applied load, i.e. crack closure occurs while the stress intensity at the crack tip (or equivalently the strain energy release rate*)

* The strain energy release rate is related to the stress intensity factor, K, via the equation $K = (GE)^{1/2}$, where E is Young modulus. (Plane stress).

has a finite value. Furthermore it was shown by these optical methods that there is a range of loads (above that required for closure) for which a closed crack remains stationary. A further increase in the applied load is needed to propagate the closed crack. The method based on photoelastic stress pattern observations was used in many stages of the present investigation, for quick inspection of the load-bearing character of a closed crack in certain specimens. It was also used to examine whether cracks can close in the epoxy resin used in this study. Crudely fractured specimens of this material examined between crossed polaroid sheets appeared to contain partially closed cracks which were load-bearing.

To the author's knowledge, this is the first time that crack closure has been observed at room temperature in an epoxy resin.

CHAPTER 7

RESULTS

7.1 Introduction

In the present chapter the main quantitative results and qualitative observations on the load bearing properties of the closed cracks are reported. The strain energy release rate has been chosen as the parameter to represent the load bearing capacity of the closed cracks. For these results, the strain energy release rate for crack propagation in virgin glass is denoted as G_v, the virtual energy release rate against which crack closure occurs (i.e. at negative crack velocity) is denoted as G_o and for any subsequent repropagation of a closed crack the strain energy release rate is denoted by G_r.

The results are presented in the form of graphs: of G_r, versus $\log_{10} v$ (where v is the crack speed) for crack repropagation tests in closed cracks aged for different times or heat-treated at a particular temperature; or in the form of G_r^* versus aging time, or G_r^* versus temperature of heat-treatment of the closed cracks, where G_r^* is the strain energy release rate at the arbitrary selected crack speed of 10^{-7} ms^{-1}.

Other results obtained from experiments in different environments are shown in the form of flow charts and tables.

Values of strain energy release rate were calculated using equations(6.7) and (6.8). In the case where the applied load was constant (equation (6.7)) the applied force, F, was measured and for a pulley of radius R,

$$F R = f m$$

Therefore, in equation (6.7), the product (f m) was substituted by (F R).

A part of the present chapter deals with a special feature, a faintly reflecting area, which appeared along the plane of closed cracks under certain experimental conditions.

7.2 Results in air

Figure 7.1 and 7.2 show the variation of G_r with crack repropagation velocity in air for soda-lime-silica glass specimens aged after crack closure for various times and for specimens heat-treated at 393 K respectively. Results from specimens heat-treated at temperature above 393 K and up to 823 K appear to lie on the same curve as those from specimens heat-treated at 393 K. On these graphs (7.1 and 7.2) there are also plotted results obtained for the initial crack propagation in virgin soda-lime-silica glass specimens, i.e. values of G_v. As can be seen excellent agreement with the results of the original investigation of Weidmann and Holloway (1974a) was found.

Each experimental point represents the mean value of crack velocity obtained from at least 8 crack propagation tests carried out on at least two different specimens at a constant value of G. The error bars printed in figures 7.1 and 7.2 represent the typical

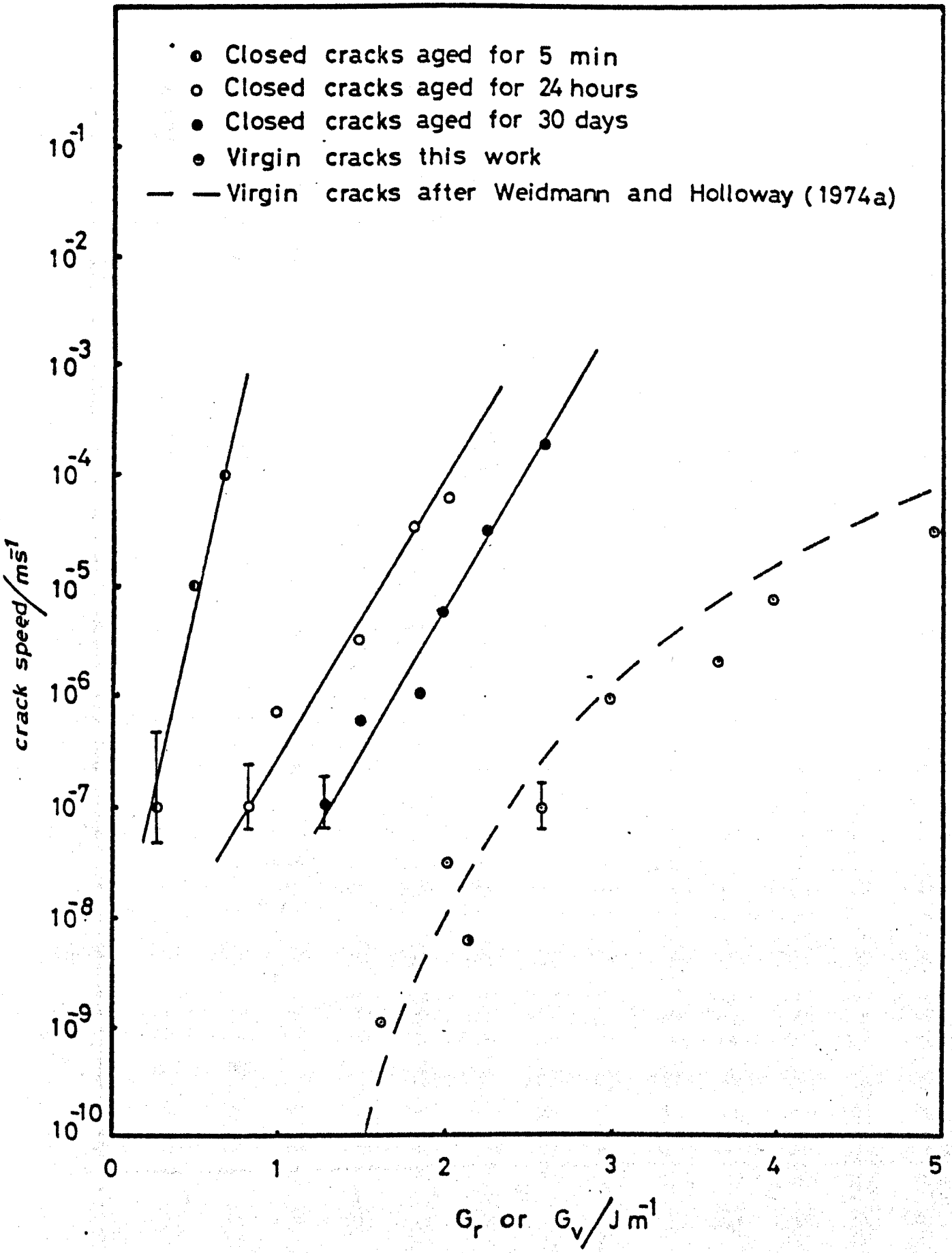

Figure 7.1 Variation of crack speed with G_r and G_v in air, for aged closed cracks and for virgin cracks respectively, in soda-lime-silica glass.

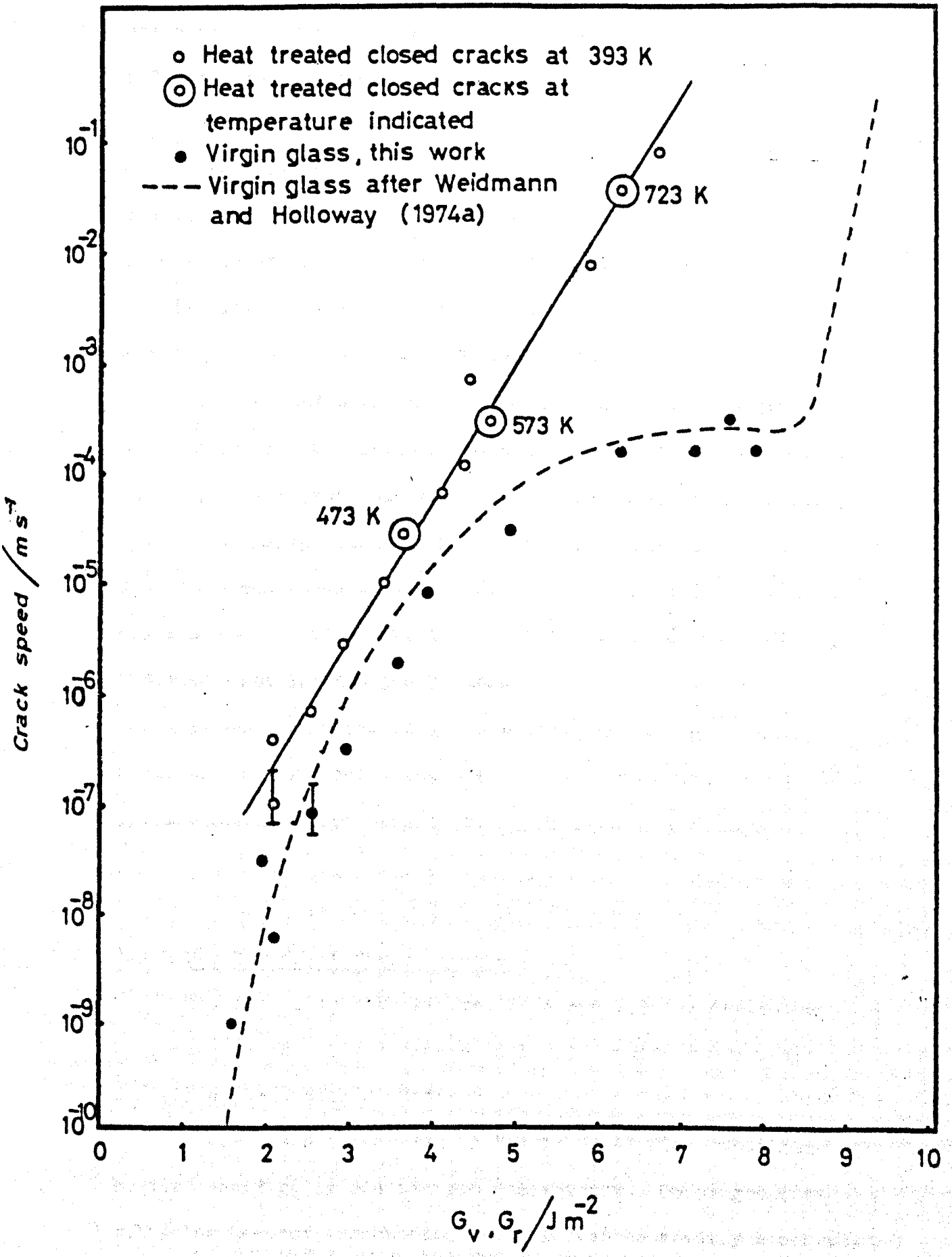

Figure 7.2 Variation of crack speed with G_r and G_v in air, for heat-treated closed cracks at 393 K and above and for virgin cracks respectively in soda-lime-silica glass.

value of the total scatter in the crack velocity value, observed under constant value of G_r or G_v.

Figures 7.3 and 7.4 show the variation of the strain energy release rate, G_r^*, required to cause repropagation of the closed crack at $\sim 10^{-7}$ ms^{-1} with aging time and temperature of heat-treatment of specimens of the three types of glasses. (No detectable difference was observed between results from experiments with fused and synthetic silica glasses).

By contrast with the results for the inorganic glasses, the strain energy release rate, G_r, in crack repropagation tests in epoxy resin specimens was found to be independent of aging time up to aging times of four months. Values obtained for G_r^*, for unhardened Araldite CT200 were identical - within the experimental scatter - with that obtained for CT200 partially hardened with 3, or 5 pph hardener.

It was not possible to heat-treat specimens of epoxy resin because the softening point of this material is very low. Specimens can deform even by being in contact with hands.

7.3 Results in different liquids

The flow charts in figures 7.5a and 7.5b summarize the behaviour of the closed cracks in liquid environments under certain experimental conditions.

Cracks were propagated in Virgin Float glass specimens in the specified liquid at room temperature. On progressive unloading however, crack closure could not be readily observed. Observations then were carried out placing the immersed specimen between crossed polaroid sheets. When water was used as the

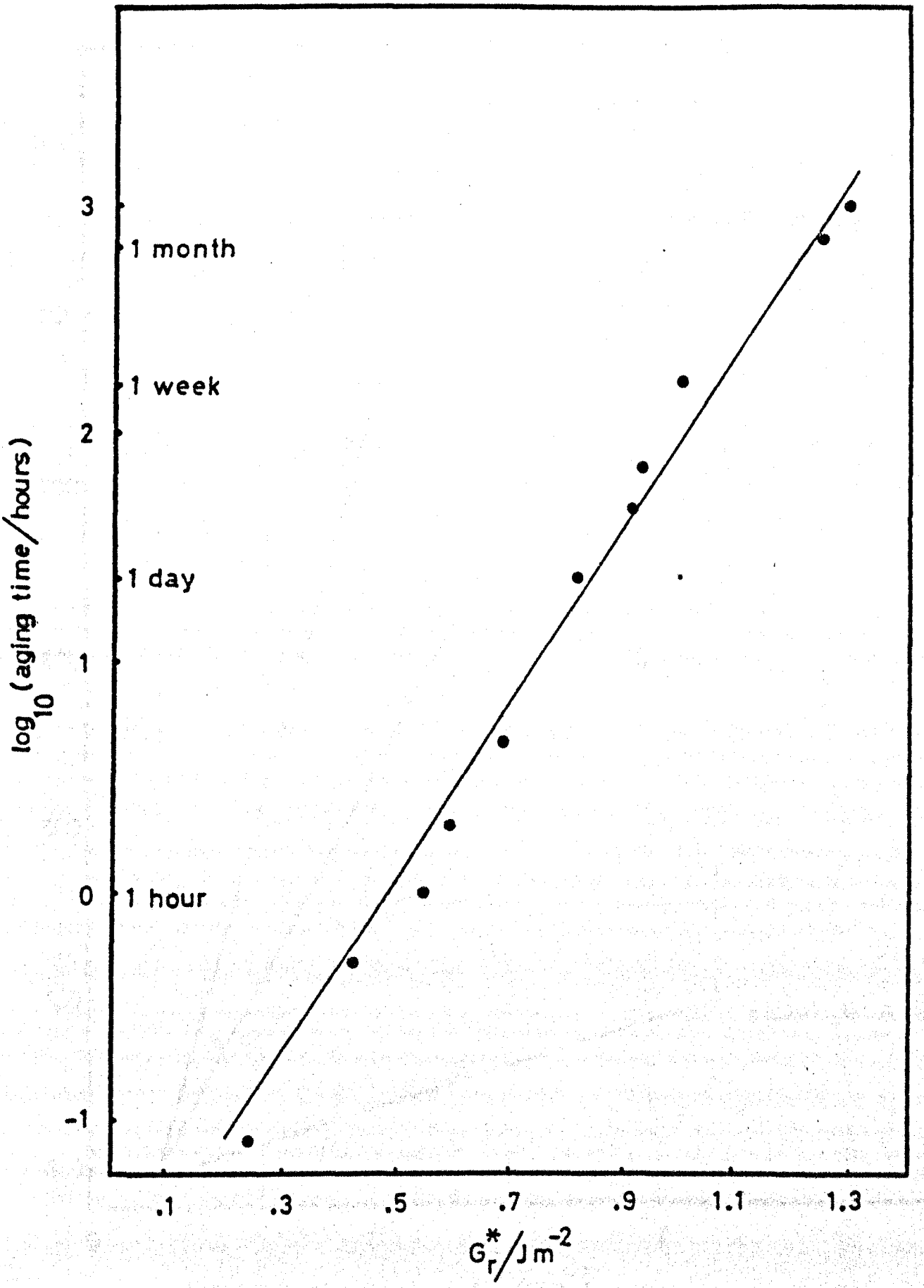

Figure 7.3 Variation of G_r^* with aging time in air in soda-lime-silica glass.

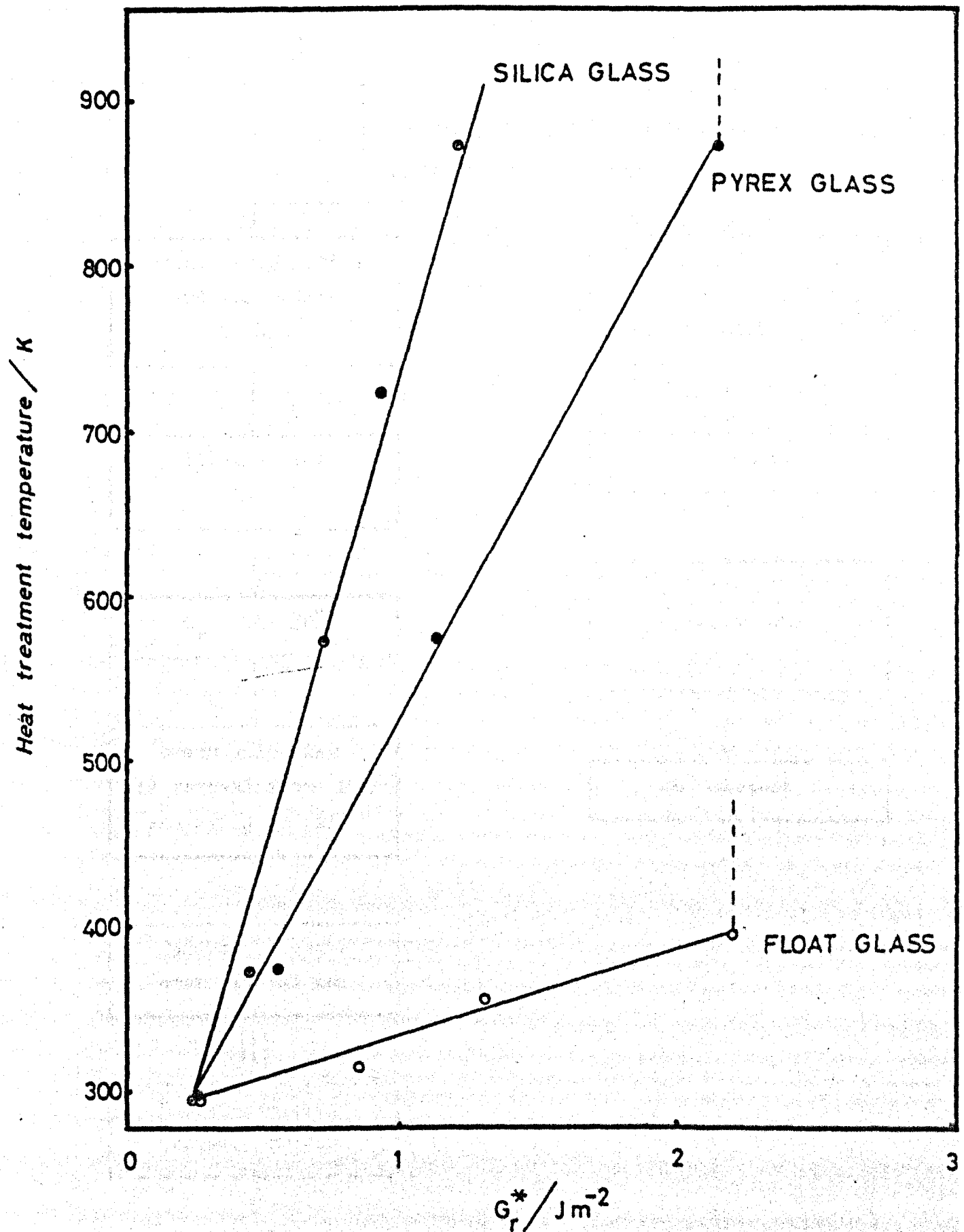

Figure 7.4 Variation of G_r^* with temperature of heat-treatment of closed crack in air. The dashed lines indicate no further increase of G_r^* with temperature. (Duration of heat-treatment 30 min).

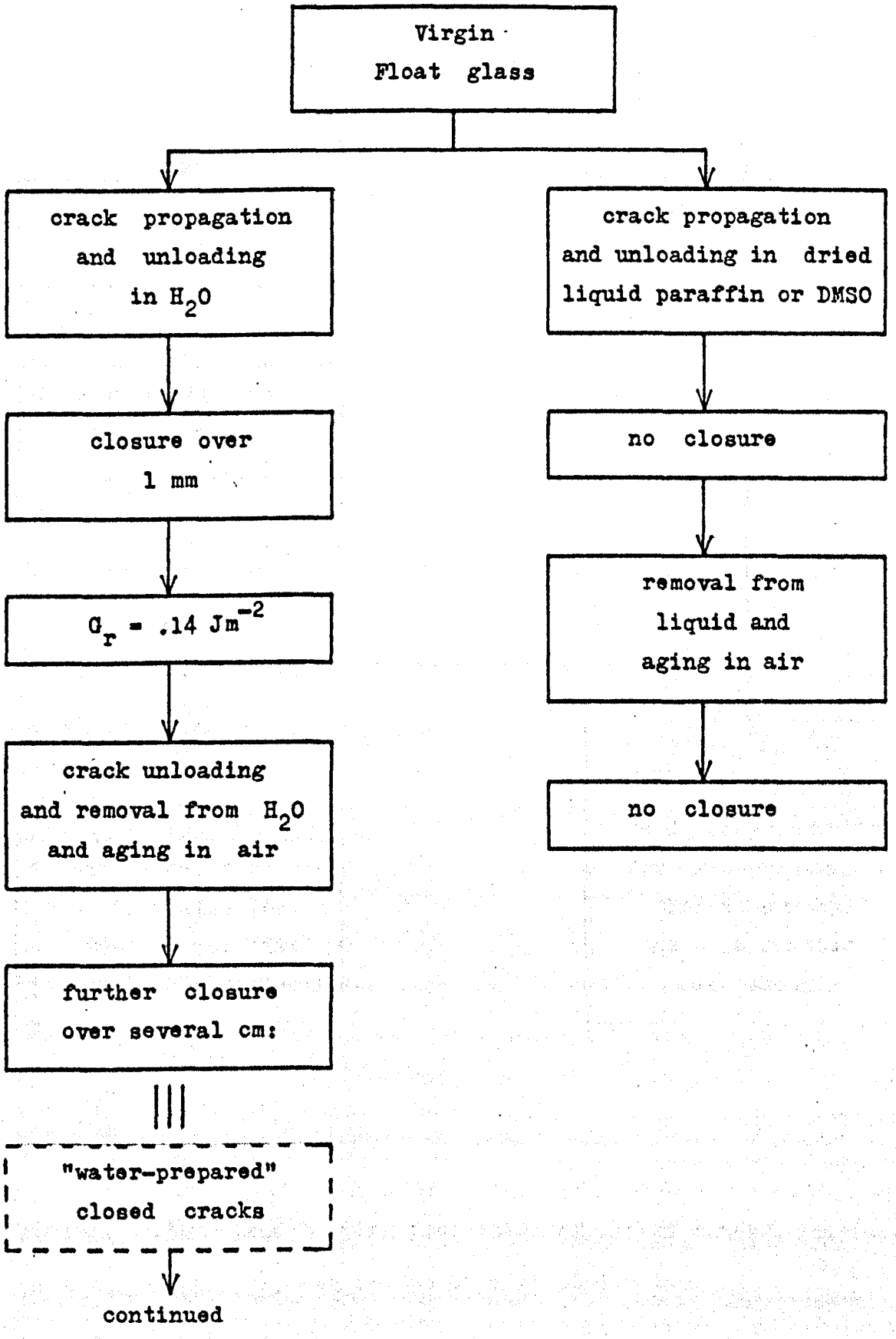

Figure 7.5a Closure characteristics of cracks in liquid environments.

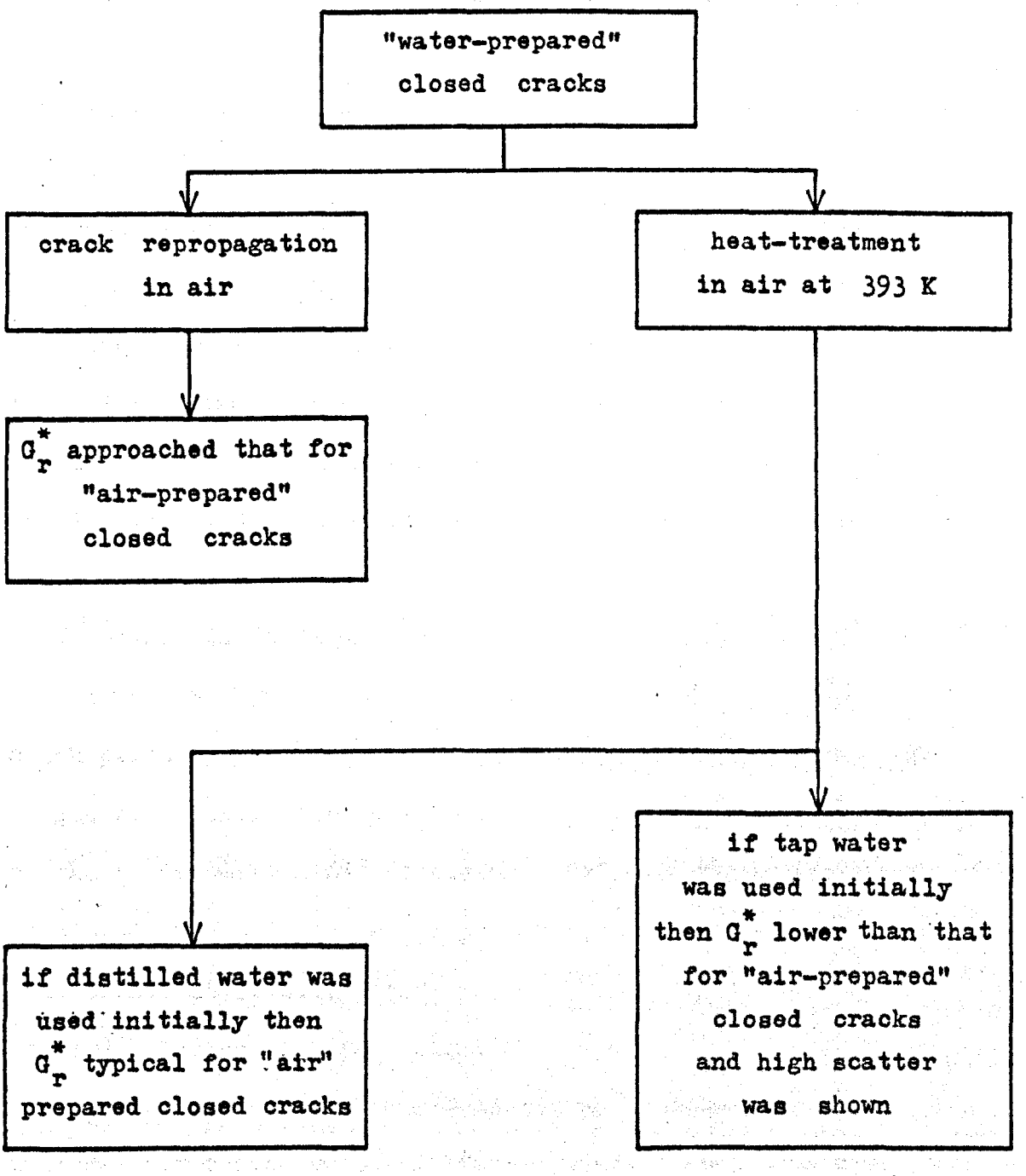

Figure 7.5b Load bearing properties of closed cracks, initially prepared in tap or distilled water.

immersion liquid some of the cracks appeared to close over approximately 1 mm from the original crack tip. No closure was observed when other liquids were used. The strain energy release rate to re-open this short, closed portion of the crack was 0.14 Jm^{-2}. No further closure could be seen when the unloaded crack remained immersed in the liquid. In a number of Float glass specimens, cracks were propagated in water and then taken out of the water and allowed to dry and age in the laboratory atmosphere. Specimens so prepared will be called hereafter "water-prepared" specimens, and specimens in which the initial crack was opened and closed in air will be called "air-prepared" specimens.

Cracks in "water-prepared" specimens closed further as they dried and aged in air. Interference fringes formed in the crack plane by the layer of water eventually disappeared. The length over which these cracks closed was typical of the closed cracks in "air-prepared" specimens. Subsequent repropagation of closed cracks in "water-prepared" specimens after aging or heat-treatment revealed that

i) G_r^* increases with aging time

ii) After aging for about 24 hours, G_r^* reaches the value measured for closed cracks in "air-prepared" specimens aged for the same period of time.

iii) "water-prepared" specimens heat-treated at 393 K showed a value of G_r^*, indistinguishable from that measured in "air-prepared" specimens heat-treated at the same temperature. When tap-water was used for the preparation of closed cracks instead of distilled water, the value of G_r^* was approximately 30% lower than in the previous case, and a larger scatter occured in the

results.

Cracks opened initially in liquid paraffin or DMSO and then unloaded and removed from the liquid did not show any tendancy to close at all.

7.4 Results in vacuum and in dry gases

The flow chart in figure 7.6 summarizes the behaviour of closed cracks formed in dry gaseous environments or vacuum.

The initial crack propagation was made in virgin Float glass specimens. The strain energy release rate, G_v, was found to be 9 Jm^{-2}. In these environments, a small increment in the value of G_v, resulted in a large increment in crack speed. This characteristic and the value obtained for G_v, agrees very well with published data by earlier investigators (e.g.Schönert and Umhauer and Klemm,1969; Weidmann and Holloway, 1974a; Lawn and Wilshaw, 1975) for crack propagation in soda-lime-silica glass in dry environments.

In the dry environments used in this investigation the cracks appeared to close down as the applied load was reduced. In subsequent repropagation tests, G_r, was found to be 1.3 Jm^{-2}. Cracks closed in vacuum and in dry gases were allowed to age up to 4 hours in the same environment and then tested; the previously obtained value of G_r, 1.3 Jm^{-2},was again obtained.

If air was allowed into the chamber while a specimen containing a closed crack was mounted on the double-torsion machine but without any external load applied to the specimen, some cracks appeared to close further over a few millimetres. Subsequent repropagation in air revealed that the strain energy

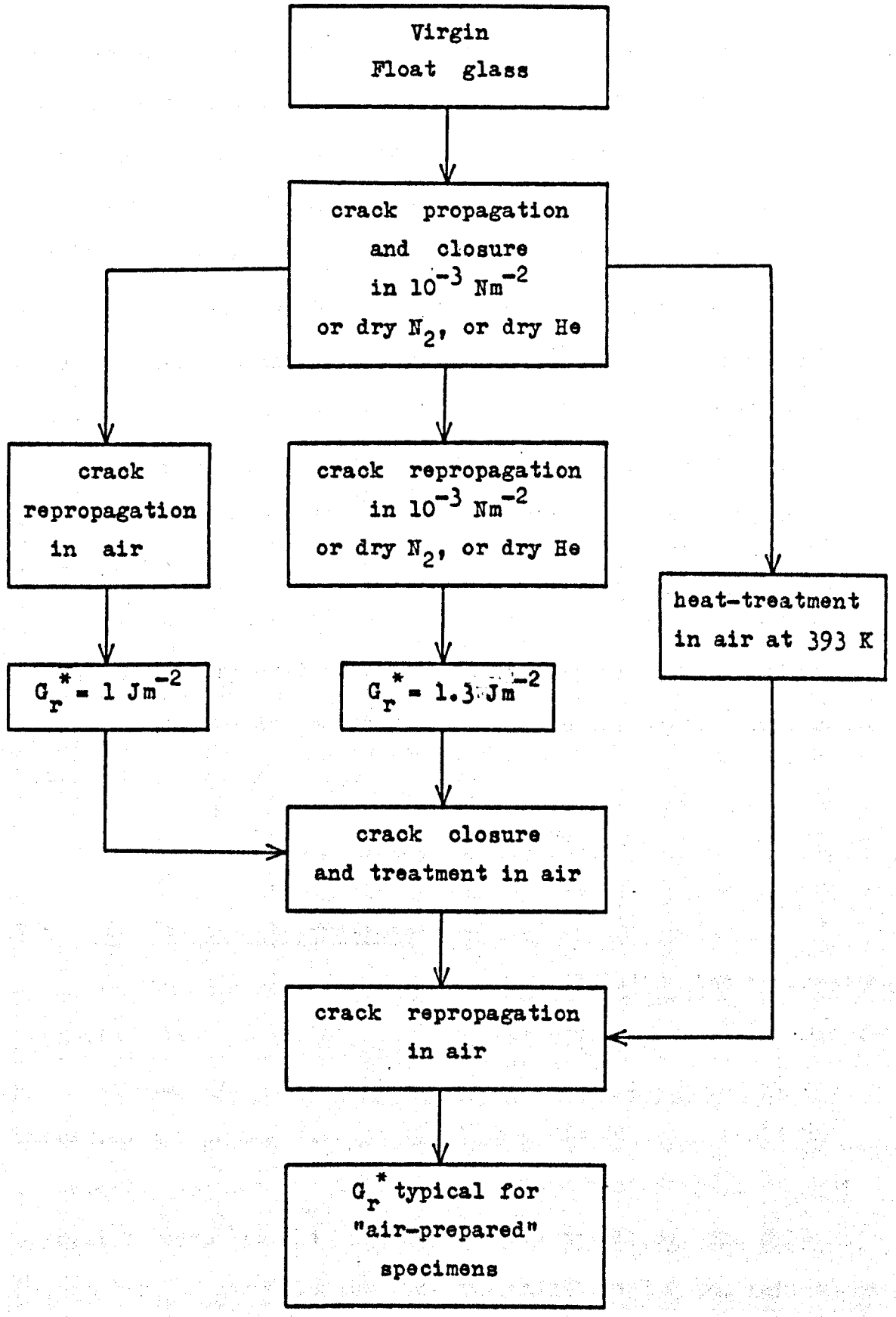

Figure 7.6 Load bearing properties of closed cracks initially prepared in dry environment.

release rate, G_r^*, for repropagation of the portion of the crack which had been closed by admission of air into the chamber is the same as for crack repropagation in an "air-prepared" specimen. But the rest of the closed crack length, which had been closed in vacuum, could be re-opened only by applying a much higher load corresponding to a strain energy release rate of approximately 1 Jm^{-2}. Closed cracks prepared in vacuum or in dry gases and subsequently heat-treated at 393 K could be repropagated in air at a load corresponding to a value of $G_r^* = 2.2\ Jm^{-2}$, i.e. the value obtained from repropagation tests in "air-prepared" specimens.

A summary of the values of G_r, obtained for different materials and under different experimental conditions is shown in table 7.1.

The value of strain energy release rate, G_c, against which an open crack appeared to close slowly (negative velocity) was also recorded for different glasses and in different environments. Table 7.2 summarizes these results.

7.5 Qualitative observations

In the following paragraphs some qualitative but interesting phenomena observed in the course of the present study are reported.

It has been noted that specimens in which cracks had undergone a repropagation test and then closed again could be allowed to age or be heat-treated and then tested again without special concern for the "history" of the specimen. The only information of significance, i.e. the only "step" which influenced the repropagation behaviour, was the treatment of the specimen after the last crack closure.

Table 7.1

Values of strain energy release rate, G_r^*, in Jm^{-2} obtained for repropagation of closed cracks under specified test conditions

Material	Aging time in air			Environment	
	5 min	7 days	30 days	water(1)	dry gas(2)
Float glass	0.25	1.05	1.25	0.14	1.30
Pyrex glass	0.25	0.45	0.55	——	1.30
Silica glass	0.25	——	0.35	——	——
Araldite CT200(3)	0.25	0.25	0.25	——	——

(1) Refers to repropagation tests on closed cracks formed and tested under the same environment.

(2) Refers to vacuum (10^{-3} Nm^{-2}), or dried nitrogen, or dried helium gas.

(3) Refers to pure Araldite CT200, or CT200 partially hardened with up to 5 pph hardener.

Table 7.2

Values of strain energy release rate, G_c, in Jm^{-2} obtained in crack closure tests[1] under specified environment

Material	Water	Air	Dry gas[2]
Float glass	0.1	0.17	0.1
Pyrex glass	—	0.15	0.1
Silica glass	—	0.15	—
Araldite CT200[3]	—	0.15	—

(1) The cracks were closing at a very slow rate (appoximately 10^{-7} ms^{-1}).

(2) Refers to vacuum (10^{-3} Nm^{-2}), or dried nitrogen, or dried helium gas.

(3) Refers to pure CT200, or CT200 partially hardener with up to 5 pph hardener.

The above feature of the behaviour permitted economical use of specimens particularly of Pyrex and silica which were available either in small quantities only, or required laborious preparation. With these materials up to three closure-repropagation cycles were performed in a single specimen.

As mentioned previously, a microscope lamp was used to facilitate detection of the crack tip position. When the lamp was operated at high light output, it was observed that some of the closed cracks exhibited a faintly reflecting area which extended from the tip of the residual open crack to the tip of the original crack. The photograph in figure 7.7 shows a specimen displaying this feature.

The faintly reflecting area has been observed in closed cracks on all the materials examined but only under certain circumstances:

i) The faintly reflecting area could be seen either after a crack had been opened and closed several times in the laboratory atmosphere or after the crack had been remained opened for approximately one minute before closure.

ii) It could be seen at small angles, θ, of glancing incidence. When θ was above a "critical" value the faint reflection could not be seen.

iii) All "water-prepared" closed cracks in glass displayed the faintly reflecting area. In these particular specimens, the feature appeared as soon as the water layer inside the crack dried out and it was brighter - as far the human eye could judge - than in "air-prepared" specimens.

On the other hand, the faint reflecting area did not appear in specimens, where the crack formed in air and was left open

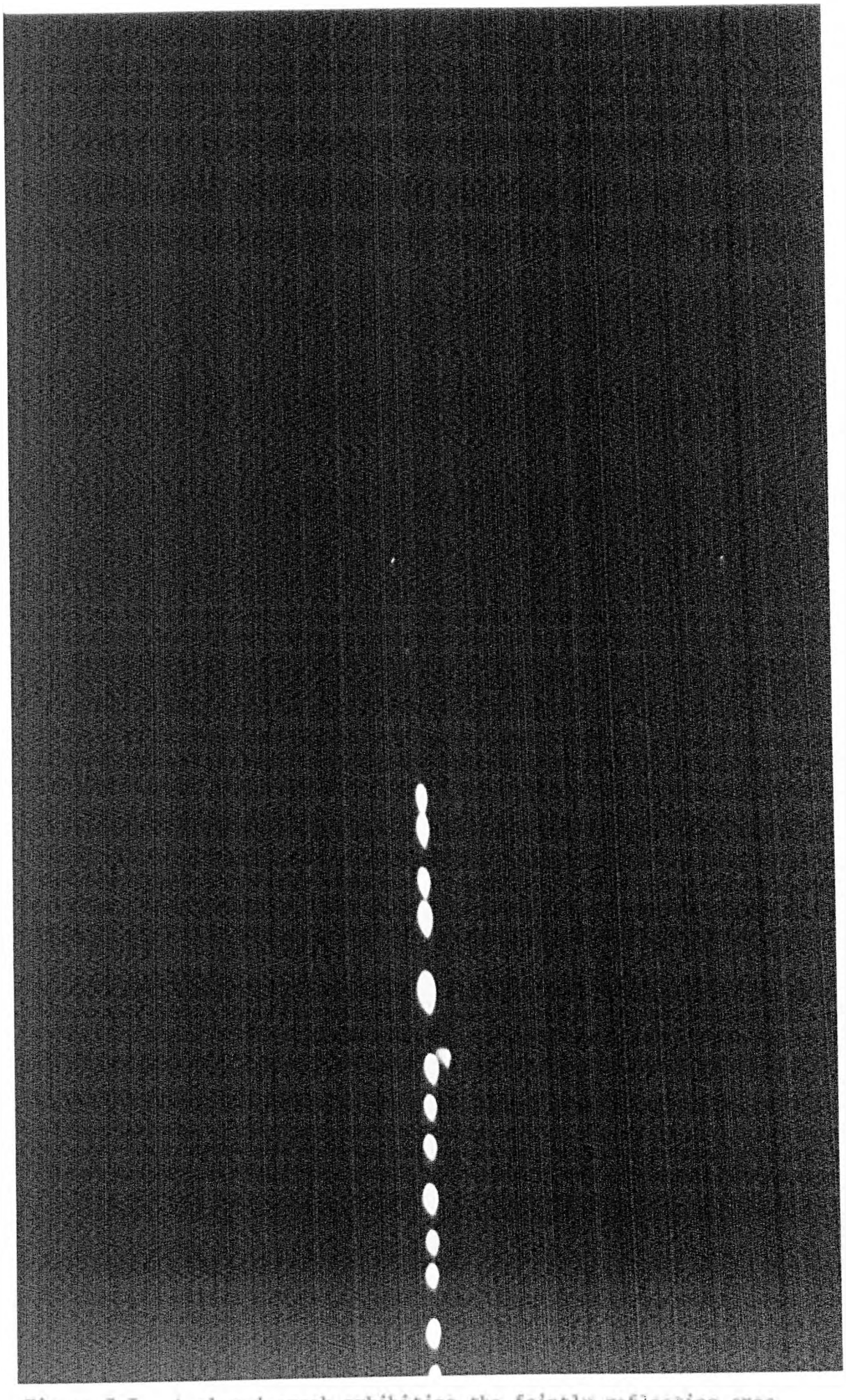

Figure 7.7. A closed crack exhibiting the faintly reflecting area.

only for a few seconds before closure, nor in specimens where the cracks opened and closed in vacuum, or in other dry gaseous environments.

However, the presence and the appearance of faint reflecting areas did not appear to influence the values of strain energy release rate, G_r and G_c.

Once the faint reflecting area has appeared it was not possible to remove it. It remained, apparently unaltered, after the specimens had undergone heat-treatment at temperatures above the softening point of the material (e.g. 973 K for soda-lime-silica glass and approximately 313 K for the epoxy resin Araldite CT200).

7.6 Identification of the faint reflecting area.

Although the results obtained (the values of G_r^*) were found not to depend on the presence of the faintly reflecting area, it was thought that information about the nature and the properties of this feature might be of importance in understanding the basic processes responsible for the load-bearing of the closed cracks. Several techniques were, therefore, employed in order to seek information about the observed faint reflecting area.

The possibility of obtaining interference effects was sought initially. Specimens with closed cracks showing the feature were mounted in the double-torsion machine attached to the stage-mounting device for microscopic observations. The illumination system was suitably arranged in order to observe possible thin film interference in reflection. Under these

conditions, however, it was not possible to detect any interference effects in the area beyond the tip of the open crack, although excellent fringes were obtained in the open portion of the crack.

Specimens showing the faintly reflecting area were then mechanically sectioned by scribing with a diamond perpendicular to the plane of the closed crack, and subsequently bending the specimen. This sectioning was intended to expose a cross-section of the faint reflecting area to be observed under phase contrast illumination. If a closed crack, showing a faintly reflecting area, was in the form of a film whose thickness was at least a quarter of a wavelength of the visible light, and its refractive index was slightly different from that of the bulk glass, it ought to be resolved by this technique. But the results were again negative: no optically detectable feature was found to correspond to the position of the reflecting area (even under phase contrast illumination of the sectioned specimens).

Sectioned surfaces normal to the plane of the faint reflecting area were sputter-coated with gold and then examined in a scanning electron microscope (Cambridge S4 - 10). But again nothing could be seen, even when the scanning electron microscope was operated at high magnification where the resolving power was about 250 Å.

The conditions under which the faint reflecting area appears, in conjuction with the results of the above attempts would be explicable if it were assumed that the faint reflecting area is a film whose thickness is a very small fraction of the wavelength of visible light. Also, the fact that the feature could be seen only at small angles of glancing incidence suggests that the effect is related to the phenomenon of frustrated total

internal reflection.

The frustration of total internal reflection occurs when electromagnetic radiation is incident on a sequence of media: dense-rare-dense at an angle greater than the critical angle at which total internal reflection would occur at the first dense-rare interface. When the thickness of the rare medium is less than about a wavelength of the electromagnetic radiation, a fraction of the incident energy is transmitted into the third medium (dense) rather than all being reflected at the first dense-rare interface. The amount of the transmitted energy is determined by the thickness of the rare medium; the smaller the thickness the greater the transmitted energy.

The circumstances under which the faintly reflecting area appears may suggest that this feature is due to adsorption and subsequent interaction of environmental species, water molecules in particular, on the freshly produced crack surfaces. A discussion on the nature of the faintly reflecting area is presented in the next chapter. As a matter of brevity the faintly reflecting area will be called hereafter film.

7.7 Estimation of the thickness of the film

An estimate of the thickness of the film can be made from measurements of the relative intensity of light, R, reflected from the film if the film is assumed to be a layer of uniform refractive index, n_f, between two glass plates of refractive index n_g, ($n_g > n_f$). The expression which relates R with the thickness of the film, d, is*

* The derivation of this expression is given in the appendix III.

$$R = \frac{1}{2}\left(\frac{\pi d}{\lambda n_g \cos\theta}\right)^2 \left[\left((n_f\cos\theta)^2 - (n_g Z)^2\right)^2 + \left((n_f Z)^2 - (n_g\cos\theta)^2\right)^2\right] \quad (7.1)$$

where

$$Z = \left[\left(\frac{n_g}{n_f}\right)^2 \sin^2\theta - 1\right]^{\frac{1}{2}} \quad (7.2)$$

where θ is the angle of incidence and λ is the wavelength of light.

The magnitude of R can be determined experimentally, θ and n_g are known but the refractive index of the film, n_f, is unknown. It is possible however to assume reasonable values for the refractive index, n_f, so that calculation of the film thickness becomes possible.

It has already been hinted that the film is probably due to adsorption (and subsequent interaction with the glass surface) of water molecules and because it appeared in all the examined materials it can be argued that the film has the same optical properties in all the materials examined. Clearly, the film in silica glass must have a refractive index lower than 1.46 ($= n_g$ of silica glass). In the present discussion the film thickness will be calcualted for two extreme values of n_f : 1.45 and 1.35.

In practice the experimental measurement of R proved to be far more difficult than was thought initially: A Float glass sample exhibiting the film was mounted on the table of a simple bench spectrometer with the direction of the film length normal to the stage of the spectrometer. Intense light was passed through the collimator onto the film and the faint reflection was detected through the telescope of the instrument. Measurements of the light intensities were made with an electronic photometer*.

However, early attempts to obtain a measurable intensity

* CdS exposure meter (Watson & sons Ltd)

of the light reflected from the film in "air-prepared" Float glass specimens failed. This major problem was overcome when "water-prepared" Float glass specimens aged for over 30 days and which exhibited relatively brighter films were used.

The angle of incidence (air-glass interface) was chosen arbitrarily so that the angle of incidence θ corresponding to the glass-film interface was 75°. Unfortunately it was not possible to investigate the variation of R with the angle of incidence: on rotating the table of the instrument (and of course the telescope about their common vertical axis) the reflection could not be received through the telescope. This was probably due to the fact that the plane of the film was not perfectly aligned with the vertical axis of the instrument. But for small rotation up to $\pm 2^{\circ}$ no detectable difference could be observed in the value of R.

The mean value of R obtained under these conditions from six measurements on two different specimens was

$$R = (1 \pm 0.3) \times 10^{-4}$$

Solving equation (7.1) for d and using this value for R and $\theta = 75^{\circ}$, $n_g = 1.51$ and $\lambda = 555$ nm it is found that

$d_1 = 5.6 \pm 0.8$ nm if $n_f = 1.45$ and

$d_2 = 3.2 \pm 0.5$ nm if $n_f = 1.35$

Certainly, the value of R for "air-prepared" specimens should be much smaller than that measured above in "water-prepared" closed cracks, so if it is assumed that $R = 1 \times 10^{-5}$ the values of d become $d_1 = 1.8$ nm and $d_2 = 1.0$ nm respectively. The above values of d must be regarded as rough approximations only. The assumptions made throughout the calcualtions and

particularly the intrinsic difficulties encountered in the measurement of R prevented any accurate determination of the film thickness and any hope for examination of a possible film "growth" or change in general terms with aging time.

It must be emphasized that the assumed film would not be necessarily a single layer of material of uniform refractive index deposited on the fracture surfaces of a closed crack as assumed in the calculation above. There are reasons to believe that the film is due to compositional changes occurring in the glass near the fracture interface and due to the adsorption water from the environment. Further discussion on this matter is given in the next chapter.

CHAPTER 8

DISCUSSION

8.1 Introduction

In this chapter results and observations reported in the part II of this thesis will be discussed and a possible interpretation will be sought.

Initially the results reported by earlier authors are discussed briefly and this is followed by a consideration of several mechanisms which might have been thought to be responsible for the formation of load-bearing closed cracks. Then the phenomena associated with the interaction of water with glass are discussed briefly and this leads to an attempt to interpret qualitatively the load-bearing properties of the closed crack in terms of the chemical reactivity of the water-glass system.

The concluding section, both of this chapter and of this thesis summarises the main conclusions that can be drawn from the studies of part I and II of this thesis.

8.2 Previous work

The methods and observations of earlier investigators on crack closure are reported in chapters 5 and 6. Among them there are two investigations in which quantitative results on "crack healing" are reported and, as has already been mentioned, these results are believed to be unreliable. Reasons for this belief are given below where the experimental procedures used to obtain these results are discussed in detail.

Cheesman and Lawn (1970) reported an investigation on closure and healing of Herzian cone cracks (figure 1.3). A Herzian cone crack is produced when the surface of a relatively brittle material is indented by a small hard spherical indenter. The radius of mutual contact between the indenting and indented materials is given by

$$a = kP^{1/3} \tag{8.1}$$

where P is the load on the sphere, and k is a function of the radius of the indenter and the elastic constants of the indenting and indented materials.

At some critical load, P_c, the elastic limit of the specimen is exceeded. As a result a circular crack initiates just outside the mutual contact zone which propagates into the bulk of the specimen forming a cone-shaped crack. Closure and "healing" of these cracks were studied by Cheesman and Lawn in soda-lime-silica glass under normal laboratory conditions. However, on unloading, these cracks did not show any tendency to disappear.

Then the authors subjected the cone cracks either to a compressive stress or to heat-treatment, where upon some of the cone cracks closed and showed load-bearing properties. In the

first case, unloaded cone cracks were subjected to a compression by a larger ball indenter so that the whole cone crack was within the compressive zone induced by the large loaded indenter. After maintaining the compression for some time - up to 3 hours - the large indenter was replaced by the original (smaller) one and the loading cycle was restarted.

In the second case, freshly formed cone cracks were heat-treated in a nitrogen atmosphere for various times. The temperature of heat-treatment ranged from 473 to 873 K and the duration of heat-treatment ranged from 1 hour to 7 days.

In order to characterize the "degree of healing" which might have occured, Cheesman and Lawn introduced a "healing parameter", H, defined as the ratio of the critical contact, radius a_{c2}, at which the treated crack re-appeared suddenly, to the critical contact radius, a_{c1}, at which the cone crack developed originally, i.e.

$$H = \frac{a_{c2}}{a_{c1}} \qquad (8.2)$$

Genuine healing as defined earlier in this thesis i.e. total restoration of the original structure and bonding, would give H = 1 and zero healing H = 0. Genuine healing was never observed. For three cone cracks subjected to a compression the healing parameter found to increase from 0.7 to 0.8, as the duration of compression increased from 10 s to a few hours.

No systematic results were obtained from experiments on heat-treated cone cracks. For instance, for three cone cracks heated at 473 K for one hour, the healing parameter was found to be 0.87, 0.79 and 0 respectively; for another set of three cracks

heated at 673 K for 24 hours, the healing parameter was found to be 0.64, 0.83 and 0 respectively.

In the author's opinion the definition of the healing parameter, (equation (8.2)), is rather misleading, that is, it does not represent the load bearing capacity of the closed cracks. It can be argued that the ratio of the fracture energies, G, gives a much better indication of the "degree of healing" than the ratio of radii of the areas of contact. In this case, because $G \propto P_c^2$ and $P_c \propto a_c^3$ the load bearing capacity can be defined as

$$h = \frac{G_2}{G_1} = \left(\frac{a_{c2}}{a_{c1}}\right)^6 \qquad (8.3)$$

It is obvious that the values quoted by Cheesman and Lawn for H will be reduced if the above definition (8.3) is adopted. For example a value of H = 0.64 would correspond to h = 0.068 and a value H = 0.9 would correspond to h = 0.53.

Despite the fact that the actual quantitative results quoted by Cheesman and Lawn are inconclusive, they do suggest that time and temperature improve the adhesion between the opposite crack faces.

Perhaps, more comparable with the present work is the work of Wiederhorn and Townsend (1970). The experimental procedure adopted by these authors was as follows. Small cracks were initiated in soda-lime-silica microscope slides by a method similar to that described in the present thesis. Crack growth and closure were induced in two different ways. Firstly, the cracks were forced to propagate in double-torsion mode by hand manipulation of the specimens in air or in an atmosphere of "superdry nitrogen". These cracks were observed to close partially as the force applied by the fingers was removed.

Secondly, specimens were placed in a small chamber containing "superdry nitrogen" and "shaken randomly". According to these authors, this mechanical shock resulted in an extension and rapid closure of the short pre-existing cracks.

Specimens containing closed cracks formed in these two ways were tested in a double-cantilever cleavage machine in an atmosphere of "superdry nitrogen". The energy required to repropagate these closed cracks could not be calculated directly as in the case of virgin specimens, but special techniques had to be used. There were two problems encountered in Wiederhorn and Townsend's work. Firstly, the cracks always deviated from the midline of the specimens towards one side, figure 8.1. Therefore in repropagation tests the crack had to follow the pre-existing off-the-midline direction. The authors assumed that the fracture energy at the point B (see figure 8.1) for instance, for a crack repropagating along the curved line AB is equal to that when the crack propagates along the straight line CB. So they carried out calibration measurements on specimens containing cracks lying varying distances, d, away from the midline of the specimen. The results from the calibration measurements were used to "correct" the fracture energy obtained from the repropagation of the curved closed cracks.

The second problem arose from the shape of the front of the closed cracks. The shape of the crack front as depicted by Wiederhorn and Townsend, figure 8.2, resembles that of the double-torsion cracks i.e., there is always a web of unbroken glass of considerable thickness near one surface of the specimen. So that when the specimen was loaded in the double-cantilever cleavage configuration, both the closed portion and the unbroken

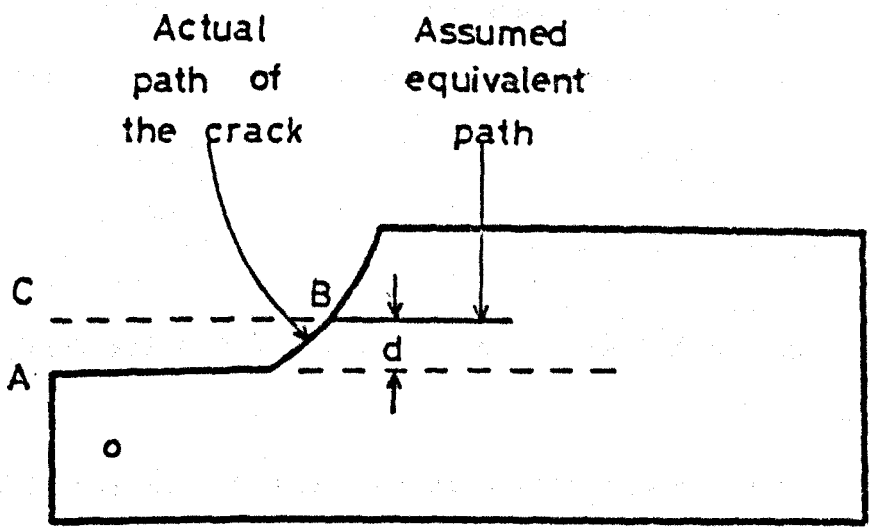

Figure 8.1 Diagram illustrating method of correction for out-of-midplane crack propagation used by Wiederhorn and Townsend (1970).

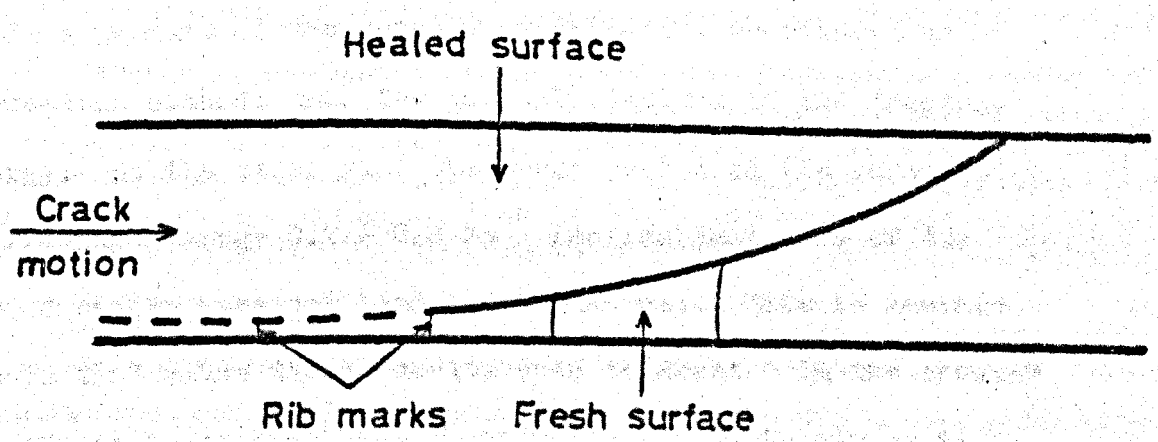

Figure 8.2 Sketch of fracture surface obtained by Wiederhorn and Townsend (1970).

glass web were being opened. Wiederhorn and Townsend estimated the fraction of the total energy used for repropagating the closed portion of the crack by measuring the thickness of the unbroken region after the specimen had been completely cleaved. The so-obtained values were $2.3 \pm 0.3\ Jm^{-2}$ for cracks induced by mechanical shock and $0.2 \pm 0.2\ Jm^{-2}$ for cracks induced by slow loading.

A direct comparison of these results with those found in the present investigation is very difficult indeed. The high value of fracture energy for repropagation of cracks which were closed quickly in a dry environment is ~ 4 times higher than that found in the present study in closed cracks formed (by relatively slow loading) and repropagated in vacuum or in a dry gas. However it cannot be appreciated whether the high value of fracture energy reported by Wiederhorn and Townsend is due to the higher load bearing capacity of the closed cracks or is a product of the complex experimental procedures and correction methods used for the calculations of the fracture energy. On the other hand the error quoted in the lower value of fracture energy $0.2 \pm 0.2\ Jm^{-2}$ implies that some of the closed cracks were not load-bearing at all. This is another reason that makes these results open to doubt. In the present investigation no crack was found which closed in air or in vacuum or in a dry gas and which was not load-bearing. All cracks closed under these conditions exhibited measurable load-bearing capacity.

Unlike the earlier reported results in glass, the results reported by previous authors for the load bearing capacity of closed cracks in mica seem to be more comparable with those

obtained in the present work: Namely, Bailey (1961) reported that in the case of crack repropagation in mica in air, the fracture energy was $G_r = 0.5\ Jm^{-2}$ at a crack repropagation velocity of 2 to 3 x 10^{-5} ms^{-1}. As shown in the graph of figure 7.1 the value of G_r for freshly formed closed cracks in soda-lime-silica glass corresponding to crack speed of 2 to 3 x 10^{-5} ms^{-1} is approximately 0.5 Jm^{-2}, that is, the same as that found by Bailey in mica. Bryant (1962) reported that in mica crystals the value of G_r is 0.3 Jm^{-2}. This author did not report the speed of the repropagating cracks, but he pointed out that more rapid separations required more energy.

Values of G_r in air reported by different authors (including the present one) for different materials are summarized in table 8.1.

Table 8.1

Investigation	Material	G_r / Jm^{-2}		
		at ~ 10^{-7} ms^{-1}	at ~ 10^{-5} ms^{-1}	unspecified
Bryant (1962)	mica	—	—	0.3
Bailey (1961)	mica	—	0.5	—
Present work	Float glass	0.25	0.5	—
Present work	Pyrex glass	0.25	—	—
Present work	Silica glass	0.25	0.5	—
Present work	Araldite	0.25	—	—

In view of those results it will be argued later in this chapter that the initial load bearing capacity of closed cracks in a

variety of materials can be explained by a common mechanism independent of the test material. The subsequent development of the load-bearing capacity of the closed cracks (i.e. the rate of change of G_r^* with aging time and with temperature) is dependent upon the nature and composition of the material.

8.3 Discussion of possible mechanisms for the formation of load-bearing closed cracks.

a) Initial load-bearing capacity of the closed crack.

The value of $G_r^* = 0.25\ Jm^{-2}$ measured in freshly closed cracks in air was found to be an order of magnitude smaller than the value of G_v ($\simeq 2.5\ Jm^{-2}$) for crack propagation in virgin silicate glasses. This fact alone can rule out the possibility that genuine crack healing can be responsible for the load-bearing capacity of the closed cracks in air.

It has been argued in chapter 5 of the present thesis that atmospheric contamination of the crack faces can be a major obstacle for the occurrence of genuine crack healing. For the cracks formed by slow loading in air it is certain that the crack faces are contaminated soon after they are formed. It appears interesting to calculate the time, t, taken for a monolayer of gas molecules to adsorb on a freshly formed crack surface at a distance L from the crack opening, figure 8.3. In the calculation below it will be assumed for simplicity that a double-torsion crack in glass held under load is suddenly exposed to a gaseous atmosphere and that each molecule striking the surface is permanently adsorbed (i.e. the sticking coefficient is 1).

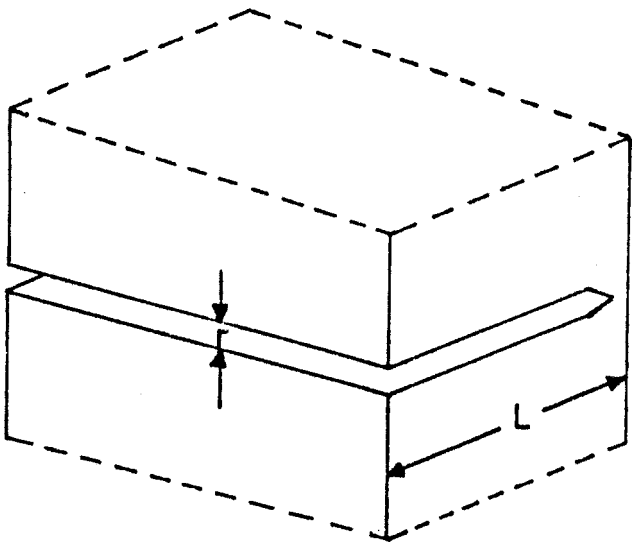

Figure 8.3 Illustration of portion of double-torsion crack length showing depth L and width r of the crack.

Under these conditions the time t is given by the Clausing's relation (see Hordon, 1966) as:

$$t = \frac{3}{8}\left(\frac{L}{r}\right)^2 \frac{1}{A\,n} \qquad (8.4)$$

where L and r are the depth and the width of the crack respectively, figure 8.3. A,is the cross sectional area of the gas molecule and n is the rate of impinging molecules. The kinetic theory of gases shows that

$$n = 2.24 \times 10^{24}\, P(MT)^{-\frac{1}{2}} \quad \text{molecules } m^{-2}\ s^{-1} \qquad (8.5)$$

where P is the partial pressure (in Nm^{-2}) of the gas species of molecular weight M, and T is the absolute temperature.

For water molecules $A \sim 2 \times 10^{-19}\ m^2$, $M = 18$, $P \simeq 1.5 \times 10^3\ Nm^{-2}$ at $T = 300$ K (assuming relative humidity 50%). For the geometry of the crack used $L \simeq 1$ mm and $r \simeq 0.01$ mm. For these values, equation (8.4) gives that $t = 3 \times 10^{-4}$ seconds.

It is pointed out that this time is the time required for water molecules to adsorb on the deepest parts of the crack walls. Naturally for areas of the crack faces closer to the crack opening the adsorption time would be considerably smaller*. It is therefore practically impossible to form and preserve virgin fracture surfaces in air, which would promote genuine healing to occur between the crack walls.

In the case of cracks formed in moderate vacuum ($\sim 10^{-3}$ Nm^{-2}) where the partial pressure of water vapour is $\sim 10^{-5}$ Nm^{-2} (at T = 300 K) equation (8.4) gives that the time required to adsorb a monolayer of H_2O molecules is approximately one hour**. This suggest that it is possible in vacuum (or in a very dry gas) to avoid excessive atmospheric contamination if the time for which the crack remains open is confined to a few seconds. This is turn suggests that if the crack faces are atomically smooth over large areas, restoration of atomic bonds of the opposite crack faces, i.e. partial genuine healing can, in principle, take place. So that the relatively high value of G_r^* observed in cracks closed in dry gases or in vacuum ($G_r^* = 1.3$ Jm^{-2}) may be due to partial genuine healing. Further discussion of this issue is presented in a later section of this chapter.

Returning to the adsorption of water molecules on the crack faces in air, it can be speculated that after the formation of a monolayer, additional molecules may be adsorbed depending on

---

* In fact, it is found that the time required to form a monolayer of water molecules on a planar surface under the same conditions is about 1/1000 of that calculated by equation (8.1).

** In practice, it is expected that the time, t, will be considerably shorter than that, due to the fact that the vacuum used was not static; the diffusion pump had to remain switched on continuously in order to maintain the pressure at the level of 10^{-3} Nm^{-2}.

the relative humidity of the atmosphere. It is not yet clear what determines the adsorption of subsequent molecules, and also if there is an equilibrium thickness for a given experimental condition. McHaffie and Lenher (1925) have reported that at relative humidities $< 50\%$ only one monolayer of H_2O is formed on a glass surface but at relative humidities $> 50\%$ the number of molecular layers increases dramatically. For example at 70%, 90% and 100% relative humidity the number of molecular layers of H_2O adsorbed at room temperature is 5, 20 and 180 in the order given. What is more plausible though is that during crack closure a number of water molecules already existing in the space between the crack faces will be adsorbed on the crack faces. It is therefore reasonable to assume that a closed crack in air at room temperature which had remained open for very short time (say 1 s) contains at least three molecular layers of water molecules between the crack faces.

In this connection it may be thought that the capillary attraction of the opposite surfaces due to the water adsorbed (condensed) inside the crack may be responsible for the initial load bearing capacity of the closed crack.

This mechanism (the capillary attraction) has been proposed in the past to explain the adhesion observed between glass beads or between flat glass surfaces (Stone, 1930; Rayleigh, 1937). Such a mechanism however cannot account for the phenomena observed in this study: The measured value of G_r^* in air is a factor of 2 larger than that expected from surface tension phenomena (surface tension of water is 0.073 Jm^{-2}). Also, cracks unloaded in water appeared to close over short distances (~ 1 mm) and showed load bearing properties (G_r^* in water = .14 Jm^{-2}).

Naturally, surface tension forces are not expected to operate when the crack is completely immersed in the liquid. On the other hand a phenomenon has been observed which may favour the surface tension hypothesis to some extent: Freshly "air-prepared" closed cracks, when immersed in water open slightly over a few mm. But closed cracks aged for as short a time as 30 minutes did not show any tendancy to open under water even when they are stored under water for over one year. This phenomenon is consistent with the observed values of G_r^* and G_c:

The value of G_r^* at which a closed-in-water crack starts propagating is 0.14 Jm^{-2}. However, the value of G_c against which a crack closes in air is 0.17 Jm^{-2}. That is, the stress intensity at the tip of a closing crack in air is higher than the stress intensity at the tip of a repropagating crack in water. The excess of the stress at the crack tip is releaved upon immersion in water by repropagation of the (immersed) closed crack. A physicochemical interpretation of this phenomenon will be attempted in a later paragraph.

b) Rate of increase of G_r^*.

Two mechanisms will be considered here which might, in principle, be responsible for the increase of G_r with time and with temperature of heat-treatment: both would result in a gradual increase of the real area of contact between the opposing crack faces.

Firstly, the possibility that air trapped between the crack faces during crack closure may migrate out of the crack as time progresses or temperature is raised so that the real area of contact increases is considered.

However the observed rate of increase of G_r^* would require

that a large amount of air migrates out of the crack at rates dependent on the composition of the glass. As a matter of fact, air pockets of various shapes and sizes have been observed in all the materials examined when the cracks were unloaded and closed very quickly; but once they have formed they remain indefinitely and unaffected from aging or/and from heat-treatment (even at temperatures above 800 K) until the cracks are re-opened and closed again at the normal slow rate. The value of G_r^* for repropagation of closed cracks exhibiting air-pockets was found to be smaller than that measured in normal specimens (depending on the size and density of the air pockets) but the rate of increase of G_r^* was identical to that in normal specimens. It is therefore unlikely that the considered mechanism was responsible for the increase of the load bearing capacity of the closed cracks.

An alternative mechanism which may be thought responsible for the increase of G_r^* and which would also result in an increase of the area of contact between the opposing crack faces is the following: Fracture is often produces surface irregularities (asperities) and shear "lips" at the crack edges as the result of the plastic deformation of the material, figure 8.4. So that when the crack closes, under the action of the relaxing elastic stress field around the crack tip contact is made only between the asperities on the opposing crack faces. As time progresses or temperature increases the actual area of contact between each pair of asperities should increase due to the creep of the material. Whether the limited amount of plastic deformation that glass is assumed to undergo can result in the formation of such features in a sub-microscopic

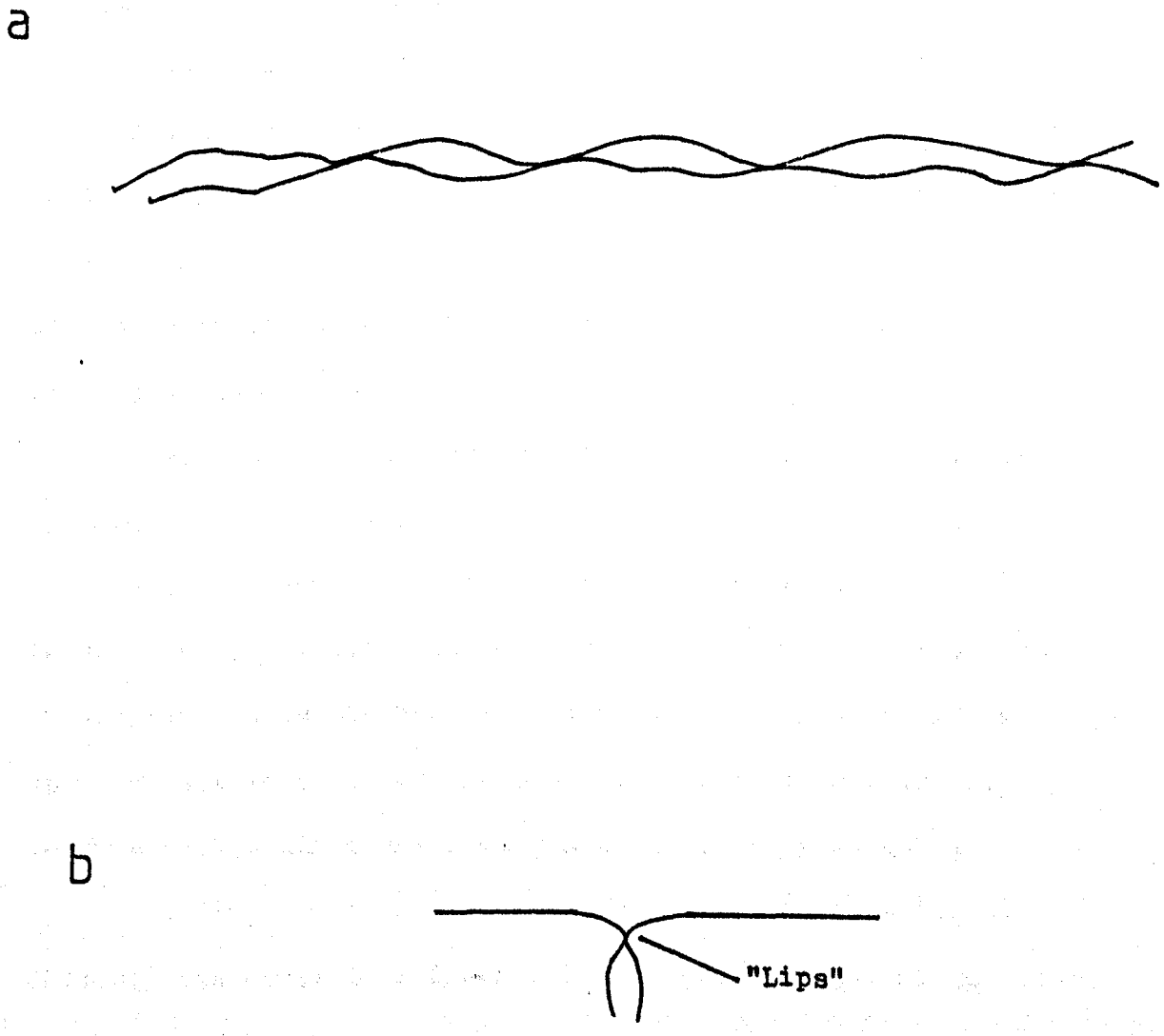

Figure 8.4 Schematic representation of the contact between two opposite crack faces possessing hypothetical surface irregularities (a) and shear "lips" (b). Plastic deformation at the points of intimate contact would result in increasing the real area of contact.

scale cannot be ruled out and it is therefore worth considering the possible influence of small asperities and shear "lips" on the rate of change of G_r^*.

However if this mechanism of gradual increase of the real area of contact operates, then the closed cracks ought to close further during aging or heat-treatment. Such a phenomenon has never been observed even after heat-treating the closed cracks at a temperature above the annealing point of the material (813 K for Float glass, 838 K for Pyrex glass).

Also, although the three silicate glasses differ substantially in chemical constitution their elastic, plastic and creep properties are approximately the same. Therefore the rate of increase of G_r^* would have been expected (in view of the mechanism considered) to be the same in all these glasses. But it is obvious that this is not the case; the rate of increase of G_r is drastically different from glass to glass, figure 7.4.

Finally, an experiment was carried out to investigate directly the possible influence of the shear "lips" on the rate of change of G_r.

A number of Float glass specimens containing closed cracks were prepared; some of them were etched in 5% HF for 5 to 30s and the others were used as control specimens. After etching some of the specimens were stored in the laboratory air and others were heat-treated in air at 413 K. In every case specimens from the control group were treated together with the etched specimens. After completion of the selected treatment, crack repropagation tests were carried out in all the specimens. The results obtained from etched specimens were indistiguisable from those obtained from the control specimens.

Observations under the optical microscope before crack repropagation and also after complete cleavage of the etched specimens, revealed that etching had removed a considerable volume of glass at the edge of the crack. In particular, the width of the crack line on the specimen surface was 5 to 10 μm and the depth of etching inside the crack was 10 - 30 μm depending on the duration of etching. It is plausible that the etched-out glass volume at the edge of the crack must have contained the shear lips (if any). The results showed clearly that the assumed shear lips do not influence the rate of increase of G_r^* with time or with temperature.

In conclusion, the two mechanisms considered are not believed to contribute to the process responsible for the observed increase of the load bearing capacity of the closed cracks. Both mechanisms require that the rate of increase of G_r^* is independent of the chemical consitution of the silicate glasses. However the results of this work showed clearly that there is a strong link between the rate of increase of G_r^* and the chemical composition of the glass.

In a later section of the present discussion it will be proposed that the rate of increase of G_r with time and with temperature may be explicable in terms of ion exchange phenomena occurring between the glass and the adsorbed water molecules.

8.4 The water-glass system

It has been argued that water molecules adsorbed on the fracture surfaces of a closed crack in air can form a thin film several molecular diameters thick and which is in effect responsible for the observed load bearing capacity of the closed cracks in the materials examined. It appears therefore interesting to seek possible ways in which the adsorbed water between the crack faces of a closed crack can lead to a load bearing interface.

The literature on water-glass surface system is immense and describe phenomena ranging from simple physical adsorption to elusive effects such as dissolution of the glass structure and even the production of new forms of water. It will not be the task of this section to give an account of the phenomena associated with the contact of water with glass; instead some of these phenomena which are believed to be the most interesting (and indeed fascinating in the author's view) and which would help to understand and perhaps interprete some of the phenomena observed in this study will be touched upon and only briefly. It appears as though most authorities in the field generally agree that silicate glass surfaces (silica glass surface in particular) consist of isolated SiOH groups, hydrogen-bonded SiOH groups, internal (subsurface) SiOH groups and molecularly adsorbed water molecules hydrogen bonded to the SiOH groups. The relative amount of these different groups on glass surfaces is dependent mainly on the "history" and environmental conditions (temperature, humidity). (Anderson and Wickersheim, 1964; Boutin and Prask, 1964 and also review by Doremus, 1973).

Research to date on the adsorption of water on silicate glasses has resulted in the publication of a great deal of

evidence that the adsorbed water must be multilayer before bulk phase properties can be detected. The evidence originates from spectroscopic studies, principally infrared, nuclear magnetic resonance, and dielectric measurements from which the characteristic spectra, relaxation times etc of the adsorbed water were found to be substantially different from those of liquid water. For example McCafferty and Zettlemoyer (1971), Kier and Zettlemoyer,(1977), have found that the dielectric relaxation time of adsorbed water was decreased from 1 s to 10^{-4}s as the thickness of the adsorbed film increased from one to several molecular diameters. These figures were compared with the dielectric relaxation time of 10^{-10}s for water in the liquid phase. Also, the nuclear correlation times for the water adsorbed on silica surfaces were found to be 2 to 4 orders of magnitude lower than for liquid water,indicating strongly that the mobility of the adsorbed water molecules was restricted (Michel, 1967). Many authors have taken the view that the first few molecular layers of the adsorbed water or water adsorbed inside narrow pores ($<$ 10 nm in diameter) is forms an oriented hydrogen-bonded network which could be more appropriately modelled by an ice-like structure and several models depicting the hypothetical structure of this hydrogen-bonded network of H_2O molecules have been proposed*.

But the most important characteristic of the water-glass system is the chemical reaction of water with the glass,which

---

* Different aspects of the hydrogen bonding of water molecules in close proximity with silicate and other oxide surfaces are reviewed by H.Knozinger, and also by L.Sobczyk, H.Engelhardt and K.Bunzl, 1976 in "The hydrogen bond-recent developments in theory and experiment" Vol. II and III. Edited by P.Schuster G.Zundel and C.Sandorty, North Holland Publishing Company.

often leads to severe deterioration of the glass surfaces. The tremendous amount of experimental work carried out in this field has revealed that dramatic changes take place on the glass in contact with water (atmospheric or liquid water) but the actual mechanism of the chemical reactions are virtually unknown and only tentatively proposed. The various models involve a diffusion of water in the form of hydrogen H^+ or hydronium H_3O^+ into the subsurface layers of the glass by an exchange process with the mobile ions present in the glass such as Na^+ or K^+. This situation is usually depicted schematically by a reaction of the form*

$$Na^+ \text{ (glass)} + H_2O \longrightarrow H^+ \text{ (glass)} + Na^+ + OH^- \qquad \text{(a)}$$

Under many conditions of service the OH^- and Na^+ ions are removed from the reacting system (for example, by rain against a window pane). Further reaction then requires the slow diffusion of alkali ions from the interior to the surface of the glass and thus the rate of attack of the glass gradually decreases.

Under some conditions however the ions produced by the reaction (a) may remain in contact with the glass; the silicon-oxygen bond can then be broken by the reaction

$$\text{glass } -Si-O-S- + OH^- \longrightarrow \text{glass } -Si-O- + Si-OH \qquad \text{(b)}$$

The rate of these reactions determine the chemical durability of the particular glass. Various empirical methods exist to classify the chemical durability or weatherability of glasses in terms of their rate of dissolution or on their

---

* Detailed chemical reactions have been proposed by Charles (1959), see also recent reviews by Doremus (1973); Hench (1975); Hench and Clark (1978) and Lanford, Davis, Lamarche, Laursen and Groleau (1979).

optical appearance under certain experimental conditions (Walter and Adams, 1975). Glasses with high proportion of metal oxides (Na_2O, K_2O etc), such as typical soda-lime-silica glass, are found to be less resistant to chemical attack by water than other glasses with small proportions of monovalent metal oxides such as Pyrex and silica glasses.

Recent studies on the composition of the glass subsurface layers using newly developed techniques revealed striking phenomena. Pentano, Dove and Onoda, (1975, 1976) examined the chemical compositions of commercial soda-lime-silica glass as a function of the depth from the surface using Auger Electron Spectroscopy (AES). Four types of surfaces were examined: a) "as-received" surface: b) ion milled surface; c) ion milled surface and then exposed to the atmosphere for 5 minutes; d) surface exposed to water at 394.5 K for one hour.

The results in each case are shown in figures 8.5 to 8.8. It is evident that weathered glass (type a) showed an excess of Na_2O and CaO at the first few layers of the surface and the bulk composition was not resumed until the depth was about 900 Å. The ion milled surfaces which in fact were exposed in vacuum for 45 hours showed an "anomaly" at the first 50 Å, in the sense that the amount of Na_2O and SiO_2 was not what was expected for a pristine surface. The authors believed that this deviation from the bulk composition was due to a trace of water vapour inside the vacuum apparatus and which in fact was detected by a residual gas analyzer. Exposure of ion milled glass surfaces to atmospheric air resulted in dramatic compositional changes and it can be seen in figures 8.8 and 8.7 that the composition of the subsurface layers of this type of surface is like that

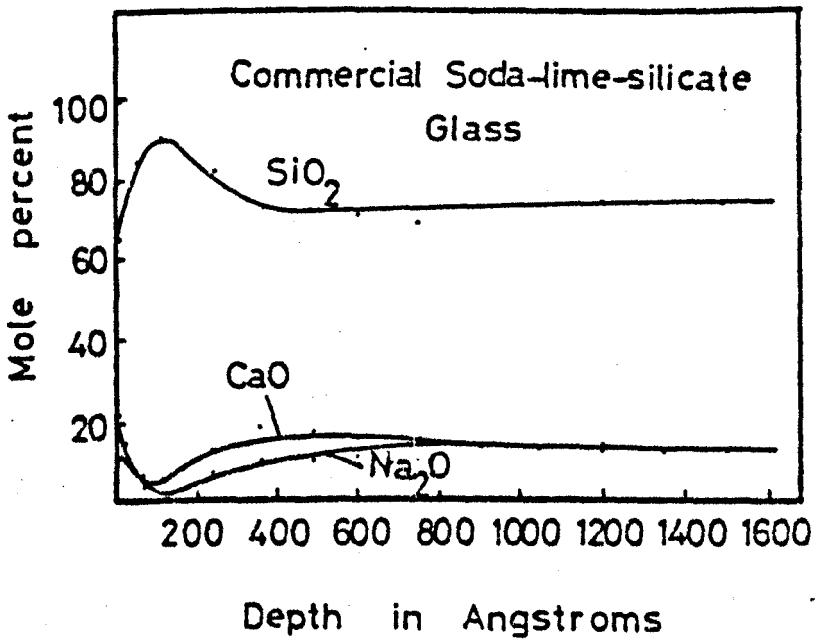

Figure 8.5 Compositional profiles for an as-received soda-lime-silicate glass surface. After Pentano et al (1975).

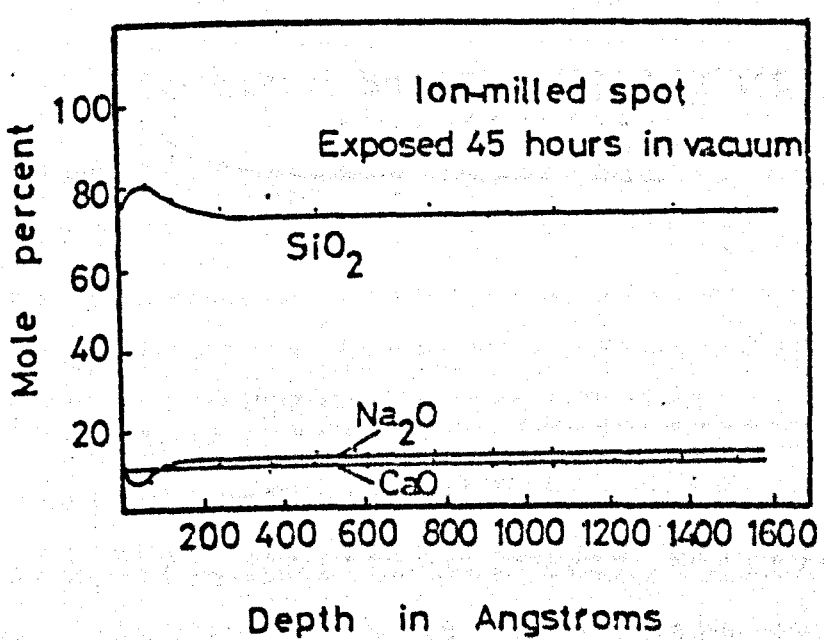

Figure 8.6 Compositional profiles for an ion-milled surface of a soda-lime-silicate glass after 45 hours exposure to a vacuum of $\sim 10^{-6}$ Nm^{-2}. After Pentano et al (1975).

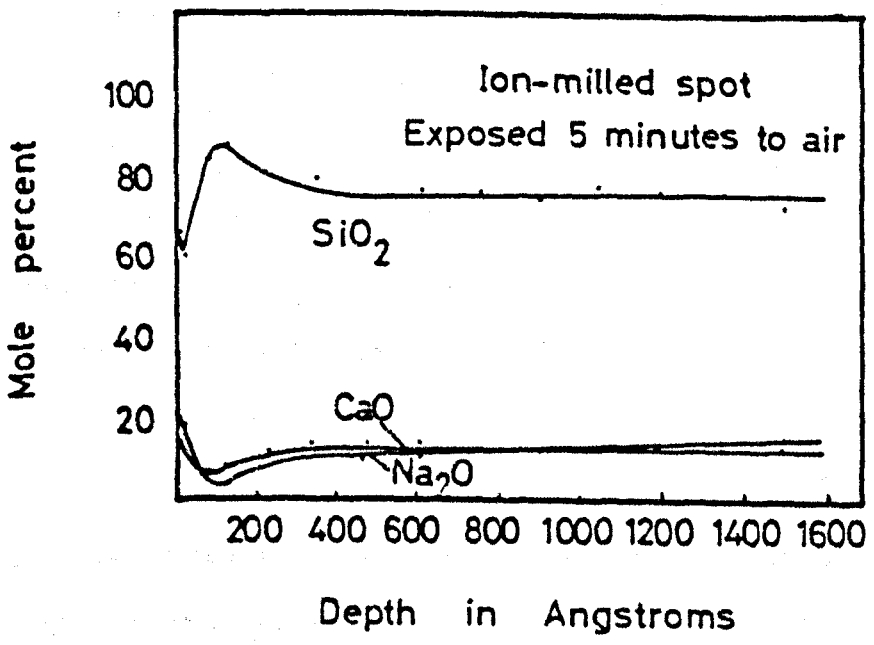

Figure 8.7 Compositional profiles for an ion-milled surface of a commercial soda-lime-silicate glass after 5 min exposure to laboratory air at room temperature. After Pentano et al (1975).

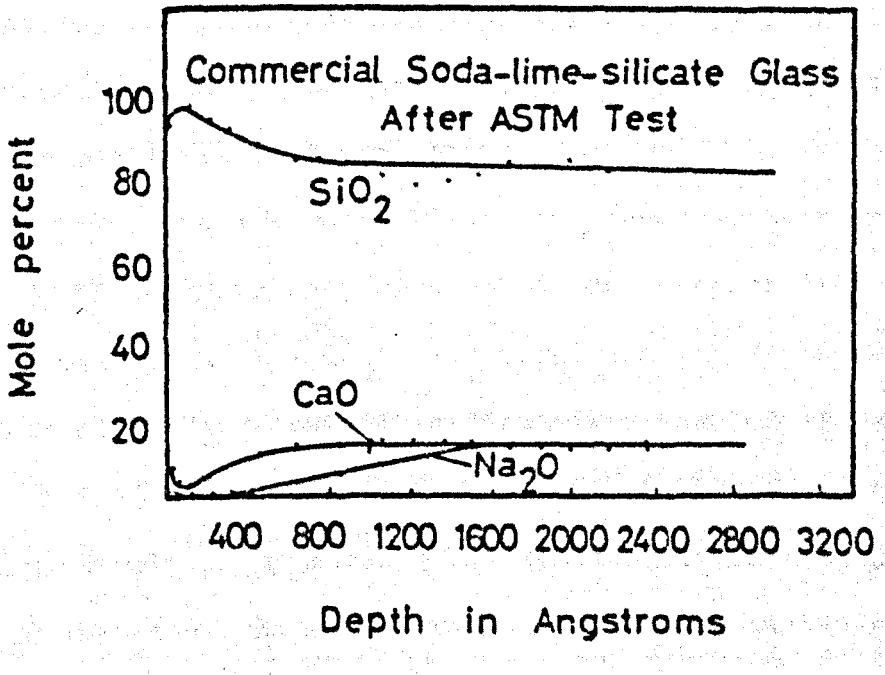

Figure 8.8 Compositional profiles for a commercial soda-lime-silicate glass surface after one hour exposure at 394.5 K in low-conductivity water. After Pentano et al (1975).

of the "as-received" samples. Finally, exposure of glass surfaces to water at 394.5 K (ASTM test) resulted in considerable changes up to a depth of 1500 Å. These authors claimed that their results agreed well with previously published results obtained from either AES or from other spectroscopic techniques such as secondary-ion mass spectroscopy (SIMS).

In a recent review article (Hench and Clark, 1978) it is reported that there exists experimental evidence to support the idea that glass articles in intimate contact can be more easily weathered than a free glass surface exposed to the same environment, and also, that freshly fractured surfaces showed signs of selective leaching and higher rates of ion exchange than other types of glass surfaces.

That fracture surfaces are much more easily attacked by water in general is also indicated by the results from durability tests of Walters and Adams (1975): The amount of Na_2O per unit area "generated" by fracture surfaces of a borosilicate glass treated at 325 K at 98% relative humudity for 20 days was six times higher than that "generated" by the surface of drawn glass under identical test conditions.

Also Gossink and Werner (1979) have reported that by using the SIMS analysis they found that the concentration of impurity atoms of Na^+ and K^+ in the first two atomic layers of the surface of an "as-received" silica glass was 100 times higher than that found at depths of $\sim$ 100 Å (which was 4 and 2 ppm respectively). By etching the samples for 10 s in 40% HF they found that the bulk concentration of the impurity atoms is detected at a depth of $\sim$ 20 Å from the surface.

Finally, it is felt that this discussion would not be

complete without some account of the story of anomalous water. Since 1960, there has been a frequent appearance of reports on the anomalous behaviour of water in fine capillaries, although a few reports on this topic appeared long before that. Everett, Haynes and McElroy (1971) gave an account of one hundred and eleven publications.

In brief, water exhibiting anomalous properties could be prepared by evaporation and condensation of purified water into freshly drawn fine capillaries of silica or Pyrex glass, of internal diameter 1 to 50 μm. After some time, which might vary from one day to a few weeks, in some of the exposed capillaries condensed liquid could be found. This liquid, as reported by various investigators, showed anomalous properties. There exists little (if any) disagreement on the properties of this condensed liquid. Its anomalous properties were higher viscosity, density and refractive index than ordinary liquid water; phase separation at temperatures below 273 K and temperature of maximum density below 277 K. Different names were given to this material: anomalous water, water II, polywater etc.

If the condensed liquid was allowed to evaporate a residue could be found inside the capillaries. Various reports described this residue as a viscous, a gel like, a granular, or a solid substance. The extreme anomalous properties were exhibited by this residue. Different degrees of anomalous behaviour could be shown though, before complete evaporation of the liquid or in solution of the residue in pure water. Some of the characteristics of the residue were a high density, about $1.4 \times 10^{3} Kgm^{-3}$ refractive index about 1.49, its boiling point was estimated to be around 523 K, although it was found stable at temperatures above 873 K,

its molecular weight was deduced to be 200 ± 50; it was described as hydroscopic and birefringent. It showed also time dependent properties: Its solubility in water was found to decrease with aging time and it hardened and became salt-like on aging. Its infrared spectra appeared to change with time also.

Many attempts were made to identify the chemical nature of the anomalous water. Spectroscopic methods (Laser - Raman, I.R., N.M.R., electron microprobe techniques, and so on) have been employed for this purpose. Then, many alkali ions, silicon, carbon, oxygen and chlorine ions were detected. However Derjaguin and his colleagues who enthusiastically introduced the idea of water II insisted that their samples prepared under ultra clean conditions contained water and only water which was in a super dense state etc. Other groups have adopted the model of a silica/water complex, a highly hydrated silica gel. This modelling seemed to be based on the fact that an appreciable amount of silica was detected in samples of anomalous water, although this observation was not confirmed by others who found silicon in trace quantities only.

The storm of spectroscopic evidence, however, which proved overwhelmingly that what was called anomalous water was in fact a contaminated form of water containing Si, Na, O, C, K, Cl, S ions, made the abandonment of the hypothesis of a new modification of water, inevitable. Derjaguin and his colleagues (1973) gave up the idea of water II and bravely acknowledged that anomalous water prepared under ultra clean conditions contained mainly O, Si and Na, and that "there are no condensates both free of impurity atoms and simultaneously exhibiting anomalous properties".

The unusual circumstance that anomalous water could only

be prepared in freshly formed capillaries received more attention. It had been suggested that fresh surfaces had special catalytic properties needed to produce anomalous water but it soon became appreciated that they were also the source of leachable impurities.

As well as the peculiar properties of the anomalous water some other interesting observations have appeared.

Olivey (1973) examined the leaching of ions from the glass during the production of anomalous water and concluded that samples prepared in Pyrex capillaries differ in the amount of contaminant from that prepared in quartz capillaries, and finally in a recent publication (Ikida and Matruda, 1976*) it is reported that mass-spectroscopic methods showed that anomalous water originates from water, silicon, carbon monoxide and possibly formyl-hydroxy-silanes.

The story of anomalous water, besides other things, gave another indication, if not a proof, that the reaction of glass with water is a complex one leading to unexpected phenomena. The application of modern spectroscopic techniques have revealed in particular that the reaction of water with glass is fast, much faster than was thought before.

In this connection it may be thought that the occurrence of load-bearing interfaces and also the glass composition dependence of the rate of change of the load-bearing capacity of the closed crack are due to the phenomena which are reported to occur when water is in contact with glass. It is repeated that most of the load-bearing properties of the closed cracks observed in this study are associated with the water (vapour)-glass system.

---

* To the author's knowledge this is the last publication to appear up to mid-1979 on the subject of anomalous water.

In the following section a mechanism is proposed, based on the previous observations mentioned briefly in the preceding section,and which,although is entirely speculative, gives some account of most aspects of the behaviour of the closed cracks observed in this study.

8.5 A mechanism for crack healing.

As a crack is formed in air,atmospheric species, water molecules in particular,are adsorbed onto the fracture surfaces of the crack. Some of the adsorbed water molecules remain undissociated and hydrogen bonded to electronegative atoms on the surface and others dissociate into H^+ and CH^- ions,possibly forming hydronium H_3O^+. After this initial surface reaction, the H^+ or H_3O^+ ions produced diffuse into the subsurface layers of the glass by an exchange process with mobile ions present in the glass (Na^+ for example). The -Si-O- network is also attacked as the result of the migration of Na^+ to the glass surface, so that the outer layers of a glass surface will consist of OH^-, H_2O molecules and various species from the bulk glass.

As the crack closes,the (immobile) H_2O molecules which are hydrogen bonded to the opposite crack faces come in contact and form localized hydrogen bonds. So that the load-bearing capacity of a crack freshly closed in air is due to a network of hydrogen bonds between the opposite crack faces.

As time progresses or temperature is raised the diffusion of H_3O^+ ions into the subsurface layers proceeds further so that the layer between the crack faces is fed with ions from the glass

while the water content of this layer is reduced and consequently the network of hydrogen bonds is destroyed. This situation can be depicted as a gradual transition from the initial state of the freshly closed cracks (in air)

$$\text{glass} \left| \begin{array}{cc} \text{hydrogen} & \text{bonded} \\ H_2O & \text{and/or } OH^- \end{array} \right| \text{glass}$$

to a relatively "solid" structure without forming sharp interfaces with the glass surfaces:

$$\text{glass} \left| \begin{array}{c} \text{structure containing} \\ Na^+,\ Si,\ OH^-\ \text{etc.} \end{array} \right| \text{glass}$$

These species concentrating between the crack faces "bridge" progressively the fracture surfaces of the closed crack by forming primary bonds but without forming necessarily an amorphous structure identical to the substrate glass. It would be more appropriate to describe this mechanism as a kind of partial genuine healing. The rate of increase of the load-bearing capacity of the closed cracks is therefore attributed to the progressive built-up of primary bonds across the faces of a closed crack. When all the "water" has diffused into the substrate glass the ("dehydrated") region between the crack faces exhibits a maximum in load-bearing ability.

The rate of increase of the number of bonds across the crack faces with aging time and with temperature would be expected to be higher in glasses containing larger proportions of network modifiers, alkali oxides in particular. In such glasses ion exchange is easier due to the high mobility of the alkali ions and leads, probably, to a "loose" structure more vulnerable to further attack which in turn would provide the essential constituents (-Si-O- groups) for the "reconstruction"

of a glass-like structure between the faces of a closed crack.

8.6 Discussion of the results in relation to the mechanism proposed.

It will now be attempted to explain the load-bearing properties of the closed cracks on the basis of the mechanism proposed.

a) Initial load-bearing capacity.

Clearly, the repropagation of a crack freshly closed in air in all the examined materials and possibly in any material with smooth fracture surfaces (mica for example) would cause the continuous breaking of hydrogen bonds which are assumed to exist between the faces of the closed crack.

It appears interesting to compare the value of $G_r^* = 0.25$ Jm^{-2} for cracks freshly closed in air with known values for the surface energy of ice where the nearest neighbour interactions are all hydrogen bonds. Mac Donald (1953) has reported that the energy per unit surface of ice calculated on the basis of breakage of hydrogen bonds is $2\gamma = 0.244$ Jm^{-2}. Besides, an experimental evaluation of the surface energy of ice based on grain boundary grooving (Ketcham and Hobbs, 1969) gave a value of $2\gamma = 0.22$ Jm^{-2}. It can be seen that a close and indeed encouraging agreement exists between the surface energy of ice and the (common) value of G_r^* for freshly closed cracks in different materials. But despite this agreement, the phenomenon in which freshly "air-prepared" closed cracks open slightly (over a few mm) upon immersion in water (or in methanol) cannot be explained in terms of the hydrogen bonding hypothesis. If it

is assumed for instance that the hydrogen bonds are destroyed when they come in contact with liquid water, it is not understood why this process (the dissolution of hydrogen bonds) does not take place over the entire length of the closed crack. But on the other hand, it is observed that when freshly "air-prepared" closed cracks are immersed in liquids which are immiscible with water such as silicon oil, liquid paraffin and n-hexane the closed crack does not open at all, a fact which is arguably in support of the hydrogen bonding hypothesis.

b) Rate of increase of G_r^*.

As shown in figure 7.4 and in table 7.1 the rate of increase of G_r^* is dependent strongly on the composition of the glass. Specifically the amount of Na_2O seems to be the dominant factor in the process with leads to the increases of G_r^* with aging time and with temperature. For instance, if the rate of increase of G_r^* with temperature is defined as $\frac{\Delta G_r^*}{\Delta T}$ it can be deduced from figure 7.4 that for Pyrex glass with $\sim$ 4% Na_2O the value of $\frac{\Delta G_r^*}{\Delta T}$ is a factor of 1/6 smaller than for soda-lime-silica glass with 13% Na_2O and a factor of 2 higher than for "pure" silica glass, which contains Na only in trace quantities. A linear relation between $\frac{\Delta G_r^*}{\Delta T}$ and the amount of Na_2O (or of the ratio $\frac{Na_2O}{SiO_2}$) would not be expected to hold due to the presence of other cationic network modifiers (table 2.1) which are known to influence the chemical durability of the glass.

In the case of the two types of silica glass used in this study, although known to have different purities, table 8.2, they showed identical behaviour (values of G_r^* and $\frac{\Delta G_r^*}{\Delta T}$). Table 8.2 shows the impurity content of the two types of silica

glass used in this study.

Table 8.2

Chemical purities of silica glasses (maximum levels in ppm)*

Element	Vitreosil 066	Spectrosil B
Ca	0.35	0.1
Al	10	0.02
Na	0.06	0.04
Fe	0.51	0.1
B	0.5	0.01
OH^-	400	1200

In principle, it might be expected that the difference in the impurity content should have led to different rates of reaction and therefore to different rates of increase of G_r^*. It may be, however, that the difference in the impurity content would play a role in the saturation value of G_r^* which was not observed in this study up to a temperature of heat-treatment of 873 K. Moreover, the larger content of Na in Vitreosil may be compensated by the relatively smaller amount of OH^- in respect to Spectrosil.

Nevertheless, it is not implied that the proposed mechanism of compositional changes at the glass fracture surfaces results in the formation of a glassy structure similar to the bulk glass. Although the saturation values of G_r measured in Float and Pyrex glasses are only ten per cent lower than that of G_v at slow crack speeds ($< 10^{-4}$ ms^{-1}), a significantly lower value of G_r appears at crack speeds above 10^{-4} ms^{-1}

* Hetherington G. and Jack K.H. Thermal Syndicate Ltd, Report RR/63/2.

(see figure 7.2). This fact suggests that heat-treatment at high temperatures (or prolonged aging) does not result in a genuine healing of the closed cracks.

In the case of closed cracks in the epoxy resin system used, it is recalled that G_r^* for cracks freshly closed in air is identical to that observed in the silicate glasses examined but no increase of G_r^* with aging time was detected (up to aging times of 4 months).

Although it is very well established that water is absorbed by these materials under common circumstances, there is no evidence suggesting the chemical reactivity in the water-epoxy resin systems. It is therefore possible that the hydrogen bonding and the lack of any reaction between the adsorbed water and the fracture surface of the epoxy resin can account for the aging time-independent value of G_r^* observed in this case.

c) Cracks closed in water.

Cracks formed and closed under water show load-bearing capacity $G_r^* = 1.4\ Jm^{-2}$ which is substantially lower than that observed in air but the closed portion of the crack is very short ~ 1 mm. It can be argued that the large number of H_2O molecules in the closed(short)portion of the crack as well as the presence of liquid water around the closed crack would inhibit the formation of a complete network of hydrogen bonds and therefore the load-bearing capacity of cracks closed in water should be lower than that in cracks closed in air. Moreover any ions leached from the glass during aging under water would migrate out to the liquid phase, a process which can account for the time-independent value of G_r^* observed in these cracks.

When these cracks are taken out of the water they gradually squeeze out the water and show a time-dependent load-bearing ability (figure 7.5). The value of G_r^* in these "water-prepared" closed cracks increases with aging time and after ~ 24 hours aging or after heat-treatment at 393 K the values of G_r^* are identical with the corresponding values obtained from "air-prepared" specimens. Presumably, the small number of H_2O molecules left between the faces of a "water-prepared" closed crack would give rise to an ion exchange process and so it would increase gradually the load-bearing ability of the closed crack.

It was mentioned earlier that when tap water instead of distilled water is used for the preparation of closed cracks, lower values of G_r^* (by up to 30%) and larger scatter in the results are shown (figure 7.5b). It is plausible (in view of the proposed mechanism) that impurities present in the water can interfere destructively in the process which leads to the bonding of the opposite crack faces. Tap water contains* in mgl^{-1}: $CaCO_3$ ~ 100-500; Cl: 200; F: 1.5 and N + Fe + Cu + Mg + Pb < 0.1. Such impurities would affect the composition and therefore the bonding in the between-the-crack faces region of closed cracks.

d) "Dry-prepared" closed cracks.

The value of G_r^* (= 1.3 Jm^{-2}) for "dry-prepared" closed cracks is found to be substantially higher than that observed in air (figure 7.6). It is proposed that this is due to partial genuine healing occurring at sites of the opposite crack faces which remained uncontaminated from atmospheric species. It is interesting to note that for repropagation of "dry-prepared" closed cracks in air, the value of G_r^* is 1 Jm^{-2} (i.e. lower

* Severn Trent Water Authority, water quality 1978/79.

than that measured in dry gases). This behaviour, that is, environment dependence of the strain energy release rate, is typical of the virgin glass and may suggest that cracks formed and closed in dry gases are held together by primary bonds similar to those found in bulk glass.

It is also found that aging in dry gas (up to 3 hours) does not have any effect on the value of G_r^*, while heat-treatment at 393 K leads to a value of G_r^* identical to that found in "air-prepared" closed cracks ($G_r^* = 2.2\ Jm^{-2}$). In this case it is plausible that the relatively small number of H_2O molecules (less than a monolayer) adsorbed on the crack faces produced in a dry gas may give rise to a rather slow ion exchange reaction which in turn would lead to the formation of additional bonds between the opposite crack faces.

e) Other properties of the closed cracks.

One of the remarkable characteristics of the closed cracks in the glasses examined is that they can undergo repeated closure-repropagation runs without measurable changes in the values of G_r^* or their rate of change with aging time or with temperature. In this case it can be speculated that during a second repropagation (third crack propagation) of a closed crack which aged or was heat-treated, two "new" surfaces of the closed crack are exposed to the atmosphere. Then, water molecules adsorb onto the fracture surfaces, so that when the crack closes (for second time) contact is made between these molecules on the opposing fracture surfaces; a network of hydrogen bonds is formed again which leads to a load-bearing interface immediately after closure ($G_r^* = 0.25\ Jm^{-2}$). As time progresses or the temperature is raised the ion exchange process takes place

involving ions from the underlying and already modified layers of glass and the adsorbed water molecules. Naturally the constitution of the layers of glass near the fracture interface must be expected to be different from that after the initial crack closure. But whether this would result necessarily in observable differences in the rate of change of the G_r cannot be anticipated.

Finally, the appearance of the faintly reflecting area may be due to the changes which are assumed to occur in the near-the-crack-face layers from the ion exchange process in silicate glass or to the absorption of water in the epoxy resin system. However the conditions under which the film appears are similar in all the examined materials (for example exposure of the crack faces in humid air for $\sim$ 100 s). But in view of the mechanism proposed, the slower reaction process in Pyrex and Silica should have delayed the appearance of the film and also heat-treatment should have resulted in more pronounced differences in the composition and therefore in the appearance of the film. It is more plausible therefore to assume that the film is due primarily to the "substance" existing between the crack faces and which is believed to be a few molecular layers thick.

Lack of direct information about the refractive index of the film prevented any accurate determination of its thickness. A crude estimate of its thickness based on measurement of the relative intensity of light reflected from the film gave values between 20 and 40 nm.

Although the film has attracted much attention in this study, it was thought that further investigation on the nature of the film would not contribute to understanding the phenomena

associated with the load-bearing properties of the closed cracks because the latter were not influenced at all by the presence or appearance of the film.

In conclusion, the mechanism for crack healing proposed in the preceding discussion seems to give some account of the observed phenomena in this study. But because it is entirely qualitative and essentially based on observation and controversial interpretation of the behaviour of the glass-water system reported by previous authors, it is not surprising that many questions can be asked which can shake belief in the mechanism. For instance: why does the ion exchange process which results in such dramatic structural and compositional changes at the crack interface not build up any stresses? Why does the repeated opening and closing of a crack in air not result in substantial increases in the visibility of the faint reflecting area? And so on. Answers to these questions can be attempted but not without introducing more arbitrary and speculative assumptions.

However, the similarities between the behaviour of the water-glass system as reported by previous authors and the behaviour of closed cracks observed in this study suggest that the mechanism proposed points towards the right direction. But plausible as this mechanism may be, there is still a serious lack of direct evidence to support it. Specifically it is not certain that ions from the glass can form primary bonds with each other and with the substrate glass structure.

Unfortunately, it has not been possible to obtain spectroscopic evidence on the constitution and on the changes that might have been occurring at the fracture interface of the

closed cracks. It was desired to obtain a series of NMR spectra to check the hypothesis of hydrogen bonding and of the diffusion of ions to the space between the crack faces. However, after a long discussion with Dr. D.V.Griffiths, Lecturer in the Chemistry Department, University of Keele, it was understood that the specimen geometry and the extremely small amount of substance to be examined - the assumed layer between the faces of the closed cracks - make such a study practically impossible. It is believed that when such direct investigation becomes a reality, it would be of great value in understanding the process which takes place at the fracture interface of closed cracks.

8.7 Concluding discussion

A fundamental conclusion that can be drawn from the results of the present study is that closed or invisible cracks in glass are load-bearing. The load-bearing capacity of the closed cracks is dependent up on the environment in which the cracks are formed and closed originally, and the subsequent treatment (aging or heat-treatment). Whether the existence of closed cracks in glass specimens can affect the macroscopic strength of the glass would depend strongly on the conditions under which the cracks were formed and treated subsequently. There exists experimental evidence that the strength of soda-lime-silica glass samples containing surface cracks produced by abrasion increases with the time of aging and with heat-treatment of the specimens.

A systematic study of these phenomena has been carried out by Mould (1960). In his investigation specimens precracked by emery cloth abrasion or grid blast with SiC particles were

allowed to age in different environments (dry and humid air, water), or were heat-treated at 843 K for 3 hours in a dry Argon atmosphere and subsequently aged in water. Strength measurements were made either under water or under liquid nitrogen. Mould's results showed that there is a general tendancy for the strength of the specimen to increase: the rate of increase was found to be dependent not only on the treatment following the initial abrasion, but also on whether the cracks were induced by emery cloth abrasion or by grid blast. The maximum strength increase was observed in specimens heat-treated and subsequently tested in liquid N_2 and it was $\sim 60\%$ higher than the strength of freshly abraded samples. Mould proposed that rounding of the crack tip due to interaction of water or of water vapour with the glass during aging or heat-treatment can account for the strength increases observed*. One of the interesting observations made by Mould was that abrasion cracks consisted of two parts: a visible part (open crack), and a "hidden" part i.e. the part of crack closed after the initial formation of the abrasion crack. But he pointed out that

> "there is no good evidence that cracks in glass can indeed heal with time... Rather than promoting the rejoining of fresh surfaces a medium such as water is much more likely to contaminate the surfaces and prevent the reformation of glassy bonds across the crack".

---

* Refering to an equation which relates the applied stress, σ_a, with the local stress at the crack tip when fracture occurs, $\sigma a = \frac{1}{2}\sqrt{\frac{r}{c}}\, S_i$, where r is the radius of the crack tip and c is the depth of the crack. Mould argued that a strength increase by $\sim 50\%$ can be obtained if r increases a factor of ~ 2.

However, the present investigation has provided evidence that closed cracks in glass can indeed "heal" under ordinary storage conditions and that water adsorbed on the crack faces can promote healing.

A quantitative discussion of Mould's results in terms of the present results does not seem possible at the present time. The complicated conditions under which the specimens were cracked, aged, treated and tested in Mould's study provide a major problem for such a discussion. Accurate knowledge of the length over which abrasion cracks can close is a preriquisite for a quantitative approach to Mould's results. Also the effect of aging and heat-treatment on the strength of abraded samples must be studied in other glass compositions so that any connection of these phenomena with the apparent crack healing observed in the present study can be identified directly.

Unfortunately, it has not been possible to investigate whether fracture is a thermodynamically reversible process (that is, for freshly closed cracks can $G_r = G_v$). This would require complete absence of environmental species but it would certainly provide vital information about the plastic deformation of glass. In the event that for freshly closed cracks (under ultra-clean conditions) $G_r = G_v$, then glass should be an ideally brittle material incapable of plastic deformation. On the other hand if $G_r < G_v$ then this would be strong evidence for plastic flow and probably a means for quantifying the plastic flow of glass.

The present work might profitably be continued and extended: the techniques used could perhaps be developed further to allow the study of adsorption and adhesion phenomena. Because fracture consistently produces ultra-clean surfaces, crack faces make a potentially useful substrate for adsorption. If the adsorption is time dependent the process can be interrupted at will by unloading the crack. Adsorbed species would remain enclosed inside the (closed) crack and the specimen could be examined subsequently in normal atmosphere. The technique for measuring the relative intensity of light reflected from a closed crack can clearly be improved. An ability to measure smaller light intensities might provide a means for studying "film" growth in more detail and this might provide further information on the reaction of water with fresh glass surfaces.

It should also be possible to introduce various other species, liquids, evaporated metal films etc. into an open crack. Subsequent crack closure and re-opening might serve to explore the adhesion between films of these materials or between these films and the substrate glass.

8.8 Final remarks.

The present thesis has dealt with two phenomena apparently related to the flow and fracture of glass. The results reported in the first part suggest that either we accept that indentation creep is not related to the flow process in tensile fracture or we need a totally new theory to account for slow crack growth and static fatigue of glass. The second part showed that the production of load-bearing closed cracks in glass seems to be

a result of the still elusive chemical action of water on glass rather than a manifestation of the reversibility of cracks in thermodynamic terms. Further research is needed to reveal the full significance and the conditions under which these phenomena are related to the deformation and fracture of glass.

-ooOoo-

APPENDIX I

TABULATED RESULTS OF INDENTATION CREEP MEASUREMENTS

Table I.1 Results at room temperature

(t/s)	$\log_{10}(t/s)$	H_v / GNm^{-2}			
		Soda-lime-silica glass	Pyrex glass	E-glass	Silica glass
1	0	5.83	——	——	——
5	0.7	5.63	5.98	6.10	6.65
20	1.3	5.35	5.73	5.89	6.37
330	2.5	5.16	——	——	——
10^3	3	——	5.37	5.51	6.06
$10^{3.5}$	3.5	5.03	——	——	——
4	4	4.88	5.12	——	5.91
5	5	4.66	4.90	5.07	5.59
6	6	4.47	——	——	——

Table I.2 Results at different temperatures for soda-lime-silica glass

(t/s)	$\log_{10}(t/s)$	H_v / GNm^{-2} at temperature T/K						
		77	295	423	573	723	773	823
1	0	——	5.83	——	——	——	——	——
5	0.7	7.04	5.63	4.97	4.27	3.18	2.80	——
20	1.3	6.81	5.35	4.78	4.10	2.99	2.50	2.07
180	2.25	——	——	——	3.68	2.56	2.19	——
330	2.5	——	5.16	——	——	——	——	——
10^3	3	6.57	——	4.39	3.58	2.34	1.72	1.14
$10^{3.5}$	3.5	——	5.03	——	——	——	——	——
10^4	4	——	4.88	4.21	3.23	1.93	1.32	——
10^5	5.0	——	4.66	4.02	——	——	——	——
10^6	6.0	——	4.47	——	——	——	——	——

Table I.3 Results at different temperatures for Pyrex glass

(t/s)	$\log_{10}(t/s)$	H_v / GNm^{-2} at temperature T/K	
		295	773
5	0.7	5.98	——
20	1.3	5.3	2.64
10^3	3	5.37	2.02
10^4	4	5.12	1.72
10^5	5	4.9	——

APPENDIX II

TABULATED RESULTS OF CRACK PROPAGATION MEASUREMENTS IN CLOSED CRACKS

Table II.1 Variation of G_r and G_v (in Jm^{-2}) in air for soda-lime-silica glass

V/ms^{-1}	Aging time/h			Heat-treatment at 393 K	Virgin glass
	0.083	24	720		
1×10^{-7}	0.25	0.83	1.25	2.2	2.5
6×10^{-7}	–	1	1.5	2.5	–
1×10^{-6}	–	–	1.8	–	3
3×10^{-6}	–	1.5	–	2.9	3.65
6×10^{-6}	–	–	2	–	–
1×10^{-5}	0.5	–	–	3.4	4
3×10^{-5}	–	1.8	2.25	–	5
6×10^{-5}	–	2	–	4.1	–
1×10^{-4}	0.8	–	2.6	4.3	6.35-8
8×10^{-4}	–	–	–	4.5	–
8×10^{-3}	–	–	–	5.9	–
8×10^{-2}	–	–	–	6.75	–

Table II.2 Variation of G_r^*/Jm^{-2} with temperature of heat-treatment for different glasses.

T/K	Soda-lime-silica	Pyrex	Silica
313	0.85	-	-
353	1.25	-	-
373	-	0.55	0.45
393	2.2	-	-
573	2.2	1.13	0.72
723	2.2	-	0.92
873	2.2	2.15	1.2

APPENDIX III

The following equations give the relative intensity of light transmitted through a thin dielectric film bounded by plane parallel interfaces in the case of the frustrated total internal reflection*. (The subscripts ($\parallel$) and ($\perp$) refer to incident light with polarization parallel to the plane of incidence and perpendicular to the plane of incidence respectively):

$$\frac{1}{T_{\parallel}} = \cosh^2\left(\frac{2\pi d n_f Z}{\lambda}\right) + \left(\frac{n_f^2 \cos^2\theta - n_g^2 Z^2}{2 n_g n_f Z \cos\theta}\right)^2 \sinh^2\left(\frac{2\pi d n_f Z}{\lambda}\right) \qquad \text{(III.1a)}$$

$$\frac{1}{T_{\perp}} = \cosh^2\left(\frac{2\pi d n_f Z}{\lambda}\right) + \left(\frac{n_f^2 Z^2 - n_g^2 \cos^2\theta}{2 n_g n_f Z \cos\theta}\right)^2 \sinh^2\left(\frac{2\pi d n_f Z}{\lambda}\right) \qquad \text{(III.1b)}$$

where $Z = \left[\left(\frac{n_g}{n_f}\right)^2 \sin^2\theta - 1\right]^{1/2}$

Because $Z < 1$, $2\pi n_f < 10$ and $d \lll \lambda$ the quantity $\frac{2\pi d n_f Z}{\lambda} < 1$

and therefore $$\cosh^2\left(\frac{2\pi d n_f Z}{\lambda}\right) \simeq 1 \qquad \text{(III.2a)}$$

and $$\sinh^2\left(\frac{2\pi d n_f Z}{\lambda}\right) = \left(\frac{2\pi d n_f Z}{\lambda}\right)^2 \qquad \text{(III.2b)}$$

The relative intensity of the reflected light, R, is only a minute fraction of T, therefore to a good approximation,

$$\frac{1}{T_{\parallel}} = R_{\parallel} \qquad \text{and} \qquad \frac{1}{T_{\perp}} = R_{\perp} \qquad \text{(III.3)}$$

For natural (unpolarized) light**

$$R = \frac{1}{2}(R_{\parallel} + R_{\perp}) \qquad \text{(III.4)}$$

---

* KAPANY, N.S. (1967) Fiber Optics ACADEMIC PRESS p.37

** BORN, M. and WOLF, E. (1964) "Principles of Optics" p.44 Pergamon Press.

Substituting equations (III.2a,b) into (III.1a,b) and using the expressions III.3 and III.4 the final expression for the reflectivity R is:

$$R = \frac{1}{2}\left(\frac{\pi d}{\lambda n_g \cos\theta}\right)^2 \left[(n_f^2 \cos^2\theta - n_g^2 Z^2)^2 + (n_f^2 Z^2 - n_g^2 \cos^2\theta)^2\right].$$

REFERENCES

AINSWORTH, L. (1954) J. Soc. Glass Technol. 38 497T.

ANDERSON, J.H. and WICKERSHEIM, K.A. (1964) Sur, Sci. 2 252.

ARORA, A., MARSHALL, D.B., LAWN, B.R. and SWAIN, M.V. (1979) J. Non-Cryst. Solids 31 415.

BAILEY, A.I. (1961) J.Appl. Phys. 32 1407.

BAILEY, A.I. (1957) 2d Int. Congress Surface Activity III p. 406.

BARTENEV, G.M. RAZUMOVSKAYA, I.V. and SANDITOV, D.S. (1969). J. Non-Cryst. Solids 1 388.

BASTIC, R.E. (1950) J.Soc. Glass Technol. 34 75.

BOUTIN, H. and PRASK, H. (1964) Surface Sci. 2 261.

BOWDEN, F.P. and TABOR, D. (1964) The Friction and Labrication of Solids Part I and II. Oxford: Clarendon Press.

BRAYANT, P.J. (1962) Trans. 9th Nat. Vac. Symp. p.311 Macmillan Co.New York.

BREARLEY, W. HASTILOW, P.A.P. and HOLLOWAY, D.G. (1962) Phys. Chem. Glasses 3 181.

BRIDGMAN, P.W. and SIMON, I. (1953) J. Appl. Phys. 24 405.

CHARLES, R.J.(1958) J.Appl. Phys. 29 1549.

CHEESMAN, R.J. and LAWN, B.R. (1970) Phys. Stat. Sol. A 3 951.

COHEN, H.M. and ROY, R. (1965) Phys. Chem. Glasses 6 149.

DERJAGUIN, B.V. (1970) Scient. Amer. 223 52.

DERJAGUIN, B.V. and CHURAEV, N.V. (1973) Nature 244 430.

DOREMUS, R.H. (1973) Glass Science Wiley-Interscience.

DOUGLAS, R.W. (1958) J.Soc. Glass Technol. 42 145T.

ERNSBERGER, F.M. (1969) J.Am. Ceram. Soc. 51 545.

(1972) Ann. Rev. Mater. Sci. 2 529.

EVANS, A.G. (1972) J.Mater. Sci. 7 1137.

(1977) Acta Metall. 25 919

EVERETT, D.H., HAYNES, J.M. and McELROY, P.J. (1971) Sci. Prog. (Oxf.) 59 279.

FINKEL, V.M. and KUTKIN, I.A. (1962) Soviet. Phys. Dokl. 7 231.

FORTY, A.J. and FORWOOD, C.T. (1963) Trans. Brit. Ceram. Soc. 62 715.

FOX, P.G. and FREEMAN, I.B. (1979) J.Mater. Sci. 14 151.

FRISCHAT, G.H. (1972) Amorphous Materials p.235, Ed. Douglas, R.W. and Ellis, B.,Wiley Interscience.

GILMAN, J.J. (1975) J.Appl. Phys. 46 1625.

GOSSINK, H.A.M. and WERNER, H.W. (1979) Silicates Industriels 44 35.

GRIFFITH, A.A. (1920) Phil. Trans. R. Soc. A 221 163.

GRIFFITHS, R. (1968) MSc Thesis,University of Keele.

GUNASEKERA, S.P. (1970) MSc. Thesis,University of Keele.

HANEMAN, D., ROOTS, W.D. and GRAND, J.T.P. (1967) J.Appl. Phys. 38 2203.

HANNEMAN, R.E. and WESTBROOK, J.H. (1968) Phys. Mag. 18 (151) 73.

HAGAN, J.T. (1979) J.Mater. Sci. 14 462.
(1979) J.Mater. Sci. 14 2975.

HENCH, L.L. (1975) J.Non-Cryst. Solids 19 27.

HENCH, L.L. and CLARK, D.E. (1978) J. Non-Cryst. Solids 28 83.

HILL, R. (1950) The mathematical theory of Plasticity, Oxford, Clarendond Press.

HILLING, W.B. (1963) Advances in Glass Technology, Part 2, Ed: Matson, F.R. and Rindone, G.E. Plenum Press, New York.

HIRST, W. and HOWSE, M.G. (1969) Proc. Roy. Soc. A 311 429.

HOLLAND, L. (1964) The Properties of Glass Surfaces, Chapman and Hall (London).

HORDON, M.J. (1966) Acta Met. 14 1966.

IKIDA, Y. and MATSUDA, (1976) Jap. J. Appl. Phys. 15 963.

IMAOKA, M. and YASUI, I. (1976) J.Non-Cryst. Solids 22 315.

IRWIN, G.R. (1957) J.Appl. Mech. 24 361.

JOHNSON, K.L. (1970) J.Mech. Phys. Solids 18 115.

KETCHAM, W.M. and HOBBS, P.V. (1969) Phil. Mag. 19 1161.

KLIER, K. and ZETTLEMOYER, A.C. (1977) J.Colloid Interface Sci. 58 216.

KIES, J.A. and CLARK, A.B.J. (1969) Proc. 2nd Int. Cont. on Fracture Brighton 1969, p.483. Chapman & Hall, London, 1970.

KOMENI, N., KAWATE, Y. and OBARA, A. (1963) Bulletin - Electrotechnical Lab. 27 919.

LANFORD, W.A., DAVIS, K., LAMARCHE, P., T.LAURSEN, GLOREAU, R. (1979) J. Non-Cryst. Solids 33 249.

LAWN, B.R. and WILSHAW, T.R. (1975) Fracture of Brittle Solids, Cambridge Univ. Press. (1975) J. Mater. Sci. 10 1049.

LAWN, B.R. and EVANS, A.G. (1977) J.Mater. Sci. 12 2195.

LEVENGOOD, W.C. (1966) Int. J. Fracture Mech. 2 400.

LEVENGOOD, W.C. and VONG, T.S. (1960) J. Appl. Phys. 31 1416.

LINGER, K.R. (1967) PhD. Thesis, University of Keele.

LEIGHLY, H.P. and OGLESBEE, R.M. (1973) The Science of Hardness Testing and its Research Applications, p.445, Ed: Westbrook, J.H. and Conrad, D., ASM, Metals Park, Ohio.

MACDONALD,J.E. (1953) J. Meteorol. 10 416.

MARSH, D.M. (1964) Proc. R. Soc. A 279 420.
(1964) Proc. R. Soc. A 282 33.

McCAFFERTY, E. and ZETTLEMOYER, A.C. (1970) J.Colloid Interface Sci. 34 452.

McHAFFIE, I.R. and LENHER, S., (1925) J.Chem. Soc. 127 1559.

McQUILLIN, B.R. (1974) PhD. Thesis, University of Keele.

MICHEL, D., (1967) Z.Naturforsch. A 22 1751

MOULD, R.E. (1960) J.Am. Cer. Soc. 43 160.

MULHEARN, T.O. (1959) J. Mech. Phys. Solids 7 85.

NADAI, A. (1931) Theory of flow and fracture of solids, Vol. 2 McGrow - Hill.

NEELY, J.E. and MACKENZIE, J.D. (1968) J. Mater. Sci. 3 603.

OBREIMOFF, J.W. (1930) Proc. R. Soc. A 127 290.

OROWAN, E. (1944) Nature 154 341.
(1948) Rep. Proc. Phys. 12 185.

OLIVEY, A. (1973) Jap. J. Appl. Phys. 12 1534.

OUTWATER, J.O. and GERRY, D.J. (1966) Report on Contract NONR 3219, Office of Naval Research, Washington D.C.
(1967) Mod. Plast. 45 156.

PENTANO, C.G., DOVE, D.B. and ONODA, G.Y. (1975) J. Non-Cryst. Solids 19 41. (1976) J. Vac. Sci. Technol. 13 414.

PETER, K.W. (1970) J. Non-Cryst. Solids 5 103.

PROD'HOMME, M. (1968) Phys. Chem. Glass 9 101.

RAYLEIGH, F.R.S. (1937) Nature 781.

RAZUMVOSKAYA, I.V., TURCHINOVICH, L.M. and DORZHIEV, D.B. (1976) Sov. Mater. Sci. 11 681.

ROBERTSON, J.H. (1963) J. Sci. Instrum. 40, p.506.

SAKKA, S. and MACKENZIE, J.D. (1969) J. Non-Cryst. Solids 1 107.

SAMUELS, L.E. and MULHEARN, T.O. (1957) J. Mech. Phys. Solids 5 125.

SCÖNERT, K., UMHAUER, H. and KLEM, W. (1969) Proc. 2d. Int. Conf. on Fracture, Brighton, (1969) p.474 Chapman & Hall, London, 1970.

SIEGER, S. (1975) J. Non-Cryst. Solids 19 213.

SMITH, R. and SANDLAND, G. (1925) J. Iron St. Inst., 111 285.

STONE, W. (1930) Phil. Mag. 9 610.

TABOR, D. (1951) The Hardness of Metals, Clarendon Press, Oxford
(1954) Endeavour 13 27.

TAYLOR, E.W. (1950) J. Soc. Glass Technol. 34 69T.

TICHANE, R.M. and WILSON, L.B. (1964) J. Appl. Phys. 35 2537.

TIMOSHENKO, S.P. and GOODIER, J.N. (1970) Theory of Elasticity p.309, 3rd. Ed. McGraw - Hill, New York.

VARCHENYA, S.A., UPIT, G.P., MANIKA, I.P. The Science of Hardness Testing and its Research Applications, p.440, Ed: Westbrook J.H. and Cnrad, D., ASM, Metals Park, Ohio.

VARNER, J.R. and FRECHETTE, V.D. (1972) Amorphous Materials p.507 Ed: Douglas, R.W. and Ellis, B. Wiley - Interscience.

WALTERS, H.V. and ADAMS, P.B. (1975) J. Non-Cryst. Solids 19 183.

WIEDMANN, G.W. (1973) PhD. Thesis, University of Keele.

WIEDMANN, G.W. and HOLLOWAY, D.G. (1974a) Phys. Chem. Glasses 15 117. (1974b) Phys. Chem. Glasses 15 68.

WESTBROOK, J.H. (1960) Phys. Chem. Glasses 1 32.

WESTBROOK, J.H. and JORGEBSEN, P.T. (1965) Trans. Met. Soc. AIME 233 425.

WESTWOOD, A.R.C., PARR, G.H., LATANISION, R.M. (1972) Amorphous Materials p.533 Ed: Douglas, R.W. and Ellis, B., J. Wiley.

WESTWOOD, A.R.C. and MACMILLAN, N.H. (1973) The Science of Hardness Testing and its Research Application, p.377 Ed: Wesrbrook, J.H. and Gonrad, D., ASM, Metals Park, Ohio.

WEYL, W.A. (1975) J. Non-Cryst. Solids 19 1.

WIEDERHORN, S.M. and TOWNSEND, P.R. (1970) J. Am. Ceram. Soc. 53 486.

WIEDERHORN, S.M. (1971) Int. Conf. on Corrosion Fatigue, Storrs Conn. 1971, paper 40.

YAMANE, M. and MACKENZIE, J.D. (1974) J. Non-Cryst. Solids 15 153.

YOUNG, R.J. and BEAUMONT, P.W.R. (1977) J. Mater. Sci. 12 684.